THE EVOLUTIONARY EMERGENCE OF NEURAL ORGANISATION IN COMPUTATIONAL MODELS OF PRIMITIVE ORGANISMS

by

Benjamin Henry Demidecki Jones

A thesis submitted to
The University of Birmingham
for the degree of
DOCTOR OF PHILOSOPHY

Natural Computation Group
School of Computer Science
The University of Birmingham
February 2010

Abstract

Over the decades, the question "why did neural organisation emerge in the way that it did?" has proved to be massively elusive. Whilst much of the literature paints a picture of *common ancestry* – the idea that a species at the root of the tree of nervous system evolution spawned numerous descendants – the actual evolutionary forces responsible for such changes, major transitions or otherwise, have been less clear. The view presented in this thesis is that via interactions with the environment, neural organisation has emerged in concert with the constraints enforced by body plan morphology and a need to process information efficiently and robustly. Whilst these factors are two smaller parts of a much greater whole, their impact during the evolutionary process cannot be ignored, for they are fundamentally significant. Thus computer simulations have been developed to provide insight into how neural organisation of an artificial agent should emerge given the constraints of its body morphology, its symmetry, feedback from the environment, and a loss of energy. The first major finding is that much of the computational process of the nervous system can be offloaded to the body morphology, which has a commensurate bearing on neural architecture, neural dynamics and motor symmetry. The second major finding is that sensory feedback strengthens the dynamic coupling between the neural system and the body plan morphology, resulting in minimal neural circuitry yet more efficient agent behaviour. The third major finding is that under the constraint of energy loss, neural circuitry again emerges to be minimalistic. Throughout, an emphasis is placed on the coupling between the nervous system and body plan morphology which are known in the literature to be tightly integrated; accordingly, both are considered on equal footings.

Acknowledgements

Somebody once told me that "a PhD was never meant to be easy". And they were right! Unequivocally so! I am therefore incredibly lucky to have been helped by 'beings' who at times, seemed to exist on several planes higher than my mere self. To begin with, I am indebted to the advice, consideration and general string pulling of my supervisors Xin Yao, Bernhard "I prefer British beer really" Sendhoff and Yaochu Jin. When I was 'stuck' I would become 'unstuck'. I am further grateful to the help and support of members of the Honda Research Institute Europe (HRI), in particular to Lisa Schramm for her help with the physics stuff (not forgetting to mention the awesome times in New Zealand), to Till Steiner, also for his help with the physics stuff, to the remarkable programming geniuses of Marc-Oliver Gewaltig and Jochen Eppler, who despite making me feel like more of a hacker than a programmer, helped me decipher some rather complicated spiking neural network software; to all the good people of the HRI-ELTEC group who offered valuable insight and discussion; to the HRI itself, for funding my research. I am further grateful to Chrisantha Fernando for his advice and encouragement, to Fiona McGettrick for her kindness and support, to Andrea Soltoggio, for some of the most productive and evocative Skype conversations I've ever had, to the coolness of Neale Samways (+family) whose cynicism matches my own (;-)); to the other awesome people I've met here at the department in Birmingham and at various conferences and academic institutions throughout the world all of whom are too innumerable to mention. I would also like to thank my family for their gentle support, kindness and encouragement and also for somehow enthusing me with tenacity. Finally, I would like to thank Maha Salem, for her remarkable kindness, friendship and patience – she read through numerous drafts of my thesis and generally kept me going when the times were tough. She'll be having punctuation nightmares for a good while yet! ;-)

Publications

Elements of this thesis have appeared in the following peer-reviewed publications.

B. Jones, Y. Jin, B. Sendhoff, and X. Yao. The evolutionary emergence of neural organization in a hydra-like animat. (Abstract only). In *The Bernstein Conference of Computational Neuroscience* and *Frontiers in Computational Neuroscience.* Frontiers Research Foundation, 2009.

B. Jones, Y. Jin, B. Sendhoff, and X. Yao. The effect of proprioceptive feedback on the distribution of sensory information in a model of an undulatory organism. In *Proceedings of the 10th European Conference on Artificial Life*, Berlin, 2009. Springer.

B. Jones, Y. Jin, X. Yao, and B. Sendhoff. Evolution of neural organization in a hydra-like animat. In *Proceedings of the 15th International Conference on Neural Information Processing of the Asia-Pacific Neural Network Assembly*, volume 1, pages 216-223, Berlin, 2008. Springer.

B. Jones, Y. Jin, B. Sendhoff, and X. Yao. Evolving functional symmetry in a three dimensional model of an elongated organism. In *Artificial Life XI: Proceedings of the Eleventh International Conference on the Simulation and Synthesis of Living Systems*, pages 305-312, Cambridge, MA, 2008. MIT Press.

Contents

List of Figures

List of Tables

Chapter 1

Introduction

The nervous system is a remarkable feat of evolution. Its capacity to humble both scientist and philosopher alike is testament to its inextricable complexity. Approaching this complexity is tough, academically speaking; yet, to pick it apart is a crucial endeavour, since, if we can shed light on how nature organises the nervous system, we will be in a better position to understand how nature adapts to make information processing more efficient. Unfortunately, the complexity of the nervous system often leaves us out in the cold, so to speak, when trying to broach the individual parts that yield the whole. It is therefore fortunate that nature, and indeed computers, give us the provisions necessary to tackle such intricacy. Firstly, we can turn to very simple organisms and look towards the most elementary of organisational principles of nervous systems; we can study *the least complex* of nervous systems. Secondly, we can turn to computers and model how such organisms might evolve and develop. In this manner, we can be more constructive in our approach; we can begin to shed light on how evolution progressed from the simplest of nervous systems – analyse exactly how they are used in a simulated environment, what their properties are, how they distribute sensory information, etc. – to those that are more organised, in the sense of distinct neural structures (the brain being the most obvious example). Importantly, this research not only contributes to understanding natural processes, it contributes to how engineers might build systems more efficiently and robustly.

Thus, the overall aim is to elucidate the evolutionary driving forces instrumental to nervous system organisation. As hinted upon above, the methodology has been to model very primitive organisms, immersing them in the simplest environments imaginable, and evolving their nervous systems (artificial neural network abstractions) and body plan morphologies

using artificial evolutionary algorithms. By keeping things this simple, extraneous factors not core to the central research theme (that of neural organisation under various constraints) have been consistently mitigated. To clarify, at no point does one address the evolutionary advantage of having a nervous system versus not having a nervous system at all. Rather, the core focus has been on how the body plan of a primitive organism, and how a need to conserve energy, constrains the evolutionary emergence of neural organisation within nervous systems that *already exist*, so that given a particular environment, particular architectural features become preferential.

1.1 Guiding Questions

The ideas in this thesis revolve around four guiding questions. Each has a guiding principle, the motivation behind the question. They are summarised as follows:

1. **Question:** *How does body plan morphology affect the evolution of the nervous system and vice-versa?* **Guiding principle:** Since the body of an organism directly interacts with the environment, it needs to have the correct niche-specific characteristics. At the same time, before these characteristics can actually be exhibited, the body needs to be properly actuated by a correctly tuned nervous system. Pointedly however, the emergence of the neural architecture is also constrained by the emergence of the body plan morphology (and vice-versa). This suggests that the evolutionary drive towards an optimal combination of these elements and the coupling between them is highly complex. The above question aims to address such coupling and the corresponding effects on body morphology characteristics and nervous system architecture.

2. **Question:** *How does body-symmetry evolve in relation to the nervous system and other body plan characteristics?* **Guiding principle:** The symmetry of an organism's body plan morphology will often preclude optimal behaviour (e.g. directional movement). At the same time, the nervous system and body plan will often adapt and fit around this symmetry in a particular way (and vice-versa) so that behaviour is made efficient and optimal. The above question investigates the process by which this occurs.

3. **Question:** *What effect does sensory feedback have on the emergence of the neural system architecture and the distribution of computational process?* **Guiding principle:** The nervous system provides actuation. This causes the host organism to move in a

particular way. Based on this behaviour, the organism either survives, or it dies. By incorporating a sensory feedback link from the motor system to the nervous system, it can be assessed whether the agent is given any kind of behavioural advantage. Of further crucial importance, is how this feedback should alter the architecture of the underlying nervous system and how the computational load is distributed between the passive dynamics of the motor system and the active dynamics of the nervous system.

4. **Question:** *What effect does energy constraint have on the evolution of both nervous system and the body plan morphology of an organism?* **Guiding principle:** In nature, an organism will ultimately die if it has no energy to survive. An energy conserving framework is therefore added to models developed earlier on, and considers how energy is lost due to the activity of the neural and motor systems and how evolution strives to minimise this, but whilst endowing the organism with maximum functional advantage. The need to conserve energy places a variety of constraints on the coupled body plan morphology and neural system. By varying the energy constraint, changes in the neural architecture and/or body plan characteristics can be observed and progressively understood.

1.2 Contributions

The contributions of this thesis are as follows:

1. **Evo-Critter:** this is a research tool inspired by the vertebrate lamprey, and designed to address the above questions. Specifically, it allows one to investigate how a spatially embedded neural control system, body plan morphology characteristics and aspects of body symmetry are all coupled together both on physical and dynamical levels. Via a process of simulated evolution, one is able to investigate the manifestation of such couplings and crucially, the commensurate changes to neural architecture.

2. **Symmetry.** It is shown that body symmetry has a direct impact on the behavioural process, for an undulatory agent. Also, that symmetry is affected by **(i)** the emergence of body segmentation characteristics and **(ii)** a need to minimise energy lost due to the activities of the neural and motor systems.

3. **Constraints of body morphology.** It is demonstrated that both neural architecture

and neural dynamics are affected by the levels of 'coupling' present within the system. This coupling concerns dependencies between the body plan morphology, aspects of the body symmetry, and organisational aspects of the neural architecture.

4. **Constraints of energy.** It is shown how the requirement to minimise energy loss (or, maximise the energy that can be conserved), results in a favouring by evolution of minimalistic neural architectures. This is firstly demonstrated in **Hydramat,** a software tool inspired by the Hydra (a type of jellyfish) and developed independently of the Evo-Critter framework. The primary objective of this tool is to elucidate the effect of energy loss in primitive neural systems alone; therefore, less emphasis is placed on body plan morphology. Energy as a constraining resource is secondly demonstrated in the context of Evo-Critter via an extra 'energy loss term' incorporated into the fitness function. This permits one to investigate not only the effect of energy loss on the emergence of neural architecture but also on the coupled emergence of symmetry and other body plan features.

1.3 Thesis layout

This thesis is split into three core parts.

- **Part I** covers background material essential to the models and experiments developed in later sections. Chapter 2 provides an overview of the 'basics' – neurons, artificial neural networks, central pattern generators, artificial evolution and genetic representations – to provide context. Chapter 3 sets out to provide the biological background core to understanding the motivation of the thesis. Evidence from biology concerning transitions of nervous systems and architectural innovations, is provided in detail. Chapter 4 provides further literature on Hydra, the freshwater jellyfish which can provide a basis for the investigation of primitive nervous systems; it then introduces literature on actual computer models concerning both the Hydra and undulatory organisms which can be used for the study of evolution of neural control systems for bio-inspired agents.

- **Part II** explores how the body plan characteristics of an organism place constraint on, and are constrained by, the nervous system. It begins with chapter 5, which introduces and describes Evo-Critter, a model designed and implemented to explore nervous system body plan morphology couplings in a 'fish-inspired' physically realistic undulatory

agent. Chapter 6 then takes this model and begins to explore questions 1 and 2 posited above (Section 1.1). Thus an investigation is made into how the body plan characteristics, and an abstract notion of body symmetry, evolve in concert with the neural control system. Then, in chapter 7, an exploration is made of the effect of proprioceptive feedback on the behaviour of the undulatory agent, with an emphasis on neural architecture, movement kinematics, and neural dynamics (essentially question 3 from above).

- **Part III** provides an exploration of energy as a constraint in the emergence of neural organisation. Thus, it considers Question 4 from above. It begins with chapter 8, which provides a model of a Hydra, a type of jellyfish, to broach this subject in the context of a radially symmetric organism, and secondly, extends the Evo-Critter framework, to broach this subject in the context of a bilaterally symmetric organism.

In Chapter 9, a *discussion*, *scope for future research directions* and some of the *wider implications* of the research are all provided. Within these sections, the contributions of each chapter are initially highlighted; having answered the research questions – having elucidated the evolutionary emergence of neural organisation in computational models of primitive organisms – everything is tied together and where required is further clarified. In other words, the whole picture is presented. Several extensions to the work conducted in this thesis are then presented and addressed as highly significant research avenues. It is hoped that myself and others will be able to take on board such avenues and further consolidate the contributions presented. Finally some of the wider implications of the research pertaining to both neuroscientists and members of the artificial life community are briefly considered.

Part I

Background

Chapter 2

Basic Principles

Synopsis

This chapter provides an overview of the fundamentals, both *biological*, and *computational*, essential to the models discussed throughout Parts II and III of this thesis. It begins in Section 2.1 by briefly describing the nervous system, since this is core to the whole thesis. Then, in Section 2.2, the artificial neural network is introduced as an approach to abstractly model biological nervous systems; an emphasis is placed on dynamic recurrent neural networks, since these are primarily used for the Evo-Critter model, developed in Chapter 5. Central pattern generators are then briefly introduced as a type of network crucial for locomotion in most metazoan organisms. Finally, from Section 2.3, artificial evolutionary algorithms are introduced as a means to optimise neural networks, with different types of encoding (*direct, indirect or implicit)* introduced as having different levels of biological plausibility. Direct and implicit encoding schemes are used for the models presented in this thesis.

2.1 Biological nervous systems

Nervous systems are comprised of vast complex networks of interconnected nerve cells. These networks allow for the transmission of information from sensors such as the eyes and major control architectures such as the brain, to points or effectors where it is needed. Principally, this endows the host organism with a control mechanism and thus enables it to survive. An example of such a nerve net is captured by Cajal[1] in one of his well renowned illustrations,

[1] http://en.wikipedia.org/wiki/Santiago_Ramon_y_Cajal

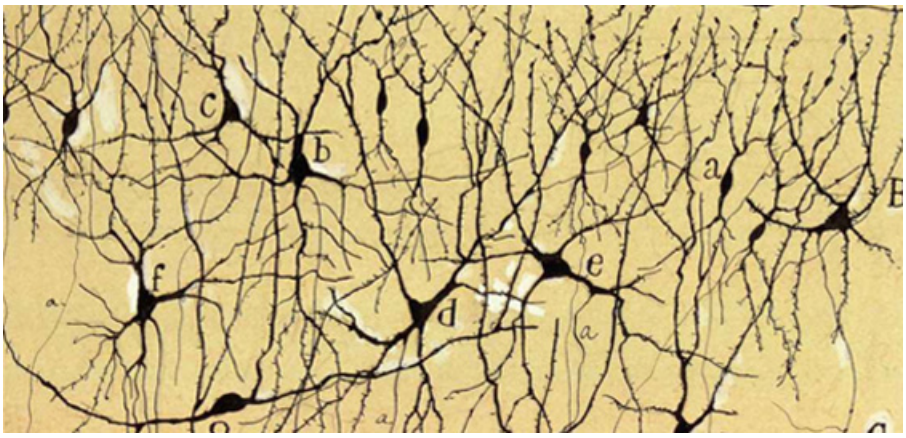

Figure 2.1: A Cajal illustration of a nervous system network (http://www.banquete.org/).

see Fig. 2.1.

The fundamental components of all nervous systems are the nerve cell and the neuritic process, namely the axon and the dendrite. During neurogenesis, nerve cells interconnect forming vast complex networks through which information is propagated in the form of electrical nerve impulses. A nerve impulse arises because of local disruptions in cell membrane potentials. In a given cell, it begins in the main cell body or *soma* and then propagates down the length of the axon, until the axon terminates at the pre-synaptic membrane. This 'pre-synapse' then forms a synaptic *connection* to a post-synapse, which is located at the end of the connected post-synaptic neuron's dendrite. The impulse then continues its journey as follows: (i) chemical neurotransmitter is released from the pre-synaptic membrane into the synaptic cleft; (ii) this neurotransmitter then travels to and binds with receptors located on the post-synaptic membrane; (iii) this causes a disruption in the post-synapse's membrane potential; (iv) consequently the 'nerve impulse' is essentially 're-propagated'. It thereafter continues its journey to the soma of the post-synaptic neuron. The whole sequence of events repeats in a vastly parallel manner as and when impulses propagate through the network. An example of this process for a single synapse is illustrated in Fig. 2.2.

Through various arrangements of neuronal connectivities, neuron types, varying synaptic efficacies, conduction delays and a variety of different neuro-transmitter substances, different functional properties including learning and memory are made possible. Ultimately, the host organism endowed with these abilities is able to survive and adapt to a variety of environmental conditions.

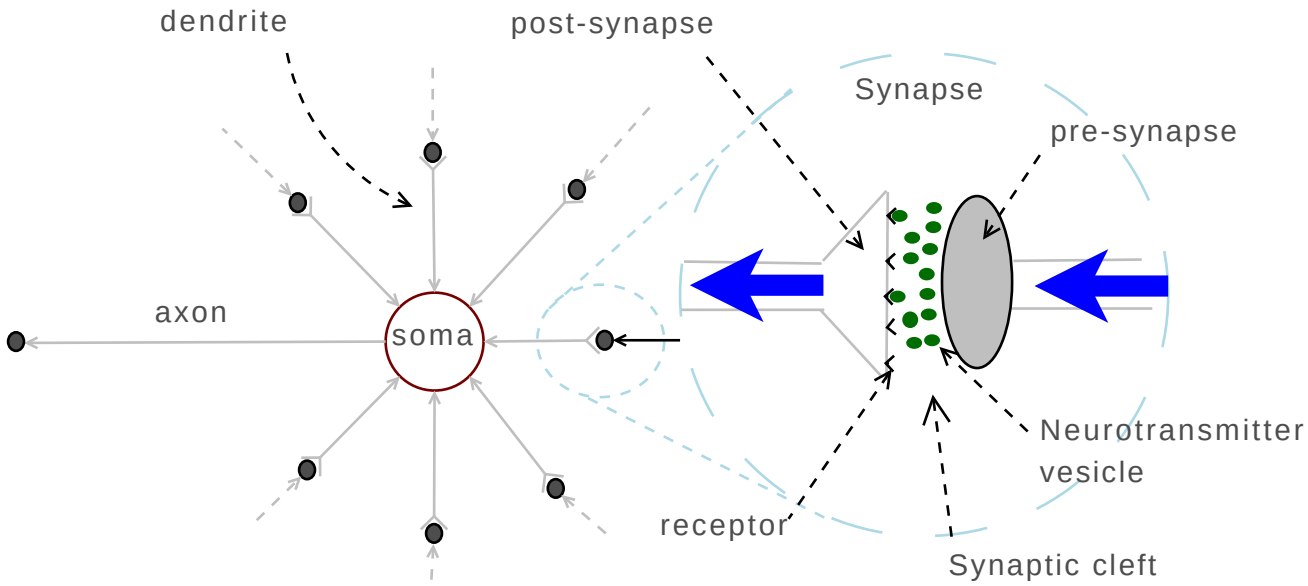

Figure 2.2: Propagation of a nerve impulse from a pre-synaptic neuron to a post-synaptic neuron. Directions of nerve impulses have been marked with arrows. As shown, at the pre-synapse, chemical neurotransmitter vesicles are released. These are detected by the post-synapse; the impulse then continues its journey to the soma of the post-synaptic neuron.

2.2 Artificial neural networks

Artificial neural networks set out to model the fundamental aspects of biological nervous systems. Chiefly, they consist of neurons ('units') which become connected together via synapses ('connection weights'), and the overall result is a directed graph with 'signals' that propagate uni-directionally. All artificial neural networks share a number of common features, but depending on how they are implemented they are more or less biologically plausible.

2.2.1 Simple feed-forward networks

The most 'primitive' of artificial neural networks is the perceptron. This primarily consists of a layer of transfer logical units (McCulloch-Pitts neurons [78]) each of which implements a binary, linearly separable function [102]. Overall, the network has N inputs and a binary output, which is then linearly separable by a hyperplane. Whilst this is ideal for simple 'yes/no' binary problems, a slightly more advanced abstraction is required for more complex computational tasks, for example, the control of some artificial life agent. An example of a more advanced abstraction is the multi-layered perceptron (MLP) (e.g. [49]), see Fig.

2.3a. This extends the computational power of the perceptron by employing units having non-linear 'activation' functions in a *hidden* or *middle* layer configuration whilst units in an *output* layer maintain linear output functions. In practice, the overall construction allows for a projection of non-linearly separable input data into a higher dimensionality. This renders the data linearly separable and therefore classifiable. A hidden unit's output is computed as

$$y_j = \mathrm{g}\left(\sum_{j=1}^{C} w_{ij} y_i + b_j\right) \tag{2.1}$$

$$\mathrm{g}(x) = \frac{1}{1 + e^{-x}} \tag{2.2}$$

where b_j is a bias term employed to ensure that the neuron will always generate some output even if the input is 0; $\mathbf{w}$ is a weight matrix, hence w_{ij} is a single connection weight from neuron i to neuron j. The sigmoid function in Eq. 2.2 is often referred to as a threshold function. The individual weights of the whole network are then tuned in a process of optimisation, minimising the network's output error; this forms the basis of 'training'. The actual network architecture – connectivity and number of hidden neurons – can also be optimised.

2.2.2 Dynamic recurrent neural networks

Recurrent neural networks are so named given their inclusion of feedback or recurrent connections. Further, in contrast to MLPs and other non-dynamic networks which operate entirely in 'one-shot' static processes, *dynamic* recurrent neural networks operate in 'time'; this means that their outputs transiently pass through a number of *intermediate states* before settling into a final *attractor* state.

Dynamic recurrent neural networks further possess 'fading memory': the state of the network at any given moment in time, progressively 'fades' such that earlier states 'resonate' throughout the system (like the waves created by a pebble thrown into a pool of water). Consequently, the 'output' or current state of the network depends not only on the current 'input', but also on all previous inputs and all previous transient states. This type of network is useful for tasks that require some patterned activity generated over time, for example, the control of undulatory locomotion, or for the control of artificial agents operating in a dynamic environment. An idealised schematic of a network that might be used in this way is presented in Fig. 2.3b.

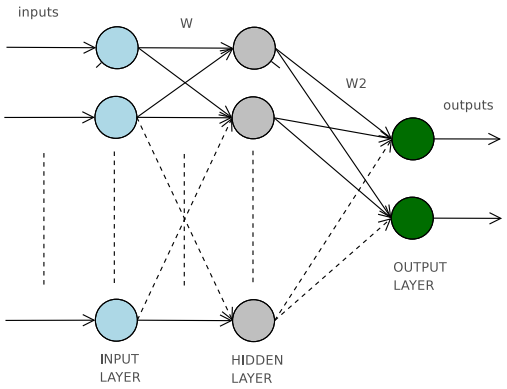

(a) A structured, multi-layered perceptron. The main component of a given unit is the sigmoidal function which serves to 'squash' the signal arriving at an incoming connection.

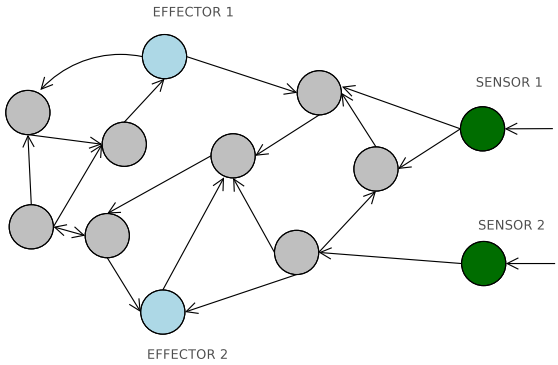

(b) An unstructured network architecture with varying levels of recurrency for a hypothetical agent having sensors and effectors.

Figure 2.3: Structured versus non-structured neural architectures.

The continuous time recurrent neural network (CTRNN) often attributed to Beer [10, 11] is the type of dynamic network used throughout most of the experiments undertaken in this thesis. A neuron in a CTRNN features a transient membrane potential, thus it reflects the non-static nature of a biological neuron. It is further modeled on the *leaky integrator* concept in which the membrane potential fractionally decreases at each time step (it 'leaks') by an amount proportional to a time constant. Conceptually, within computational neuroscience, this is argued to be one of the more plausible models of membrane potential [12].

The process of leaky integration for a neuron, j, can be summarised as,

$$\tau_j \frac{du_j}{dt} = -u_j + RI_i(t) \tag{2.3}$$

where u_j is the membrane potential; τ_j is the time-constant controlling the rate at which u changes over time; RI is the resistance of the synaptic connections on the in-coming pre-synaptic current. The above definitions can then be expanded as follows,

$$\tau_j \frac{du_j}{dt} = -u_j + \sum_{i=1}^{C} w_{ij} a_i + I_j \tag{2.4}$$

$$a_i = \frac{e^{2x_i} - 1}{e^{2x_i} + 1} \tag{2.5}$$

$$x_i = u_i - b_i \tag{2.6}$$

where w_{ij} is a connection weight from neuron i to neuron j; a_i is the activation of neuron i which is typically computed using the hyperbolic tangent function, Eq. 2.5, b_i is a bias term and I_j is some external input current. The variables u_j and τ_j are the neuron's membrane potential and time constant. The Evo-Critter framework introduced in Chapter 5 uses such a CTRNN model.

2.2.3 Spiking neural networks

Spiking neural networks are often cited as the latest generation of artificial neural network, e.g. [123]. They are based on the idea of *nerve impulses*, spikes of activity generated by individual neurons at different time intervals. This of course reflects the spiking activity of real biological neurons, therefore, out of all neural network models, spiking neural networks are often considered the most biologically plausible. Unfortunately, they are difficult to implement and often require substantial computational overhead. Fortunately, a number of simulation environments designed to explore spiking neural networks are readily available, for example, the Neuro Simulation Toolkit (NEST) [44].

One of the most simple spiking neuron models is the 'Integrate-and-Fire' neuron, which revolves around the leaky integrator concept introduced above. In essence, this works by accumulating (i.e. integrating) the membrane potential of a neuron. When this reaches a certain threshold the neuron 'fires' (spikes) after which it is immediately reset to its resting potential. A straightforward implementation takes the standard CTRNN model as given in Eq. 5.14 but makes the following changes. Firstly, the activation function given in 2.5 is replaced with the following threshold function:

$$a_j(t) = \begin{cases} 1 & u_j(t) = \vartheta \\ 0 & \text{otherwise} \end{cases} \tag{2.7}$$

where $a_j(t)$ is the activation of neuron j at time t and ϑ is a constant threshold. The binary value 1, represents a pulse, a firing of the neuron. When the neuron fires at time $t^{(f)}$ the membrane potential is immediately reset to its resting potential,

$$u(t^{(f)}) = u_r \tag{2.8}$$

where u_r is a predefined constant. The process of leaky integration can then be repeated.

The Hydramat model introduced in Chapter 8 employs an integrate and fire model for the neural control.

2.2.4 Central pattern generators

Central pattern generators (CPGs) are a class of neural network that by virtue of their inherent dynamics are capable of generating rhythmic or oscillatory patterns of activity without any external input [76]. These can be successfully implemented with CTRNNs given the ease with which CTRNNs can generate patterned activity. In nature, CPGs are utilised for fictive patterns of activity, for example *breathing*, *pacemakers*, and *locomotion*. The diverse range of structures requiring rhythmic process highlights how CPG motifs will not only emerge to provide optimal neural dynamics, but with the secondary constraint of more optimally fitting with the surrounding body structure. Finally, CPGs are very well understood thus are suitable for study in simulation where, for example, the emphasis is on neural control of locomotion. As such, they are heavily utilised in the simulations outlined in this thesis. A depiction of a very simple CPG is presented in Fig. 2.4.

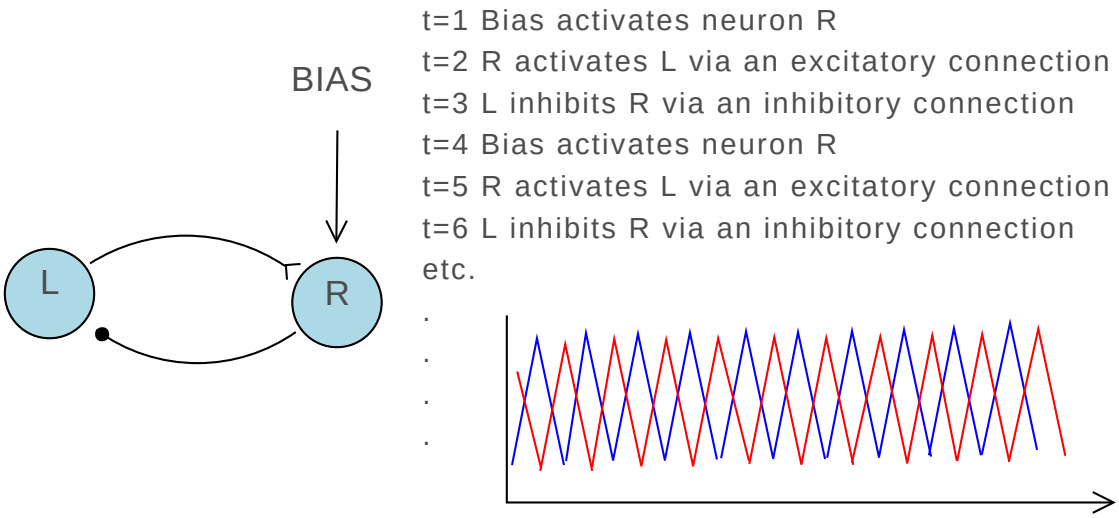

Figure 2.4: A depiction of a simple CPG neural oscillator for inhibitory neuron L and excitatory neuron R. The dynamic generates oscillating activity for L and R directly in antiphase with each other.

2.3 Neuroevolution

Artificial neural networks need to be optimised if they are to carry out some task correctly. This process can involve the optimisation of any number of neural parameters, but typically includes the weight matrix and/or synaptic connectivity. One way of doing this involves the use of evolutionary algorithms, so named since they are inspired by natural evolution. A good but slightly dated review can be found in [127]. A more up to date review can be found in [41].

2.3.1 Basic operation

In an evolutionary algorithm, a population of individuals compete to pass on their parameter values (genes); this is based on the notion of *survival of the fittest.* Individuals represent solutions to a given problem or task and will survive if they meet some fitness criterion; this is often a fitness function or the ability to undertake some target behaviour. Thus in terms of a neural network, the fitness function might simply be the sum squared error output that needs to be minimised, or perhaps the distance that a virtual agent has to 'swim' forwards. This manifestation of error output or behaviour is due to the *phenotype*, the actual physical entity as encoded for by the genetic code or *genotype*; thus only the phenotype is evaluated. In finding the correct phenotype, the algorithm searches over the genotype space which is the space encoding those parameters (e.g. connection weights) needing to be optimised. In such algorithms, the process of selecting progressively better solutions is akin to survival in evolutionary terms (i.e. the poorer solutions or individuals die out over time). Those individuals having better fitness are selected with a higher probability, to eventually form an offspring population. This offspring population then becomes the 'parent' population in the next consecutive round (generation) of the algorithm.

Together with selection, individuals probabilistically *reproduce* by having certain of their parameter values *recombined.* In effect, this enhances genetic diversity since it expands the gene pool; thus, the likelihood of a fitter solution being acquired as a result is increased. Individuals are also subjected to probabilistic *mutation.* This involves changing the value of a parameter: if it is real valued, then a small amount of normal or uniform noise can be added to it. If it is boolean, then it can be flipped. The whole process is visually depicted in Fig. 2.5.

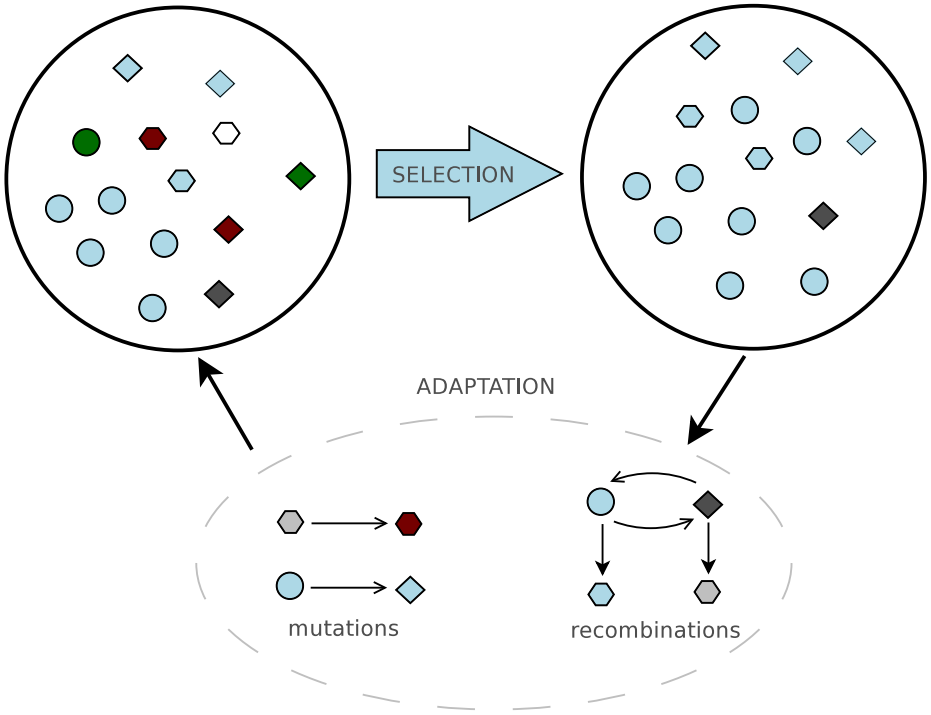

Figure 2.5: A generic evolutionary process. In this toy example, individuals have certain phenotypic traits such as shape and colour. They are evaluated and selected in favour of the colour blue. The gene parameters responsible for these features are then adapted and the whole process repeats in a loop. The eventual result will be an optimised set of individuals.

2.3.2 Encoding schemes

Depending on the type of neural network being optimised and the genetic representation itself, a variety of encoding schemes can be used for the optimisation process. An encoding scheme basically describes how the phenotype should be numerically quantified. The different types (*direct, indirect, implicit)* are outlined here.

2.3.2.1 Direct

Direct encoding schemes provide a direct one to one mapping between the genotype and phenotype. For example, if there are 50 phenotype traits (for example, 50 connection weights), the genetic representation will consist of 50 parameters. A problem with this is that the search space becomes intractable with larger networks; it is therefore considered the least biologically plausible of all representations. An example is Neuroevolution of Augmenting Topologies (NEAT) developed by Stanley and Miikkulainen [115].

2.3.2.2 Indirect

Indirect encoding schemes provide a generative process in which the phenotype is progressively developed from the genotype. An example is that implemented by Kitano, who, in his seminal work, outlined how a genotype rule grammar can be used to build up larger neural architectures [61], see Fig. 2.6. Since indirect approaches are not 1:1 mappings, the problem with scalability is intrinsically countered and, given the developmental abstraction, more conceivably fits with biology.

$$S \qquad \begin{matrix} A & B \\ C & D \end{matrix} \qquad \begin{matrix} c & p & a & a \\ a & c & a & e \\ a & a & a & a \\ a & a & a & b \end{matrix} \qquad \begin{matrix} 1 & 0 & 1 & 1 & 0 & 0 & 0 & 0 \\ 0 & 1 & 1 & 1 & 0 & 0 & 0 & 0 \\ 0 & 0 & 1 & 0 & 0 & 0 & 0 & 1 \\ 0 & 0 & 0 & 1 & 0 & 0 & 0 & 1 \\ 0 & 0 & 0 & 0 & 0 & 0 & 0 & 0 \\ 0 & 0 & 0 & 0 & 0 & 0 & 0 & 0 \\ 0 & 0 & 0 & 0 & 0 & 0 & 0 & 0 \\ 0 & 0 & 0 & 0 & 0 & 0 & 0 & 1 \end{matrix}$$

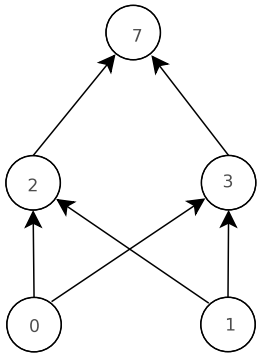

$$S \rightarrow \begin{bmatrix} A & B \\ C & D \end{bmatrix} \quad A \rightarrow \begin{bmatrix} c & p \\ a & c \end{bmatrix} \quad B \rightarrow \begin{bmatrix} a & a \\ a & e \end{bmatrix} \quad C \rightarrow \begin{bmatrix} a & a \\ a & a \end{bmatrix} \quad D \rightarrow \begin{bmatrix} a & a \\ a & b \end{bmatrix}$$

$$a \rightarrow \begin{bmatrix} 0 & 0 \\ 0 & 0 \end{bmatrix} \quad b \rightarrow \begin{bmatrix} 0 & 0 \\ 0 & 1 \end{bmatrix} \quad c \rightarrow \begin{bmatrix} 1 & 0 \\ 0 & 0 \end{bmatrix} \quad e \rightarrow \begin{bmatrix} 0 & 1 \\ 0 & 1 \end{bmatrix} \quad p \rightarrow \begin{bmatrix} 1 & 1 \\ 1 & 1 \end{bmatrix}$$

Figure 2.6: An example encoding of a neural architecture using Kitano's Graph Generation System, showing how rules are progressively employed to build up the overall connectivity of a neural network. Adapted from Figs. 3 and 4 of [61].

Others have approached encoding in a similar fashion. For example, Gruau [48] developed a system in which rules are encoded in 'cells' representative of neurons that can undergo division and/or invoke neuritic growth. These cells are progressively interpreted and the architecture of the neural network is built up. Others have been more interested in geometrical information, for example, using the angles of outgoing connections and the x,y coordinate positions of neurons in determining connectivity [95]. Rust et al. [103] and further Astor and Adami [6] have independently developed models that grow synaptic connections according to chemical gradients present within the environment. Chvál [28] uses Lindenmayer systems

to provide a generative mapping. Eggenberger [35, 34] employs a gene regulatory network with an emphasis on how local gene interaction can generate relatively complex networks.

2.3.2.3 Implicit

In implicit encodings, properties are implicit within the system as a result of other properties. For example, connectivity and/or connection weights might be derived as a function of interneuronal distance in which case these parameters are not explicitly encoded, but are implicitly given by neuron positional information. This approach, depicted in Fig. 2.7, is used as the basis for all models presented in this thesis. A further example is the Analog Genetic Encoding scheme (AGE) [41]. In AGE, sequences of characters of arbitrary length describe different neuron types. These sequences are joined together but are delimited by pre-specified characters; this forms a single long string representation of characters. A weight value is then derived according to an interaction function which takes two such character sequences from the whole string and outputs the weight value. In other words, weight values are implicit in how the character sequences interact with each other.

The representations used by the models in this thesis utilise properties of both implicit and direct encoding schemes. Firstly, they are implicit in the sense that they rely on neuron positional information to derive weight values and connectivity. Secondly, they are direct in the sense that several neural properties such as time constant and bias value are directly represented.

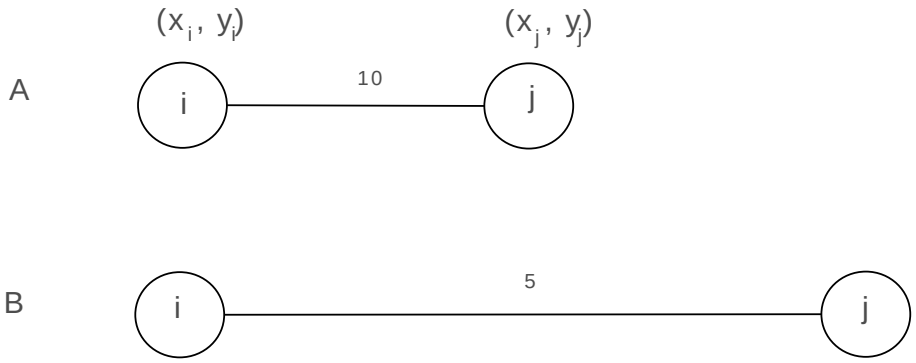

Figure 2.7: A basic example of implicit encoding. In this scheme, the (x,y) coordinate positions of neurons i and j are genetically represented and evolved. The weight value is derived from the Euclidean distance between the two neurons; the further the two neurons are apart, the smaller the weight value. Thus, in scenario B, the connection weight (the 'line') is smaller than in scenario A. In other words, the weight values are not directly encoded, but are implicitly derived from functions of other parameters.

2.4 Summary

This chapter began with an overview of the nervous system, describing its constituent components, the *neuron* and the *synapse*. It was explained how artificial neural networks composed of 'units' and connection 'weights' can be used to model neural systems. In explaining these, an example of how a network might control an artificial agent moving around in a virtual environment was provided, since, note, the models developed in this thesis are all based on artificial agents. Neuroevolution was then introduced as a means to 'evolve' the network. Direct and indirect encoding schemes were introduced with the latter being cited as the more biologically plausible given its development centric nature. Kitano's grammar based approach and Gruau's cellular encoding scheme (amongst others) were identified as examples. Finally, two examples of implicit encoding schemes were given. Firstly, a 'toy' example in which connection weights are derived according to interneuronal euclidean distance; secondly, AGE in which weights are dervied from functions of parts of the genotype.

Chapter 3

Related Biological Background

Synopsis

This chapter sets out to provide the biological context and motivational grounding for the experiments undertaken in Parts II and III of this thesis. Accordingly, it goes into some depth explaining, with regards to evolutionary transitions, the intricacies of neural organisation. Thus, the first point of focus explores theories and literature outlining the evolutionary transition of *symmetry breaking*, the theory that radially symmetric organisms evolved a more advanced bilateral symmetry; a focus is placed on the commensurate changes to the nervous system. Essentially, the literature exemplifies how in a given animal, the nervous system is strongly coupled to its body plan morphology. Both the jellyfish and flatworm are introduced as examples of radial and bilateral organisms respectively since these are considered baseline in neural organisation (these two organisms also provide motivational grounding for the models described in later chapters). The second point of focus presented in Section 3.3 considers how, in terms of the wire length and metabolism, energy is a constraining resource in the evolution of neural organisation. This idea is further expanded upon and investigated in Part III of this thesis.

3.1 Evolutionary transitions

Survivability is the fundamental hallmark of a well adapted organism. Even with slight environmental perturbation, the organism is able to reproduce successfully and pass on its genetic characteristics. This of course is evolution in a nutshell. Yet the ability for an organism to

survive is progressively shaped by the niche that it finds itself in; a jellyfish, for example, survives in an aquatic environment because of millions of years of evolutionary refinement and would not survive if it were suddenly removed and placed elsewhere. Likewise, a giraffe would probably not survive if trees – and tall ones at that – were to suddenly vanish. Organisms survive because environmental selection pressures have resulted in evolution selecting in favour of particular traits.

Arguably the most important trait of a given animal is its body shape since this firstly potentiates some ability for the animal to fit in and act correctly in the environment. It can be thought of as an interface residing between the animal's need to survive, and the environment. At the same time, in order that the body can be made to successfully interact with the environment, the animal has to have an effective control system – a nervous system; without it, the body, no matter how carefully crafted, would be useless. These two aspects evolve together in a highly coupled manner, so that a change in one invariably results in a commensurate change in the other. Consequently, during certain moments or periods of evolution whereby the genetic makeup of the animal underwent drastic changes, so called *evolutionary transitions,* adaptations in nervous system architecture, went hand in hand with adaptations in body plan morphology (e.g. [5]).

Such body plan morphologies revolve around types of symmetry with *radial* and *bilateral* being the two core types, Fig. 3.1. In animals having these types of symmetry, the nervous systems are architecturally distinct given that they are coupled to their respective body plans in distinctive manners. For example, the jellyfish which has a radially symmetric body plan has a two dimensional and highly diffuse nerve net whilst in bilaterally symmetric organisms such as the flatworm, the nervous system is far more organised having distinct brain-like regions. In the literature, there is often conflicting evidence regarding which type of organism came first; clearly both the jellyfish and flatworm have been evolving for millions of years, both symmetries have a distinct place in nature. Yet at some point during evolutionary history, some environmental constraint emerged that made it advantageous for certain animals to become bilaterally symmetric. Hence the evolutionary process that resulted in a change in body plan symmetry – *symmetry breaking* – together with a coupled adaptation in nervous system architecture is often cited (e.g. [40]) as being fundamental in early evolutionary transitions of neural organisation.

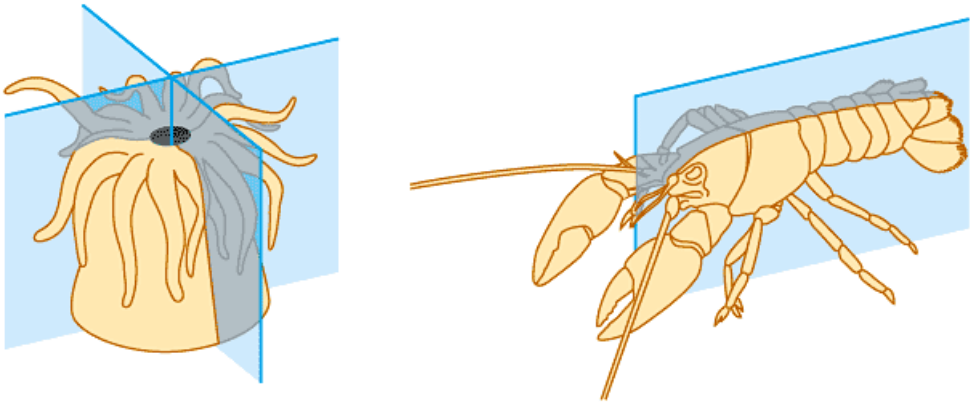

(a) Radial (b) Bilateral

Figure 3.1: A comparison of body-symmetries (©Pearson Education Inc., publishing as Benjamin Cummings). In radially symmetric organisms, a mirror plane can be turned 360^o along a single pole of symmetry. By comparison, in bilateral animals, a mirror plane splits the animal into two halves.

3.2 Body symmetry

At some point during evolutionary history, bilateral organisation emerged as an advantage. This organisation is in contrast to cnidarian which exhibits only one pole of symmetry (an oral-aboral axis), meaning that a mirror plane running through the pole can be turned 360^o with the result being mirrored symmetry at all angles. In contrast, bilateral symmetry is physiologically characterised by the presence of a dorso-ventral axis and an anterior-posterior axis (e.g. [72]), thus, the process that led to the emergence of this axis development is key in understanding bilateral organisation, and the evolution thereof [82]. Bilaterian organisms are also characterised by their triploblasty (they have three germ layers; cnidaria are diploblastic, having only two) [77].

It is important to understand the emergence of the (primitive) body plan because the nervous system is heavily coupled to it; to understand evolutionary transitions of body plan morphologies is to understand evolutionary transitions of nervous systems. However, because of the inherent physiological properties of a nervous system, we must keep in mind that some aspects will always be 'emerged novelties' [51], nevertheless, any major evolutionary transition of nervous systems beyond such plastic lifetime effects would have been commensurate with change in body plan morphology. An example is how the formation of a dorso-ventral axis in Bilateria is actually a precondition for a central nervous system [82]. More simple is the

invertebrate *Hydra*[1]; indeed most literature considers a hydra-like animal to be the common ancestor of both extant Cnidaria and Bilateria, e.g. [40]. It therefore serves as an excellent model organism.

3.2.1 Phylum Cnidaria

Together with the advantage of being considered ancestrally common to the Radiata and Bilateria, the Hydra and the Cnidaria in general are cited as good model organisms for studying nervous system evolution [74, 63] because of their well understood primitive diploblasty, diffuse nerve net and radial symmetry. Furthermore, in the case of Hydra, nerve cells are coupled to the body plan morphology in every sense of the word: the epithelial cells undergo continuous movement and since the nerve cells reside within the epithelial tissue, they too are constantly displaced [63]. And on a molecular level, experimental evidence indicates that nerve cells within the Hydra become differentiated in very region-specific manners (e.g. [17, 65, 66, 16]) and of course, region is defined by the body itself. At a lower level, the nerves themselves are also regarded as primitive given their ability to propagate signals bidirectionally (*amacrine process*), and further have no distinguishable axonal or dendritic processes [116].

3.2.2 Emergence of bilateral organisation

Given the above evidence, more advanced bilateral organisation and indeed more advanced neural organisation is supposed to have emerged as a condition secondary to the Cnidaria (e.g. [4]), with the flatworm often regarded as basal in bilaterian organisation [100]. At the more advanced end of the spectrum is the vertebrate organism *agnathan*, a type of lamprey, which is basal with regard to neuromeres (embryonic compartments or segmented units) [86][2]. Note however, that whether bilaterian body plans emerged out of cnidarian body plans or vice-versa is conjectural at best [33], especially if we consider how some Radiata exhibit biradial symmetry (e.g. the *Ctenephora* or comb-jellies), if not actual bilateral symmetry [77]. The debate is expansive and beyond the scope of this thesis. Also, we must always keep in mind

[1]The Hydra is a radially symmetric organism of the class *Hydrozoa* and phylum *Cnidaria*. The Cnidaria also comprises the *Anthozoa* (sea anenomes and corals) and the *Scyphozoa* (jellyfish).

[2]The lamprey is a very interesting study organism because its central pattern generating neural dynamics are well understood and established (e.g. [46]). We will therefore pick up on the lamprey as a model organism at a later point.

that evolution can hone in on particular design principles and traits that are functionally useful even if they have emerged along different lineages; in other words, evolution may converge on common design principles [90].

It is generally accepted that bilateral body symmetry is a complex property that at some point emerged during evolution. And given the propensity of arguments suggesting that the common ancestor *was* hydra-like, many evolutionary and developmental biologists have turned to the Hydra as a "living fossil" which can be used to elucidate the *how* and the *why* of nervous system evolution. In doing so, an abundance of common genetic markers present in both Hydra and more advanced Bilateria have been identified; this is indicative of genetic similarity [82]. It is known for example, that certain gene complexes – most notably, so called *homeobox* genes – are present in all metazoan organisms [108] (yet some are also bilaterian inventions [97]); for example, the gene *cyngsc* which is present in Hydra, is homologous to *goosecoid,* a gene found in bilaterians, responsible for axis formation and axial patterning [23]. Further genetic similarities have also been found in terms of the number of germ layers [114] and in terms of head formation [84]. Physiological evidence also indicates similarities in sensory systems and neuronal pathways [99][60]. In sum, these molecular and physiological studies exemplify an abundance of *genetic conservation* [50].

Genetic conservation Genetic conservation fundamentally implies that features have been maintained over successive evolutionary generations because of their fitness-enhancing properties. This implies that body plan morphology and neural circuitry, and the coupling between, has emerged in a way that is robust; the jellyfish and flatworm are robust to their own particular niches, given that none of their principle features – radial/bilateral symmetry and diffuse/organised nerve net – have been lost. In line with this, Ghysen [45] explains how, in order for different "life-forms, lifestyles and habitats" to emerge, neural circuits previously attained during evolution need to be robust so that their overall functional coherence can be maintained. In order to maintain this coherence, he explains, mutations occurring in the most genetically conserved parts of the animal's DNA need to be 'screened', so that problematic – in the sense of fitness depleting – changes within the genome can be prevented.

Genetic and developmental novelty In parallel to genetic conservation, different species can also maintain genetic novelty. For example, Bosch and Khalturin [21] found that Hydra have certain genes responsible for hydra-specific characteristics. Yet novelty can also come

about during development. For example, Katz [60] examines how the progressive acquisition of behaviour in the leech (swimming and crawling) is reflected by changes in neural circuitry given varying connection strengths. The sea cucumber *stichopus japanicus* is a further example. During life, it undergoes a very drastic change in body plan morphology and neural circuitry; it starts out as a symmetric larva but then later establishes penteradial symmetry [87] (a relative to this animal is the star-fish). Meinhardt [80] further suggests how axis formation in higher organisms might actually be the result of a self-organising process.

3.2.3 Theories for the transition

What evolutionary forces were instrumental in shaping the nervous system? What need is there that a certain animal should be elongated? These questions are crucial in understanding the transition from simple, radially symmetric organisms, to more advanced, bilaterally symmetric organisms (and the commensurate changes to the nervous system). Of course, we might turn towards fossil evidence, but this helps little in our understanding, since features of a given animal can only be observed once they have evolved [32]. Fossils only provide records of emerged features. Fortunately, we can turn to extant organisms such as the Hydra and flatworm, and based on gene homologues, theoretical frameworks and models can be constructed which attempt to underpin the evolutionary processes and forces responsible (see [51] and [32] for comprehensive reviews). Many suggest an elongation of the organism out of functional necessity so that it might crawl – it is endowed with directional ability –, with for example, a commensurate build up of nerve tissue in half of the animal ("polyp with a half nerve net scenario" attributed to Lacalli [67]). Directional ability is heavily regarded to be the main driving force of neural organisation in the flatworm [101]. The nerve cord might also be derived from the nerve ring of Cnidaria – Koizumi [64] has postulated that the nerve ring of Hydra might be a primitive central nervous system and Mackie [74] considers the nerve ring of more advanced *aglantha* jellyfish to be a central nervous system. Whatever the theory, it is clear that the nervous system is heavily coupled to the body plan morphology.

3.3 Energy and efficiency

It is conjectured that the architecture of a nervous system is shaped by body plan morphology. Along with this, it needs to provide functional advantage. Yet, if the organism is to evolve,

it needs to live in an energy efficient manner; it needs to conserve a certain level of energy if it is to survive. Therefore, not only does the neural architecture need to optimally fit with the body plan morphology, it also needs to be wired – and needs to operate – in a way that conserves energy. The ability to process information efficiently can be observed at all levels of variation, from the single cell [39] to the multicellular Hydra, in which nerve cells are proximal to the tentacles and therefore located such that they are more functionally 'useful', e.g. [64].

Cost-effective information processing was suggested as the evolutionary driving force in [8]. The recent study by Niven et al. [93, 94] on fly photoreceptors was one of the first to analyse the balance between energy costs and performance in the evolution of nervous systems. One of the interesting conclusions is that the fixed cost of maintaining a cell ready to signal increases with its maximum information rate. Thus, even if the improved functionality is not used or required, it has to be paid for if it is available. Another argument is that selection pressure has likely arisen from a need to minimise energy consumption [121, 122]. This is also supported by the observation of decreasing brain size and complexity [92] when the need for this evolutionary trait diminishes. Often also is the assumption that evolution drove a minimisation of conduction delays in axons, passive cable attenuation in dendrites, and the wire length [26]. Interestingly, it has been suggested that efficiency maximisation and energy minimisation together may be responsible for the small-world characteristics [124] of the larger-classed brain networks [8].

Wire length The longer a piece of wire, the more energy it will lose. Thus, the longer the neuritic process connecting two neurons, or the further a spike has to propagate to get to a target destination, the more energy expended as a result. In terms of development, Chen et al. [25] explore the possibility that laying down 'wire' is energetically expensive; thus, it is proposed that evolution economises via a minimisation of wire length. Optimal wire length may also reduce metabolic costs [68]. The total energy cost can be formulated as follows ([25, 26, 27])

$$C^{tot} = C^{int} + C^{ext} \tag{3.1}$$

in which the total cost C^{tot}, is equal to the internal cost, C^{int} (connections between neurons), added to the external cost, C^{ext} (connections between neurons and peripheral devices like

sensors and effectors). The internal cost is calculated as

$$C^{int} = \frac{1}{2\alpha}\sum_i\sum_j A_{ij}\,|x_i - x_j|^{\zeta} \tag{3.2}$$

where matrix A represents connectivity between neurons i and j, and x_i and x_j are neuron locations. The parameter α is an unknown coefficient but is typically proportional to the number of synapses between two neurons; ζ is typically set to 2 [25]. The external cost is then similarly calculated as,

$$C^{ext} = \sum_i\sum_k S_{ik}\,|x_i - s_k|^{\zeta} + \frac{1}{\alpha}\sum_i\sum_l M_{il}\,|x_i - m_l|^{\zeta} \tag{3.3}$$

where matrices S and M are representative of connections from neurons to sensors and motors respectively. Chen et al. and Chklovskii [25, 27] independently show via a minimisation of such a cost, that the layout of a model of 279 non-pharyngeal neurons of the *Caenorhabditis elegans* closely matches biological data. This highlights the importance of wire length in an energy conserving framework.

Metabolism A further important factor concerning energy cost is metabolism; in terms of neural processing, this equates to the amount of energy expended during the computational efforts of the neural system. In [68], it is found that even during rest, neural processing is metabolically expensive with a significant 20% of total energy consumed by the brain during a resting state. A further example is the fly, in which consumption of energy in bright light due to the activity of the fly's photoreceptors *alone* is 8% of the total energy consumption. Both of these proportions are significant [68]. In related work, Olshausen and Field [96] consider how sparse coding of sensory input can be energy saving given lower firing rates of the sensory neurons, i.e. less neural activity.

3.4 Summary and Conclusion

This chapter began by elucidating the need to understand the evolution of body plan morphology; that, if we are to understand the evolution of the nervous system, we need to examine body plan morphology transitions, given the tight coupling between both. This was presented in terms of the evolutionary transition from radial symmetry to bilateral symmetry.

Literature was then presented describing how, given the vast number of genetic homologues between species, neural organisation must have evolved from a common ancestor which was likely to have been hydra-like; further, that neural circuits have likely evolved in a way that is both robust (due to genetic conservation) and efficient. Several biological theories were then given, to outline how evolution may have progressed from simple to more advanced organisms. Finally, energy conservation as a driving factor in the evolutionary process, with a focus on the minimisation of wire length, was further presented.

In conclusion, the importance of the couplings existing between the body plan morphology, its symmetry, and the nervous system was firstly clarified; further, a need to untangle precisely why these couplings emerged was highlighted. Later in this thesis, several methodologies set out to explicate this 'why?': computational models of primitive organisms are introduced and described. These models principally feature nervous system abstractions spatially constrained by abstract body plan morphologies. Thus conceptually, it will be demonstrated how architecture – being at the fore of our understanding – influences neural dynamics, the dynamics of the motor system, and ultimately the behaviour of the agent.

The significance of energy as a constraining factor on the evolutionary emergence of neural architecture was secondly introduced, with literature concerning wire length and metabolism. It can be argued that on account of this literature, current methodologies are perhaps 'lacking'. Typically, they only consider 'static' neural network treatments without considering any kind of online agent behaviour, the effect of body morphology and moreover nor do they consider the effect of environmental selection pressure. Thus many of the pictures presented by current studies might benefit if they also consider such unexplored properties and processes. The investigations presented in this thesis aim to fill in some of these gaps: models incorporating a more diverse range of features including body morphology, body symmetry, and energy are accordingly brought forward in later chapters.

Chapter 4

Towards Models of Primitive Organisms

Synopsis

The core aim of this thesis is to shed light on how, in models of primitive organisms, neural organisation should emerge when constraints of the body and the constraint of energy conservation are taken into consideration. Having discussed in the prior chapter how these processes are heavily coupled, it is important to think about modelling neural organisation in similar terms - that of body plan–nervous system couplings, the behaviour that should ensue, evolutionary selection pressure, and, the actual types of organism that we can base our models upon; we also need to think in terms of computational neuroethology [30] since behaviour is core to the evolutionary process. This chapter therefore begins with an overview of the Hydra and related models, since this organism is considered basal in nervous system evolution and is further used as the basis for a model introduced in Chapter 8. An overview of models of bilaterally symmetric organisms with an emphasis on biophysically realistic undulatory behaviour is then given. The Evo-Critter agent which is used to assess body plan and nervous system couplings (see Chapter 5) is based on the same type of undulatory behaviour.

4.1 The Hydra

The Hydra is often regarded as basal in nervous system and body plan evolution [73]. Because of this, it serves as an excellent basis in modelling an evolutionarily early stage of the nervous system. The genus Hydra is a freshwater organism of the phylum *Cnidaria* and of the class *Hydrozoa*, and for the most part maintains a sessile lifestyle. It is characterised by

its diploblasty, radial symmetry and diffuse nervous system architecture, see Fig. 4.1. It also utilises tentacles to sting, paralyse and capture zooplanktic prey. The nervous system itself is diffuse with nerve cells residing within the epithelial tissue, however, denser aggregations of nerve cells also reside around the hypostomal (mouth) region and pedal disc (foot) region; see for example [63, 116]. These cells become differentiated from interstitial precursor cells in a position dependent manner, for example, cells near to the hypostome may differentiate to become sensory cells [83, 16, 14, 17]. The Hydra also maintains remarkable tissue dynamics: during its lifetime, the epithelial cells undergo constant migration eventually becoming sloughed off at the body extremities [15]. Peripheral nerve cells are then also lost because of their presence within the epithelial tissue. Interstitial cells then differentiate to replace them.

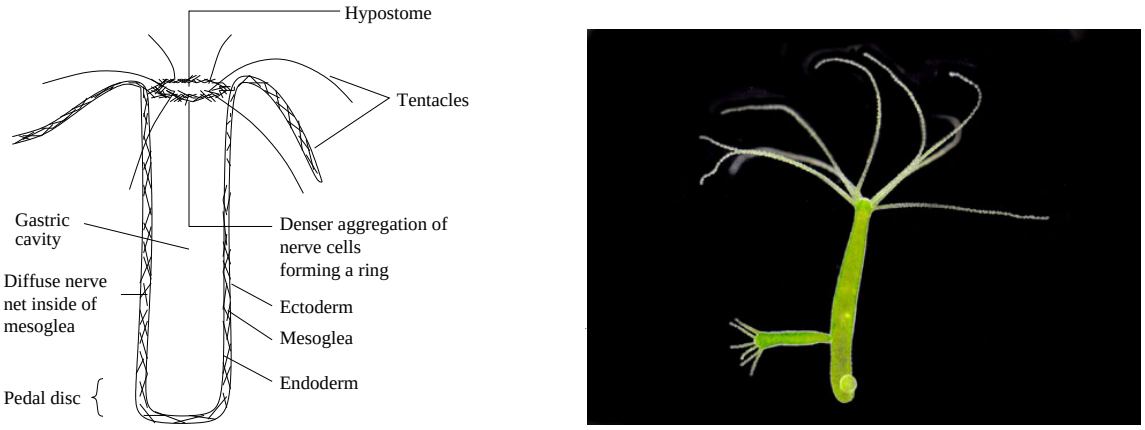

Figure 4.1: A diagram of Hydra (left) and a photo of green Hydra (right) (photo © Peter J. Bryant http://nathistoc.bio.uci.edu/Cnidaria/HydraV.htm)

In terms of a computational model, Albert [3, 1, 2] was the first to construct an agent resembling a Hydra, in which a tube would have to react to food particles falling from the top of a virtual aquatic environment. His motivation was to emulate an early stage of neural evolution, namely, the stage at which the nervous system emerged from a non-nervous sponge or *porifera-type* ancestor. At no stage did this model incorporate an evolutionary process; Albert was only interested in a snapshot of evolutionary history. The model also incorporated epithelial conduction since this is utilised by the sponge [70], yet is also known to be part of the Hydra's neuro-anatomy [75]. Neural and muscle cell models were further incorporated. Connections would then be formed between neurons according to number and lengths of potential partner cells and processes. The tube would then be able to undertake basic movements given stimulus thresholds within the muscle cells; the most successful individuals

were those that could catch the most pieces of food. A main finding was that fitness could be increased by having a larger number of nerve cells, and, above a certain number of nerve cells, by lengthening the allowed connections. This demonstrates the advantage of having a nervous system alone, before even considering the specifics of its organisation. A depiction of Albert's simulation environment is provided in Fig. 4.2 and a diagram of the agent's cellular histology is given in Fig. 4.3. The work reported in the first half of Chapter 8, is based on the work of Albert yet further incorporates evolution and a novel energy measure abstraction (also see [59]).

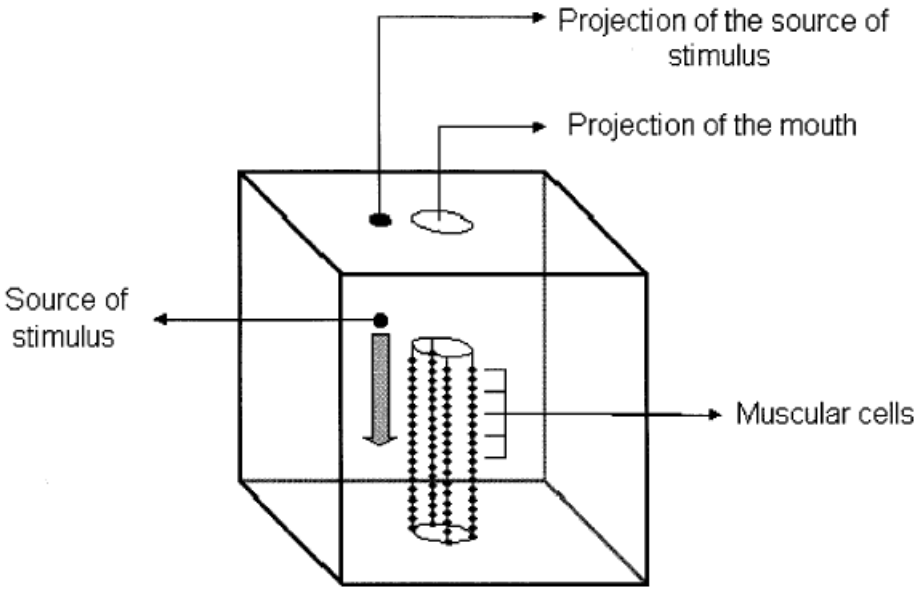

Figure 4.2: The simulation environment developed by Albert which sets out to model a Hydra (Figure 3 of [1]). The agent is tasked with catching food particles falling from the top of the environment.

Schramm et al. [55] further model the neurogenetic processes of Hydra, basing the developmental program on a genetic regulatory network (GRN) originally developed in [105]. The model permits basic cellular events – *cell growth*, *cell migration* and *axon growth;* thus the GRN is evolved until the correct ordering of events ((i) cell growth, (ii) cell migration, (iii) cell differentiation, (iv) connection formation [63]) can be established. The weights and connectivity of the network are further evolved for a food catching task.

The work of Leung and Berzins [69] considers a model of organism growth based on surface mesh generation. Their approach uses meshes to generate "geometries associated

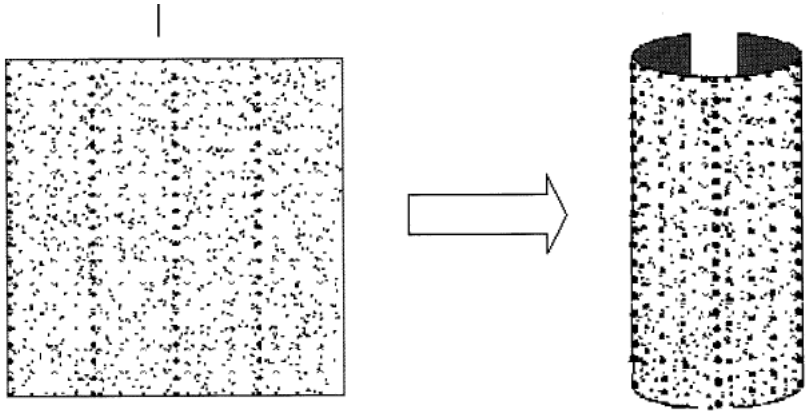

Figure 4.3: A diagram of the histology of the model developed by Albert (adapted from Figure 1 of [1]). As shown, a cellular matrix is embedded into the agent's skin which then gets 'wrapped' around to form a cylindrical geometry.

with biological forms or organisms"; it works via an abstract notion of morphogens which serve to identify precisely where components of the mesh should be deformed. Their aim was to evolve morphologies for models of organisms including Hydra with the eventual aim of investigating morphological symmetry breaking. Some visualisations of their work are given in Fig. 4.4.

4.2 Modeling bilateral organisms

A core interest of the research presented in this thesis regards body plan morphology and nervous system couplings in both the 'simplest' radially symmetric organisms and in the more 'advanced' bilaterally symmetric organisms. As an example of a radially symmetric organism, the Hydra has already been discussed above. In terms of bilaterally symmetric organisms, as mentioned in Chapter 3, the platyhelminthe (flatworm) is often cited to be baseline [100]. Problematically however, the flatworm's movement kinematics ('pedal locomotion') are very difficult to model; yet, an accurate representation of behaviour is essential if we are to understand how body plan morphology, neural system and environment become coupled together. And so we must turn to something *simpler*, a form of locomotion that *is* well understood, even if not principally the type employed by the simpler of bilaterian invertebrates. Provided that we can still use it to study principles of neural organisation and nervous system body plan couplings, it will suffice.

A simpler type of locomotion that *is* well understood, is *undulatory.* In undulatory loco-

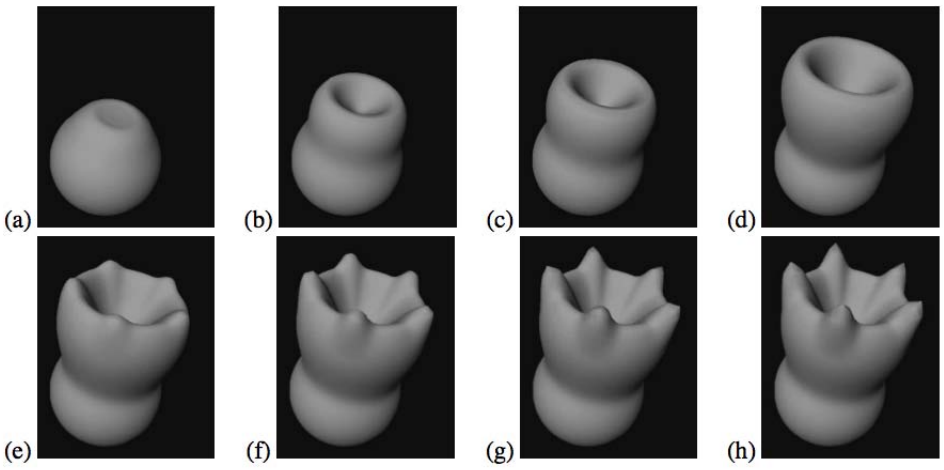

Figure 4.4: Example development in Leung and Berzins model of organism body morphogenesis showing how a Hydra-like body can be constructed in stages from an initial 'blastula' sphere (Figure 9 of [69]).

motion, a wave of contraction commencing at the head of the animal propagates towards the tail where its amplitude is greatest. The animal therefore uses its whole body in generating thrust and not just a part of it [85]. A common example of an animal seen to utilise undulatory locomotion is the eel, the mechanics of which have been extensively explored by Müller [85], who demonstrated how several flow fields are generated around the eel as it propels itself forwards. Gillis [46] also explains how "the size and shape of the animal can affect the nature of the propulsive forces generated during undulatory locomotion". Thus, for a given animal, the evolutionary advantage of having certain body characteristics is paramount to its survivability.

Many models address the underlying physical mechanics of undulatory locomotion. The agents central to these models are typically immersed in virtual 'water', so that their ability to swim can be analysed. In the context of an evolutionary scenario, the agent's fitness is often attributed to the distance that it can swim. We will first explore undulatory locomotion models motivated by biophysical realism; secondly, artificial life models of the Karl Sims [109] variety will be introduced.

4.2.1 Biophysical models

Many of the undulatory locomotion models focus on two dimensional abstractions of lamprey with an emphasis placed on biophysical realism. In the earliest examples, neural control cir-

cuits were typically hand-coded to reflect true lamprey central pattern generators and data gathered from real-life experiments. Most prominent is the work of Ekeberg [36, 37, 38] whose models are comparable to pharmacological data. Implementation-wise, they utilise a set of rigid links connected by joints and springs, see Fig. 4.5. Each link is actuated by a neural circuit which, via the alteration of a spring constant, controls the level of permitted spring distension; the circuits are also endowed with sensory feedback via 'stretch receptors'. Ekeberg's findings were comparable to undulatory behaviour in real lamprey; but interestingly, he also found that the amplitude of the undulatory wave, from the head to the tail, increases as a result of the body kinematics and not as a result of the neural system [36]. In other words, the passive body dynamics are utilised in attaining optimal behaviour. A visualisation of a model based on Ekeberg's is shown in Fig. 4.6.

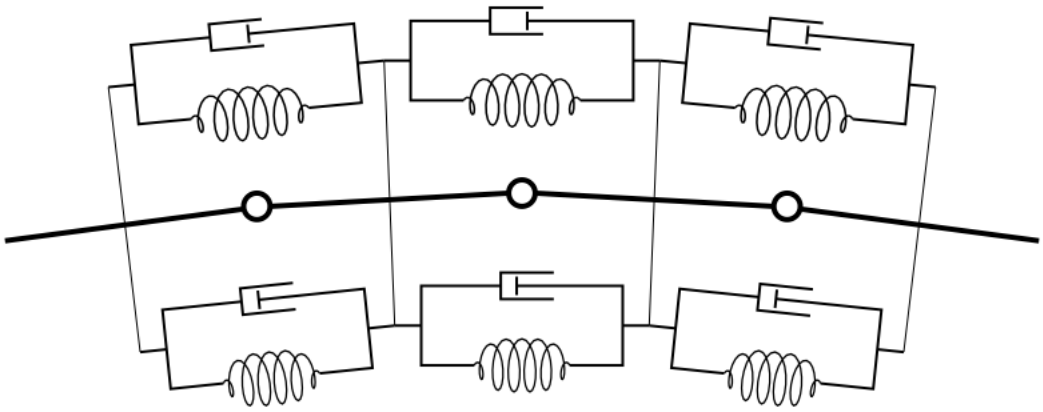

Figure 4.5: The physical construction employed by Ekeberg and others in the modeling of an undulatory organism, showing how a chain of rigid links are controlled by a set of springs (taken from Fig. 2 of [37]).

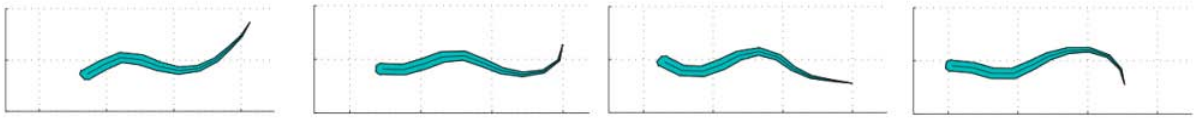

Figure 4.6: An example two dimensional biophysical model of a lamprey of the type employed by Ekeberg and Ijspeert shown at successive behavioural time-steps to move from right to left (adapted from Figure 3 of [54]).

The work of Ekeberg was then extended by Ijspeert et al. [54] who incorporated a genetic

algorithm (GA), for the purpose of optimising the neural controller. Their motivation was to find out whether controllers trained by the GA would function as well as the hand-coded controller developed by Ekeberg. This GA worked in three phases: **(a)** the evolution of a segmental oscillator in isolation, since they argued, biological CPGs are known to oscillate in isolation (also see [76]); these segmental oscillators would then be replicated for each body segment (actuated link), thus the parameter space of the GA could be drastically reduced; **(b)** evolution of connections between a set of segmental oscillators; **(c)** evolution of sensory feedback from stretch-sensitive cells noting from Ekeberg's experiments that agents having feedback would swim more efficiently. Their findings did indeed demonstrate that the GA would find successful controllers.

Ijspeert and Kodjabachian [52] later incorporated a developmental process employing 'Simple Geometry Oriented Cellular Encoding' (SGOCE)[62] [24]. SGOCE is based on Gruau's cellular encoding scheme [48] but has the addition that geometry constrains neuronal connectivity. Primarily, their findings demonstrate how a variety of CPG controllers can be evolved and developed. A less crucial finding is how agents would always evolve to have some 'residual' fitness, even in those without properly evolved CPG circuits; this was found to be due to all agents having initial body contortions which would have the effect of 'pushing' the agent slightly forwards.

Grillner et al. [47] have realistically implemented a model lamprey, relying on models of spinal CPGs, sensory mechanisms, a postural control system (pitch and head tilt), and a command system to initialise locomotion. The model captures both the realism of spiking neural dynamics and the realism of biophysical locomotion. However, it lacks an evolutionary mechanism.

On related tracks, Sfakiotakis and Tsakiris [107] developed Simuun for the simulation of snake-like mechanisms, a toolbox built around Simulink[1]. Their motivation was to develop a tool that can be used for biologically grounded and computational neuroethological studies. Ijspeert and Arbib [53] developed a mechanical model of a salamander capable of locomoting on both land and water, featuring a neural control system and novel vision-based control circuit. Their study highlights the effect of body movement in terms of its influence on perception. A further aim of their study was to shed light on the central nervous system of vertebrates, and its relationship to body kinematics. Terzopoules et al. [118, 119] constructed three dimensional artificial fishes using soft bodied spring systems, with novel features such as

[1]See http://www.mathworks.co.uk/products/simulink/

perception and foveated retinal image streams. Although highly advanced, this work lacked any neural control mechanism; nevertheless, it demonstrated a richness and diversity in the types of behaviour that could emerge (predator prey relationships, fish-schooling etc.).

4.2.2 Karl Sims models and other solid body approaches

In his seminal work on the coevolution of creature morphology and neural control, Karl Sims [110] built physically realistic three dimensional models of 'creatures' constructed out of solid units - blocks and spheres and rods, etc., that would operate in highly physically realistic environments obeying such laws as gravity. Many have taken his solid body representation in inspiration for their own simulation environments, whilst asking questions that have mostly concerned the coevolution of 'brain' and 'body'; this field is often referred to as *embodied cognition.* Although these models were not developed for the sole purpose of studying undulatory locomotion, they can still be used to successfully do so. Therefore, we may refer to models having simulation environments similar to that employed by Karl Sims as 'Karl Sims style models'. They differ from the simpler two dimensional models in terms of the physical representation but more importantly they also attempt to broach the issue of creature morphology, with 'creatures' that are not always biologically realistic but always physically possible. A good review of such models is provided in [117].

Towards morphology and control Crucially, the solid body approach to agent modelling adopted by Karl Sims can be used in the investigation of creature morphology and control. One pitfall of the simpler two dimensional biophysical models introduced above is that their body plan characteristics are statically defined. Thus some of the more interesting investigations involving coevolution of body plan morphology and neural control are not possible with these models. In comparison, the large variety of coevolved configurations made possible by Sims' models, allows for behaviours such as swimming, jumping, and running [110], see Fig. 4.7. In the Sims genotype, several parameters including joint type, part dimensions, and part positions in relation to connected parts, are encoded. For the neural system, abstract neuron types implemented as logical functions (*sum, min, max, sum-threshold, abs,* etc.) and connectivity between them are also represented. Sensors and effectors remain position fixed. A sensor measures aspects of the world relative to the part that it belongs to, or, in the case of an effector, a particular joint is actuated. In terms of swimming behaviour (which is what we are primarily interested in), many combined creature morphologies and controllers can be

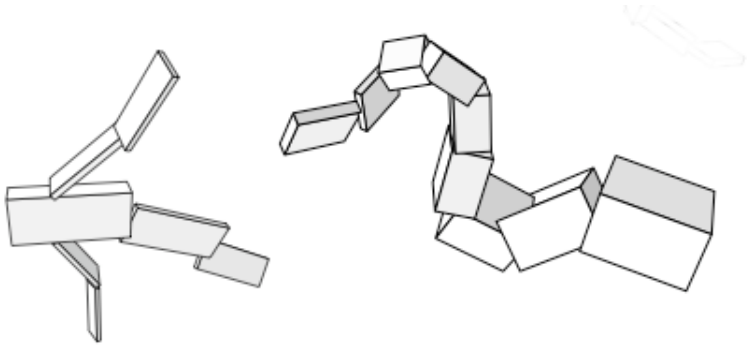

Figure 4.7: Examples of swimmers evolved by Karl Sims. The rightmost has apparent undulatory locomotion. (Taken from Figure 6 of [110]).

evolved with some of the agents exhibiting undulatory behaviour (see Fig. 4.7).

The work of Taylor and Massey [117] replicates the work of Sims, but primarily focuses on the evolution of creatures optimised for swimming. An interesting discussion about the importance of having an adequate fitness function is also provided. This goes as follows: a higher number of behavioural iterations used during the evaluation process requires more computational overhead; yet, there is a trade-off between too much overhead and too little. If the computational time is too short, the evolutionary process may result in creatures getting stuck in local optima. Also, because of numerical inconsistencies and implementational artifacts, creatures might 'fold over', 'twist around', or 'explode'. All of these factors, they argue, have to be taken into account. One useful suggestion is that simulations can be aborted early if such artifacts are detected. Indeed, this methodology is successfully incorporated into the Evo-Critter framework (see Chapter 5).

Further is the work of Bongard [18, 19] who has explored in detail the coevolution of creature morphology and control. Together with Pfeifer, he models an artificial ontogeny, developing agents operating in a physically realistic environment [18]. The agents are constructed out of spheres which serve as the main structural units. If and when these units reach a certain size, they split into two – a reflection of organism growth. Neuron units include 'sensory', 'motor', 'internal', 'bias' and 'oscillatory', providing for a variety of control architectures. Growth gene products determine where 'child' units connect to 'parent' units. The genome is treated as a genetic regulatory network and cellular encoding [48] is used for the neural network; weights and connections are defined by virtual gene products. In simulation, they discover how a body axis will evolve in a target-dictated direction and loco-

motion towards this target proceeds with waves of oscillation occurring along the body axis. A more crucial finding is that modification to creature morphology alone is often sufficient in significantly enhancing fitness.

Finally, some very exciting yet still preliminary work is that being developed by Schramm et al. [106] who apply a genetic regulatory network in the evolution of body plan morphology of a locomoting agent. The body plan is constructed out of individual spheres, analogous to biological cells, with springs connecting them. These cells can then replicate or die as seen fit by the evolutionary process. The movement mechanism works by alternating the natural resting lengths of the lateral, outer springs, to one of two values, with a periodicity defined by an evolved parameter. Using this setup, a variety of animats capable of both undulatory and peristaltic forms of locomotion can be evolved (peristaltic being the form of locomotion observed in the caterpillar); crucially, this exemplifies a direct coupling between the control mechanism and the body plan morphology. An example visualisation showing such an agent having undulatory locomotion is given in Fig. 4.8. In future work, they hope to replace the rudimentary control mechanism with a neural network (e.g., a CTRNN), together with a neural growth process.

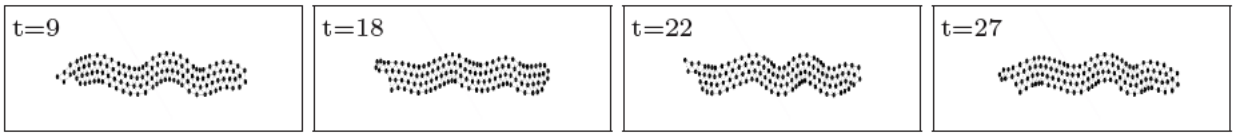

Figure 4.8: A sequence of behavioural iterations for one of the animats developed by Schramm et al. showing an agent constructed out of spheres and rods locomoting from left to right (taken from Figure 7 of [106]).

4.3 Summary and Conclusions

This chapter began with a description of Hydra, the freshwater jellyfish organism regarded as baseline in primitive neural organisation. A few studies exemplifying its use as a model organism were then described, with the work of Albert outlined as the most significant. The process of modeling bilaterally symmetric organisms was secondly discussed. In line with this, the flatworm was identified as a model organism but the difficulty in modeling its pedal locomotion was highlighted as problematic. Undulatory locomotion was therefore proposed as a much simpler and far better understood locomotion mechanism. Biophysical models

with an emphasis on reflecting real biological organisms (e.g. the lamprey or salamander) were thus initially described. Secondly, artificial life models of the type proposed by Karl Sims were introduced as ideal tools for studying embodied cognition.

In conclusion, several models investigate neural organisation and the coupling to body plan morphology at a variety of levels of abstraction. However, on a spatial level, many of them fail to address how the nervous system should emerge in concert with the body plan morphology and body symmetry and thus fail to wholly explain the drive towards optimal agent behaviour. Moreover, they fail to exemplify how on an evolutionary time-scale, certain types of body characteristic, for example symmetry, should emerge at various points of evolution ('points of transition'). Many of the studies fail to address how the environment should shape these couplings – why is it that a certain body plan–neural architecture combination should proliferate in a given environment? There is a need to understand this. Finally, as far as the author is aware, none of the studies address how a minimisation of energy loss (or alternatively its conservation) places constraint on the emergence of the couplings and the organisation of neural structure. However, if we are to understand the evolutionary emergence of neural organisation, there is a clear need to broach this.

Part II

A Model for Body and Nervous System Coevolution

Chapter 5

Evo-Critter: A Model of an Undulatory Organism

Synopsis

This chapter introduces Evo-Critter, a simulation environment designed to explore how the neural system and body plan morphology of an eel-like organism become architecturally coupled during a process of simulated evolution. A mechanically realistic agent serves as the eel-like organism (animat[1]) which is physically endowed with the potential to locomote (i.e., 'swim') in a particular direction; however, the underlying movement dynamics are not hardcoded but come about due to continuous refinements undertaken during an evolutionary process. These refinements concern the architecture of the neural system which is constrained by the shell of the animat body, the computational properties of the neural system (some of which are implicitly determined by the neural architecture), and certain features of the animat's body plan itself. Taken together, these different aspects present a richly coupled system of interacting components, an interaction that needs to be optimally tuned in order that optimal behaviour - in this case swimming - can be attained.

Models of undulatory locomotion have already been reviewed in Chapter 4. A distinction was made between two classes of model: those placing more of an emphasis on understanding biophysical processes, and those that are more concerned with behaviour that just looks like it could be *life-like* but has little biological grounding. We should understand that in Evo-Critter, the view is taken that both are important. On the one hand, physically

[1]**Note:** Throughout this thesis, *agent* and *animat* are used interchangeably.

realistic mechanisms are necessary since the agent needs to be appropriately constrained by the environment. On the other hand, *any* behaviour that emerges is important since this is what drives evolution. Thus the model is inspired by early two dimensional paradigms but also takes note from the three dimensional 'Karl Sims style' [109] creatures, since these are predominantly used in investigating morphology and control.

In answering the questions posited in Section 1.1 of the introductory chapter, Evo-Critter has formed a core part of the research described in this thesis. An example of an animat having been evolved is presented in Fig. 5.1. To begin with, some intuitive yet important background information on fish kinematics and morphology is given, after which the model itself is described in detail.

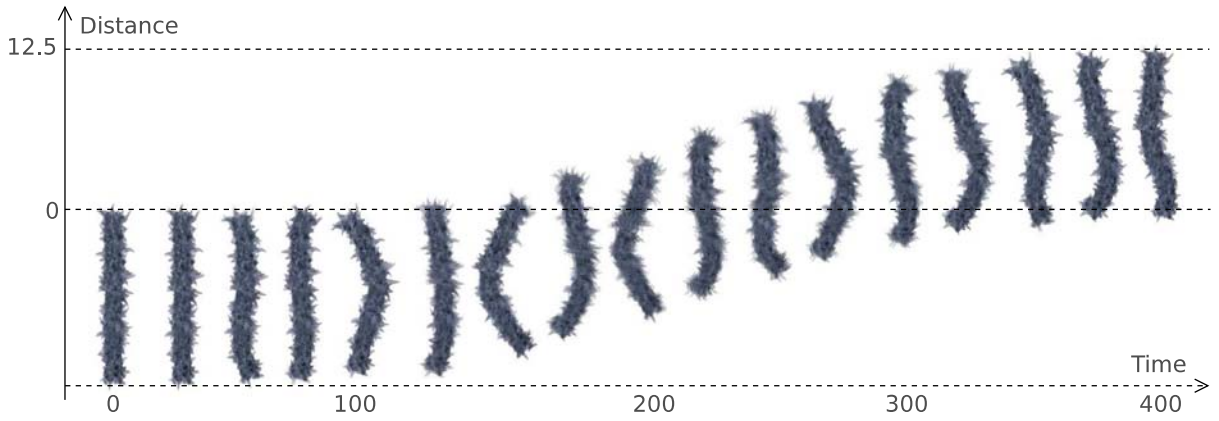

Figure 5.1: An example of an Evo-Critter agent swimming forwards via undulatory locomotion. Snapshots of the simulation environment are taken every 25 behavioural iterations.

5.1 Body mechanics

First of all, a fish will swim forwards because the oscillating movements of its tail generate thrust. However, its velocity is proportional to the amplitude and surface area of the beating tail, since this pushes against the water so is naturally opposed by it. Hence an evolutionary advantage of fish tail fins being flat and having a large surface area is apparent. We can then imagine how an aquatic organism's length will also govern the effectiveness of its swimming, since this will change the afore-described surface area and therefore the kinematics of its swimming behaviour. The *anguilliform anguilla* for example is long and elongated and resultantly utilises undulatory locomotion for its swimming behaviour, see Fig. 5.2.

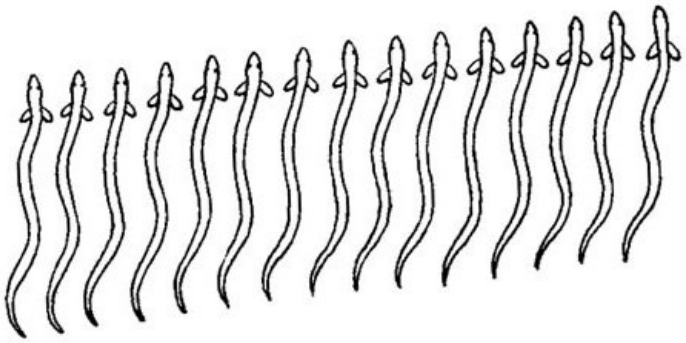

Figure 5.2: Undulatory locomotion of the type observed in the *anguilliform anguilla.* The animal is shown to move forward through time (Credit: Florida Museum of Natural History).

On the other hand, a non-anguilliform fish is less elongated and propels itself forward by beating its tail, with *carangiform* and *ostraciiform* types of locomotion being examples of this, see [46, 79, 120].

With kinematics in mind, differences in length of the animat's body plan are accounted for in the model. Furthermore, the animat is constrained to be segmented, since in all but the simplest organisms, segmentation or *metamerism* is argued to be generic in metazoan organisation, [88, 126].[2] Thus the model also incorporates the evolution of the number of body segments and the respective length of each segment, both of which will evolve out of functional necessity. Model individuals having a smaller number of segments might be expected to swim more like carangiform fish whilst those having a larger number of segments might be expected to exhibit more anguilliform type behaviour.

5.2 Simulation environment

For speed and efficiency, the simulation environment is implemented in C++ and consists of the animat geometry, the physics engine, the nervous system, and the evolutionary process. They are explained in the following subsections.

[2] As referenced in [126], Clark [29] discusses how segmentation may facilitate some types of behaviour, for example, undulatory locomotion, arguing that localised motor contractions are more energy efficient whilst also allowing sequential segment contraction.

5.2.1 Geometry

The animat is three dimensional, constructed out of 'points' and 'edges'. Edges are connected together to form 4-sided layers which are then connected to form cuboids ('body segments'). These cuboids are finally connected to form the overall elongated morphology, see Fig. 5.3. Although the layers are essentially two dimensional squares, they are constructed in a 'circular' (polygonal) fashion; this is for the sake of implementational convenience since historically, the individual layers were N-sided polygons (and squares are 4-sided polygons). The equations governing this initialisation are simply:

$$\begin{aligned} x &= \sin\left(\tfrac{\alpha\pi}{180}\right) \cdot r \\ z &= \cos\left(\tfrac{\alpha\pi}{180}\right) \cdot r \end{aligned} \tag{5.1}$$

where x and z are the geometrical coordinates of the point, α is the angle, and r is the radius (thus the first, second, third and fourth vertex points making up a layer are initialised with the angles 90°, 180°, 270° and 360° respectively). Further, the geometrical elements are initialised such that the layers are stacked in a vertical 'upright' configuration (i.e., head at the top, tail at the bottom); again, this is for implementational convenience. The radius r of a layer is calculated as

$$r = \frac{A/\omega}{1.5} \tag{5.2}$$

where A is the total length of the animat, set to 25, and ω is a width factor, set to 20.5. These values were empirically chosen during a testing and debugging phase in consideration of both the agent's elongation and, more crucially, in consideration of numerical stability; certain spring lengths would cause the agent's springs to become numerically unstable during its behaviour. The length of a segment is given by

$$S_i^{length} = \left(\frac{A}{0.5 \cdot (s+1)}\right) \cdot F_i \tag{5.3}$$

where s is the number of body segments within the integer range $[3, 4 \ldots 20]$ and F_i is a parameter that varies the length of the segment such that $0.2 \leqslant F_i \leqslant 2.0$. In the model, s and F_i are evolved parameters.

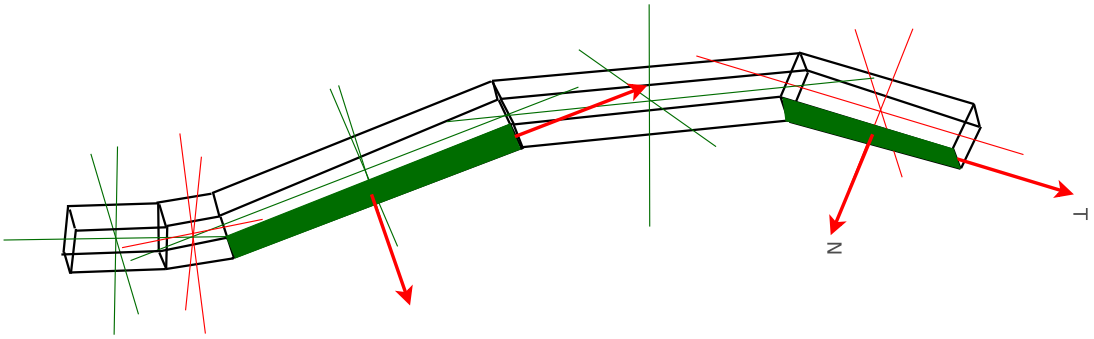

Figure 5.3: Agent geometry and highlighted water force model. Each animat segment has a 'compass system' which is used for deriving the directional components of opposing water forces. Two such faces have been filled in with green colour; example vector components used in calculating water force are highlighted with red arrows. 'T' represents the tangent component and 'N' represents the normal component.

5.2.2 Physics

All agent physics are handled by a mass-particle based physics engine, which has been implemented entirely from scratch. This is based on point masses and springs. In terms of the agent, each vertex point is secondly a point mass, and each edge is secondly a spring; thus the animat is shaped by a 'spring mesh'. The engine handles the agent's movements and how it should interact with the surrounding environment (friction or drag). This 'soft-bodied' approach is less complicated than a rigid body simulator which must consider more complex aspects, for example, collision detection; it is far easier to implement. To the best of the author's knowledge, there is only one other related piece of work that implements the overall construction of a 3D fish model in the form of a spring mesh, see [119].

In the model, three primary forces act upon the point masses. Firstly, the spring movements are subject to the internal forces of the connected point masses; a point mass has a velocity so is largely carried by its inherent momentum. Secondly, specific springs are subjected to forces because of neural system 'actuation'; this is the key way in which movement of the agent is realised. Thirdly, the springs are subjected to forces from the external environment. During a single time step, all forces are accumulated before being integrated.

Spring system Each spring in the model obeys Hooke's law. This states that,

$$\mathbf{F} = kdq\mathbf{X} \tag{5.4}$$

where $\mathbf{F}$ is a force vector, k is the spring constant set to 200, and d is the difference between the current spring length and the spring resting length; q is a dampener set to 0.4. The values k and q were empirically chosen for their numerical stability. Finally, $\mathbf{X}$ is the normalised vector between the two end point masses. A spring is thus compressed by applying equal but symmetric forces to each of the two end point masses, forcing them together. The point mass dynamics, namely acceleration $\mathbf{a}$, velocity $\mathbf{v}$ and position $\mathbf{p}$, are then integrated according to the following differentials:

$$\dot{\mathbf{a}} = \frac{\mathbf{A}}{m} \qquad \dot{\mathbf{v}} = \mathbf{a} \cdot \delta t \qquad \dot{\mathbf{p}} = \mathbf{v} \cdot \delta t \tag{5.5}$$

where $\mathbf{A}$ is a force accumulator which gets updated each time an internal or external force is to be applied; m is mass set to 5.0. Once all forces have been accumulated for all point masses, an integrator is applied in one sweep and the point mass positions are updated. The value δt is the integration timestep. Tuning this value alters the dynamics of the spring system: too small and the simulation takes too long; too big and the spring dynamics become unstable. In all simulations, it is set to 0.05. A simple Euler integration method is employed.

The water force model Given the environment, the animat succumbs to the friction or rather, the *drag* of the surrounding 'water'. In effect, this slows the animat down, ultimately affecting how it should locomote. External 'water force' pushes against each face of an animat segment, the magnitude of which depends on the opposing force of the face *pushing back*. It is sufficient to use the face's velocity as an approximate measure of this 'pushing-back' force magnitude, since, from this vector alone, the opposing water force can be computed. The face velocity is taken to be the average over all four constituent point mass velocities (one at each corner of the face). Note that this whole approach assumes that water is static with zero momentum. The approach is simple, reliable and efficient in its implementation and is further the approach taken by others (e.g. [107]).

In terms of the implementation, the face's velocity vector is initially split into two velocity components, the tangent component and the normal component (as highlighted in Fig. 5.3):

$$t = \hat{\mathbf{t}} \cdot \mathbf{v} \qquad\qquad n = \hat{\mathbf{n}} \cdot \mathbf{v} \tag{5.6}$$

where $\hat{\mathbf{t}}$ and $\hat{\mathbf{n}}$ are normalised tangent and normal vector components of the segment face ($\mathbf{t}$ and $\mathbf{n}$ are represented by 'T' and 'N' in Fig. 5.3) and $\mathbf{v}$ is the velocity of the face. From real

values t and n, force magnitudes are then computed,

$$\Xi(t) = -\gamma_t \text{sgn}(t) t^2 \tag{5.7}$$
$$\Xi(n) = -\gamma_n \text{sgn}(n) n^2$$

where the γ parameters control the levels of each. The function sgn basically indicates the sign of a given vector component. These are required in order to determine the direction in which water should push back against the undulatory agent. The actual water force, $\mathbf{w}$, to be applied to each of the four point masses making up the face is derived from force, $\mathbf{f}$, as follows:

$$\mathbf{f} = \Xi(t)\hat{\mathbf{t}} + \Xi(n)\hat{\mathbf{n}} \tag{5.8}$$

$$\mathbf{w} = \mathbf{f} c d A \tag{5.9}$$

where c is a viscosity coefficient, d is drag, and A is the area of the segment face. The viscosity coefficient can be thought of as the thickness of the fluid. Note that in the model c and d are set to 1 since it is sufficient to tune the γ parameters. As noted in [107] the ratio of γ_n/γ_t is also important in determining how the resulting animat should undertake undulatory locomotion finding that γ_n/γ_t should be >1 i.e. $\gamma_t \ll \gamma_n$. In the model, it was found to be sufficient to set $\gamma_t = 0.9$. Any smaller and the dynamics of the physics engine would become unstable. Any larger and the animat would swim far too slowly. The value, $\gamma_n = 1.0$, was also found to be appropriate.

5.2.3 Neural system

Spatial distribution The neural architecture is embedded within the animat wire frame but is intrinsically segmented in the following fashion. Inside of each segment are ten neuron units, four of which are motor neurons and six of which are general interneurons. Spatially, the interneuron positions are randomly distributed and this distribution affects both connection strength and neuron to neuron connectivity. For a given general interneuron, the (x,z) part of its three dimensional (x,y,z) coordinate triplet is initialised using the equations specified in Eq. 5.1 with radii and angle values that have been uniformally generated. The y-coordinate is then further initialised as a random real value (recall that the animat is initialised in an upright position, with the head at the top and the 'foot' at the bottom meaning that a neuron's y-coordinate represents the position of the neuron along the length of the animat

body). These positional parameters are optimised over a period of simulated evolution; the motor neurons remain position-fixed. Note further that if the length of a body segment changes, which can happen because of a change in the value F_i (see Eq. 5.3), then the neural spread within the segment is commensurately altered. If the segment length increases, then the neural spread over the y coordinate plane is 'expanded'. If it decreases, then the neural spread over the y coordinate plane is 'compressed'. Specifically, whenever the segment length F_i changes, the y coordinate of each neuron within the segment i is updated as follows:

$$n_y \leftarrow n_y \cdot F_i \tag{5.10}$$

In other words, the architecture of the neural system is directly coupled to the geometrical properties of the body segmentation. This is an abstraction of development, so that changes in body characteristics are reflected by changes in the neural architecture.

Connection strengths The weight values are computed from the interneuronal euclidean distance. The closer two neurons are to each other, the higher the weight value between them,

$$w_{ij} = \xi / d_{ij} \tag{5.11}$$

where ξ has been empirically set to 20.0 to ensure that a suitable range of weights can be generated. Given that the maximum possible length of a segment as defined by Eq. 5.3 is 25 and that the radius of a layer as defined by Eq. 5.2 is ≈ 8.3, the maximum possible distance between two neurons is ≈ 26.34 which therefore gives the smallest possible weight $w = w^{min}$ that can form as $\approx \frac{20.0}{26.34} = 0.76$. Note further that given the operation of Eq. 5.10, if the length of the segment decreases from S_i^{max}, w will increase, whilst if the length increases from S_i^{min}, w will decrease (see "Spatial distribution").

Connectivity Connectivity also comes about as a function of distance given the sigmoid,

$$\sigma(\lambda, s, d_{ij}) = \frac{2}{2 + \exp((\lambda/s) * d_{ij})} \tag{5.12}$$

where λ is an evolved parameter, s is a scaling parameter, which is set to the total length of the agent, and d_{ij} is the euclidean distance between neurons i and j. As shown in Fig. 5.4, a connection is established if the function produces a value >0.5. The scaling parameter serves to alter the magnitude of the λ parameter as the length of the animat changes. This ensures

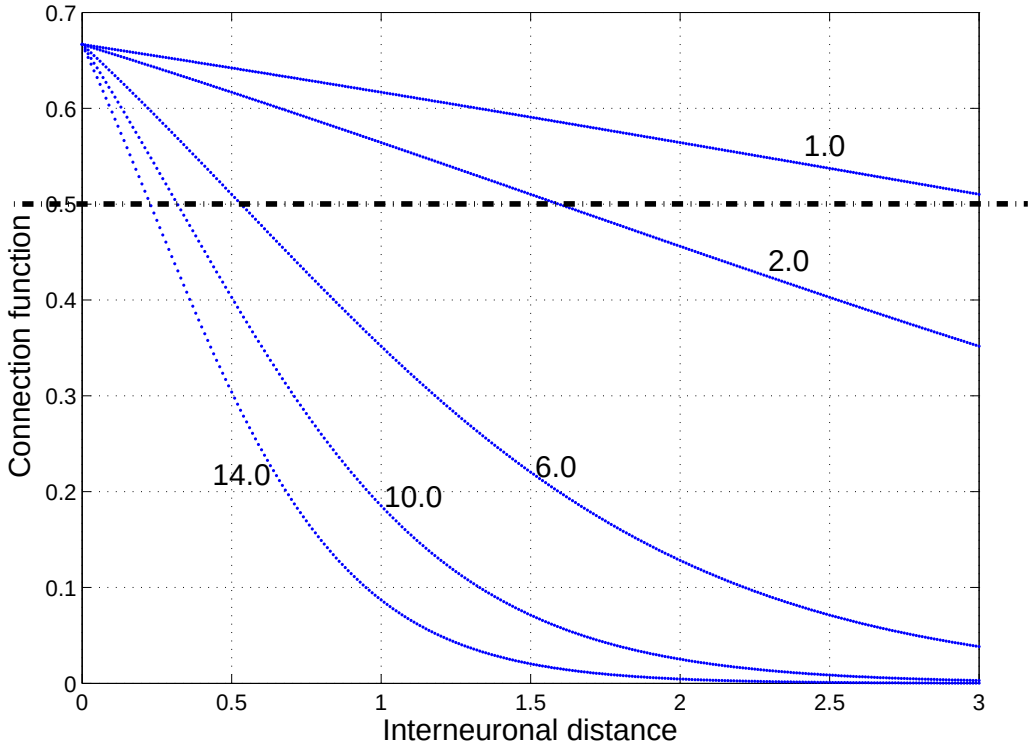

Figure 5.4: A graph showing how connectivity between two different neurons depends on both the λ parameter (labelled) and the interneuronal distance. All neuron pairs generating values above the dotted line become connected.

that the effect of the λ parameter is consistent across a variety of elongations. Note further that a set of four λ values is employed each of which caters for one type of connection: λ_{II}, λ_{IE}, λ_{SE}, λ_{AA} where I=interneuron, E=effector neuron, S=sensory neuron; AA indicates connections between interneurons in adjacent segments. Note that connections can form between the motors and interneurons/sensors but not between the motors themselves.

Motor symmetry In Chapter 3, the importance of body plan symmetry as something that changes during evolution and its coupling to the nervous system was introduced and discussed. It was further remarked how the jellyfish, with is radial body plan, is viewed as being baseline in terms of body symmetry. Symmetry is also accounted for in the Evo-Critter system and is represented by a 'motor symmetry configuration'. Loosely speaking, the motor symmetry configuration determines which motorneurons become driving effectors during movement behaviour (**note:** motorneurons not emerging as effectors can serve as

additional excitatory interneurons, but have no direct influence on movement behaviour). Example motor symmetries are visualised in Fig. 5.5 and several are described below:

1. All motor neurons evolve to become driving effectors. The symmetry of the agent is considered radially symmetric. The part of the genotype encoding motor symmetry is 1111 (Fig. 5.5C).

2. None of the motor neurons evolve to become driving effectors. The behavioural evaluation is aborted since it is impossible for the agent to move in this situation. The part of the genotype encoding motor symmetry is 0000.

3. Motors on either side of the animat evolve to become driving effectors. The symmetry of the agent is considered bilaterally symmetric. The part of the genotype encoding motor symmetry is 1010 or 0101 (Fig. 5.5A).

The motors are actually considered part of the body plan, thus, an emergence in the above property provides a rudimentary means of studying symmetry breaking, a core evolutionary transition of nervous systems (see Chapter 3).

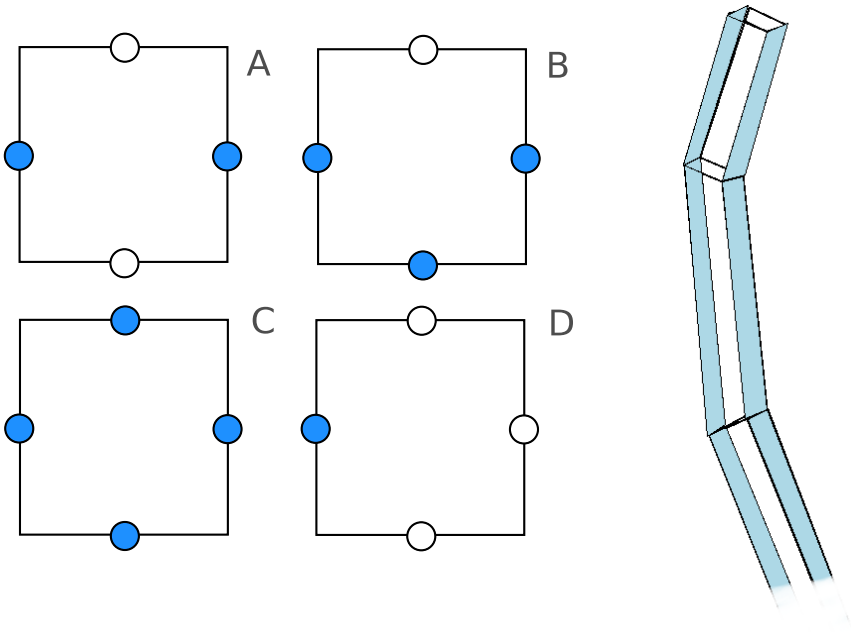

Figure 5.5: Examples of different active motor configurations. Boxes A-D represent example motor symmetries, as viewed from the end of the agent, with filled circles as effectors and unfilled circles as general interneurons. The right hand wire frame diagram exemplifies the 'A' configuration highlighting how both left and right sides become actuated during movement.

Computational motor system Each face of a segment has a motor neuron located at its centre. Thus each segment has four motor neurons. In a given segment face, a motor neuron actuates a vertical spring-pair, see Fig. 5.6. The amount of force applied to each spring in this pair is proportional to the motor neuron's membrane potential but is normalised to within the range [0, 120]; values higher than 120 result in the spring dynamics becoming unstable. Also, a spring is only ever actuated if the motor neuron's membrane potential is between 0 and 1.

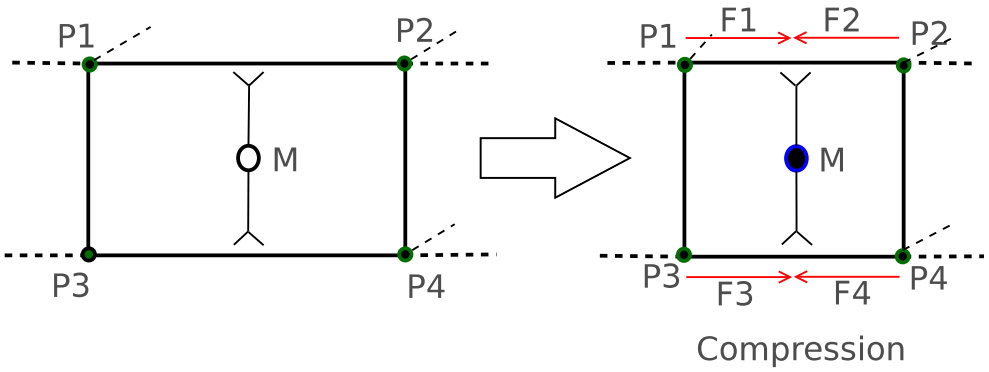

Figure 5.6: Motor force system: the effect of a motor M in the centre of one of the segment faces contracting spring P1$\Longleftrightarrow$P2 by applying equal but opposite forces F1 and F2 to point masses P1 and P2 and contracting spring P3$\Longleftrightarrow$P4 by applying equal but opposite forces F3 and F4 to point masses P3 and P4.

Sensory system The animat has a very rudimentary sensory system consisting of 4 sensory neurons that remain position-fixed at the head of the animat (one at the top-middle of each segment face). The head segment therefore has 14 neurons rather than the normal 10. Current is injected into all sensors according to the angle of the target from each, see Fig. 5.7a.

This approach is based on the bearing-based tracking model [53] computed as

$$I_s = \exp(-\alpha(\Delta\phi - 90)^2) \tag{5.13}$$

where α is set to 0.0005 and $\Delta\phi$ is the angle of the target from the sensor. As shown in the figure, the sensor maintains a 180° receptive arc along the sensor plane. If the target is exactly perpendicular to the plane, i.e. the animat is pointing directly towards the target, then Eq. 5.13 results in an input current of 1.0. When there is a deviation from this orthogonality, if

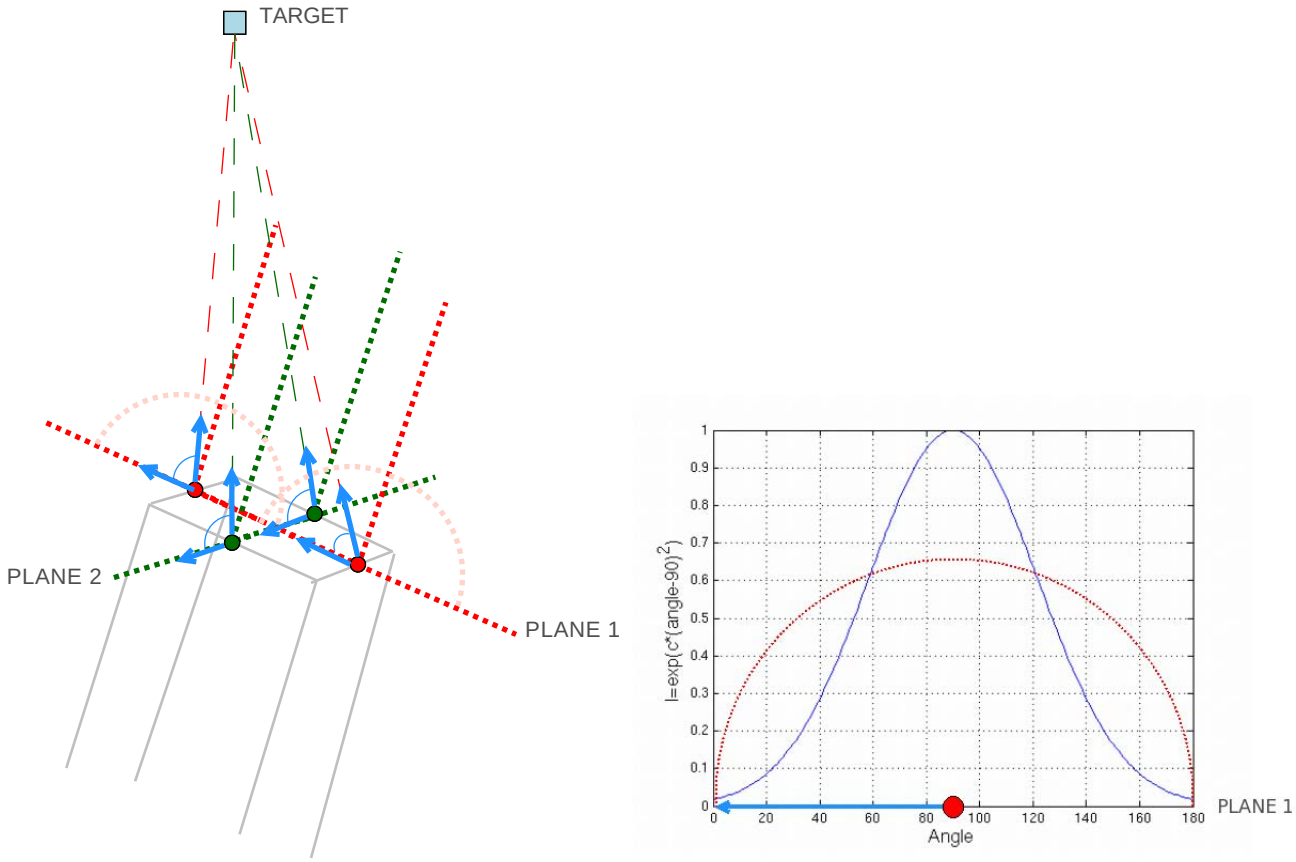

(a) (b)

Figure 5.7: **(a)** A diagram showing how angular information is used for sensory input. The end of the head segment is depicted. The filled circles at the top represent sensory neurons. For a given sensor, the short blue arrows represent the unit vectors used to calculate the angle of the target from the sensor. The large dotted arcs on PLANE 1 highlight how a given sensor has a 180° receptive arc. The sensors on PLANE 2 have concordant arcs but they have been omitted for clarity**;** **(b)**, A graph showing how the current is generated for one sensor.

$0 < \Delta\phi < 90$ or $90 < \Delta\phi < 180$, then $I_s < 1$. This calculation is highlighted for one sensor in Fig. 5.7b. The bias value of each sensory neuron is set to 0.5, and the time constant is set to 1.0. These have been empirically set to ensure that the sensory neurons will become activated over a range of angles.

Other models have also incorporated such vision systems, for example, Beauregard and Kennedy [9] have incorporated a similar abstraction, modeling a 2D lamprey able to undertake tracking of a moving object; also, Ijspeert [53] has incorporated a similar model in the the visual system of a simulated salamander.

Computational model The neural system is based on a continuous time recurrent neural network (see Section 2.2.2). The membrane potential u_j of a neuron is modelled as follows [13]:

$$\frac{du_j}{dt} = \frac{1}{\tau_j}\left(-u_j + \sum_{i=1}^{C} w_{ji}a_i + I_j\right) \tag{5.14}$$

where τ_j is a time constant,w_{ji} is a vector of presynaptic connection weights and I_j is an external input current. The value a_i is a presynaptic neuron's membrane activity computed as follows:

$$a_i = \tanh(u_i - \beta_i) \tag{5.15}$$

where β_i is a bias value. If a neuron is inhibitory then all of its outgoing connection weights are made to be negative. There are three other important aspects of the model:

1. The motor neurons in each adjacent animat segment are all excitatory. This is in view of biological muscles which are considered excitatory, only ever having periods of contraction (excitation).

2. Motors in each animat segment have equivalent parameters (the motors in segment N have the same bias values and time constants as those in segment M). This restriction cuts down on computational overhead. Also, the view is taken that *muscle tissue is muscle tissue* and that the corresponding neurons should have as little computational disparity between them as possible.

3. All sensory neurons have the same time constant and threshold values (1.0 and 0.5 respectively) to ensure that each triggers the neural system in exactly the same way.

5.2.4 Simulation loop

The behaviour of the animat is conceptualised in one 'giant algorithm' named the Simulation Loop. This takes care of updating the simulation including the neural dynamics of the CTRNN, the dynamics of the physics engine, and finally the animat's body posture and geometry, see Algorithm 5.1.

Algorithm 5.1 Pseudocode of the simulation loop during one behavioural evaluation. In total, 40 simulation steps are permitted, but within that, the CTRNN is integrated over 10 time steps and then for each CTRNN time step, the physics engine/animat movements are integrated and updated over 20 time steps.

```
WHILE simSteps < 40
        WHILE netSteps < 10
                ctrnn.update
                WHILE physSteps < 20
                        apply motor activations
                        apply water forces
                        accumulate all forces
                        integrate physics
                        update animat geometry
                END WHILE
        END WHILE
END WHILE
```

5.3 Evolutionary process

An evolutionary algorithm that harnesses both the power of adaptive mutation and local selection is used to evolve all or part of the genotype presented in Fig. 5.8.

5.3.1 Local selection strategy

At an early stage of implementation, a simple binary tournament selection scheme was used for the selection process. However, this was later swapped with a local selection process of the type described in [104], since, (a) preliminary investigation showed it to have far better convergence; (b) within the field of Neuroevolution, a similar strategy has on prior occasion been employed to great success, see for example [112, 111]; (c) the fact that local selection results in gradual phenotypic change is a practical advantage since it allows for

evolutionary process to be more easily tracked. Diagrams visualising the local selection scheme are presented in Fig. 5.9.

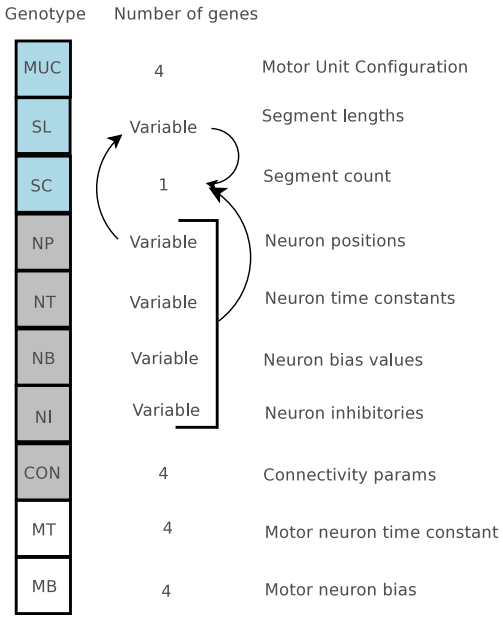

Figure 5.8: The full Evo-Critter genotype. The arrows reflect dependencies between different parts of the genotype. Thus we can observe how neuronal parameter genes and segment length factor genes all depend on the number of segments ('segment count').

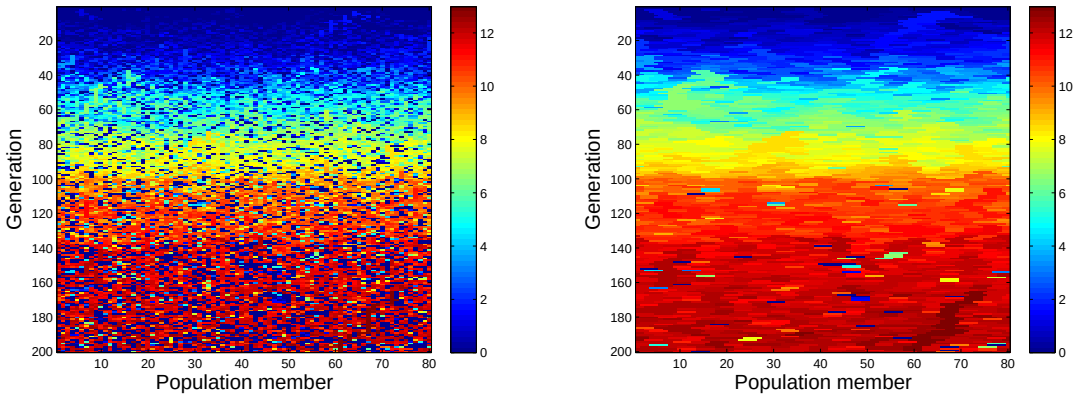

(a) Before selection

(b) After selection

Figure 5.9: Visualisations of population fitness before and after local selection has been applied. Note that for the 'after selection' visualisation, the fitness values are shown immediately before the next generation, i.e., prior to resetting them to 0. Color indicates fitness.

Process The local selection strategy is tournament based. For each successive 4 members (the tournament size), the fittest of the 4 replaces the other 3. After selection, this results in contiguous 'bands' of equally fit individuals, see Fig. 5.9b. A random offset of size *tournament size* is also employed (i.e. 4). Thus suppose we have a population of size 8 with members [a,b,c,d,e,f,g,h] and the 'offset' is randomly initialised to 0 and the fittest member in the first subset of 4 members ([a,b,c,d]) is found to be individual c and the fittest member in the second subset of 4 members ([e,f,g,h]) is found to be individual h, then the resulting selectees would be [c,c,c,c,h,h,h,h]. Or, if the offset is randomly initialised to 1, the selection process begins with the second individual; thus, the first subset of 4 individuals would be [b,c,d,e] and the second set would be [f,g,h,a] i.e. a circular array implementation is employed. Having an offset ensures that for a given population member, it has a fair chance of mixing well with the rest of the population. The effect is two-fold - an enhancement of diversity and an avoidance of local minima.

5.3.2 Other evolutionary operators

Subsequent to selection, except for the fittest member (the elite chromosome), discrete recombination and adaptive mutation are applied to the selectee chromosome pool (the offspring population). Discrete recombination exchanges gene values between two offspring candidates selected uniformally from the offspring population. The adaptation process relies on the setting of two strategy parameters, $\tau_0 = 1.0/\sqrt{2.0 * D}$ and $\tau_1 = 1.0/\sqrt{2.0 * \sqrt{D}}$, where D represents the dimensionality of the vector being evolved. These parameters have been shown to be optimal in a process of self-adaptation [7]. Note that within the evolutionary framework, different gene groupings (λ parameters, neuron angles, segment lengths etc.) require different τ values since each gene grouping may have a different number of genes. For any real valued gene, the σ values are adapted as follows:

$$\sigma_i \leftarrow \sigma_i * exp\left(N(0,\tau_0) + N_i(0,\tau_1)\right) \tag{5.16}$$

The full animat genotype has a mixed boolean, real and integer valued representation, thus boolean mutations incorporate bit flips. The motor symmetry configuration and the neuron inhibitory values are all booleans. The segment count is integer whilst all remaining parameters are real. Furthermore, as depicted in Fig. 5.8, dependencies exist between different gene groupings. Because of this, the genotype is not of a fixed length but ultimately depends

on the number of body segments. This has been accounted for in the evolutionary process as follows. When the number of body segments increases, a new segment length gene and new neuron parameter genes (positions, time constants, biases and inhibitories) are created. When the number of body segments decreases, the corresponding segment length gene and neuron gene groupings are removed.

5.4 Evaluating neural and motor activity

For the experiments conducted in later chapters, a number of measures are made to assess levels of neural activity. They are defined as follows:

- **Definition: Oscillation Count.** This is defined as the number of times that the membrane potential, u, of a given neuron, i, changes from a positive state (>0) to a negative state (<0) or vice-versa, during the behaviour of the agent,

$$o_i = \sum_{n=1}^{|\mathbf{p}_i|} c_n \tag{5.17}$$

$$c_n = \begin{cases} 1 & u_{n-1} < 0 \bigwedge u_n > 0 \\ 1 & u_{n-1} > 0 \bigwedge u_n < 0 \\ 0 & \text{otherwise} \end{cases} \tag{5.18}$$

  where $c_n \epsilon \mathbf{p}_i$.

- **Definition: Oscillation Period.** This is defined as the average time lapse between a pair of successive membrane oscillations, as generated by a single neuron, i, during the behaviour of the agent,

$$\lambda_i = \frac{1}{|\mathbf{p}_i| - 1} \sum_{n=2}^{|\mathbf{p}_i|} (c_n(t) - c_{n-1}(t)) \tag{5.19}$$

- **Definition: Motor Contraction Count.** This is defined as the total number of times that all motors (springs) become actuated by the motor neurons during the behaviour of the agent (thus it discludes kinematic events triggered by passive spring movements). Since as mentioned in Section 5.2.3 ("Computational Motor System") that

a motor neuron will only actuate a motor when its membrane potential is between 0 and 1, a more precise definition can be formulated,

$$m = \sum_{i=1}^{|\mathbf{m}_p||\mathbf{m}_q|} \sum_{j=1} c_{ij} \tag{5.20}$$

$$c_{ij} = \begin{cases} 1 & u_{m_i} > 0 \bigwedge u_{m_i} < 1 \\ 0 & \text{otherwise} \end{cases}, \forall c_{ij} \epsilon \mathbf{M} \tag{5.21}$$

where $\mathbf{m_p}$ and $\mathbf{m_q}$ are column and row vectors of a matrix $\mathbf{M}$ storing the 'contraction events' of each specific motor.

5.5 Summary and Conclusions

This chapter introduced Evo-Critter, the system used for many of the experiments described in this thesis. It began with identifying the need to have a simulation environment capable of exploring body plan and nervous system couplings. Secondly, the kinematics of fish swimming were described, with explanations of how different types of fish locomotion, of which undulatory is an example, require subtly different body plan morphologies, control systems and levels of elongation. The simulation environment was then introduced with descriptions of how the animat is constructed out of springs and point masses and how a water force model is used to model an aquatic environment. The neural architecture was explained as being spatially embedded relying on geometric information to determine connection strengths and interneuronal connectivity. At this point, the sensory and motor systems were also introduced. It was explained that the sensory system relies on angular information to determine the location of a target within the environment. An abstract notion of motor symmetry was introduced as a means to assess functional symmetry, thus providing an abstract notion of general body plan symmetry. An outline of the evolutionary process used to evolve the agent was given, with explanations of how the genome is a mixed real, integer and boolean valued representation and how local selection and self adaptation are two of the main features of the implementation. Finally, three measures of neural activity used in the later chapters, were defined.

In conclusion, the Evo-Critter framework is a novel research tool that enables us to study how the nervous system architecture of an undulatory agent should emerge when under

the constraints of body plan morphology characteristics and symmetry. The framework is extensible; it is easy to change the neural model, for example, from an analog to a spiking variant; certain parts of the neural architecture are easily constrained; an energy consumption term is easily added (which will be discussed in Chapter 8). Specifically, the contributions are as follows:

1. The neural architecture is spatially embedded which makes it possible to directly link the effect of architecture to neural dynamics. Thus it contributes to our understanding of how neural architecture directly relates to the behaviour of the agent.

2. The segmentation characteristics of the agent are evolvable; we are therefore able to observe the effect that these characteristics have on the behaviour of the agent and the effect it has on neural architecture. This contributes to our understanding of how body plan morphology affects the neural architecture and the resulting agent behaviour.

3. The local selection scheme enables us to more easily identify points of transition in the evolutionary process.

4. The evolvable motor symmetry configuration allows us to identify how symmetry of the agent can facilitate optimal swimming behaviour. Furthermore, we can track how it changes during the evolutionary process. Thus together with the local selection scheme, we can observe 'points of transition'. As discussed in Chapter 3, symmetry is a very important study point given its rich association with the nervous system architecture and the body plan morphology.

5. Crucially, the framework contributes to an understanding of how the nervous system is coupled to body plan morphology and motor symmetry. The framework allows us to ask such questions as – how does the body plan constrain the emergence of the neural architecture? How does the motor symmetry then also change as a result of this? Basically, the model provides us with the ability to understand different types of coupling, as reflected by the arrows in Fig. 5.8. In the following chapter, these couplings are explored in more depth.

Chapter 6

Body plan morphology: a constraining factor in the emergence of neural organisation

Synopsis

In this chapter, experiments that were conducted using the Evo-Critter system, with an emphasis on the coupling between the agent's body plan morphology and nervous system, are discussed in detail. Specifically, questions 1 and 2 as posited in Section 1.1 of the Introduction are addressed. For convenience, they are repeated here:

1. **Question:** *How does body plan morphology affect the evolution of the nervous system and vice-versa?* **Guiding principle:** Since the body of an organism directly interacts with the environment, it needs to have the correct niche-specific characteristics. At the same time, before these characteristics can actually be exhibited, the body needs to be properly actuated by a correctly tuned nervous system. Pointedly however, the emergence of the neural architecture is also constrained by the emergence of the body plan morphology (and vice-versa). This suggests that the evolutionary drive towards an optimal combination of these elements and the coupling between them is highly complex. The above question aims to address such coupling and the corresponding effects on body morphology characteristics and nervous system architecture.

2. **Question:** *How does body-symmetry evolve in relation to the nervous system and other body plan characteristics?* **Guiding principle:** The symmetry of an organism's body plan morphology will often preclude optimal behaviour (e.g. directional movement).

At the same time, the nervous system and body plan will often adapt and fit around this symmetry in a particular way (and vice-versa) so that behaviour is made efficient and optimal. The above question investigates the process by which this occurs. Note that much of the work concerning functional symmetry is presented in [56].

Note: At no point do the investigations described in this chapter incorporate a notion of 'energy' since this is investigated separately in Chapter 8. The reasoning behind this, is that given the model, we need to first understand the effect of body plan morphology *alone* before we also tackle the importance of energy.

The layout of this chapter is as follows: Section 6.1 begins by building upon the biological literature presented in Chapter 3. An emphasis is placed on the significance of nervous system body plan morphology couplings, body symmetry and neural control. This provides context for the actual aim of this chapter which is to shed light on the above questions. Then, the types of coupling that are present in the Evo-Critter framework (*environmental, genetic, implicit)* are identified in Section 6.2. The actual experiments that were carried out are defined in Section 6.3, and the findings are presented in Sections 6.4 and 6.5. A discussion is finally presented in Section 6.6. Evo-Critter, the model developed in Chapter 5 is used throughout.

6.1 Significance of body plan nervous system couplings

In biological organisation, organismic components ('cells', 'tissues', 'organs', 'systems', etc.) are coupled; they are part of a holistic system. A morphological change in one component, either via evolution or during development, will often impact on the organisation of another component. Consequently, major evolutionary transitions have resulted in drastic shifts in body shape and form, underlying component architecture and morphology. This is fundamental since it presents biological organisation as being richly dynamic, survival as being dependent on the interoperability that exists between all morphological aspects (as opposed to between only a few of them); the behaviour that results from this is crucial for the animal's survival.

Thus, we must recognise that animal behaviour is ultimately shaped by the coupling existing between its nervous system and body plan morphology. Moreover, the body can actually be thought of as an 'interface' residing between the nervous system and the environment,

since in an 'exterior-sense' it is only the body that is directly presented to the environment. Just as a jellyfish needs to be large and flat so that it can be carried by water currents, a giraffe needs to have a long neck so that it can reach tall trees.

The interacting body then requires an efficient nervous system for control, so that basically, the body can do what it is 'designed' to do. To be efficient, its architecture needs to be coupled to the body in a way that allows for optimal behaviour. Given environmental pressure, the body might evolve in order that it can *fit* better; and when this happens, the nervous system will commensurately be adapted in order that it can maintain optimal coupling. What this all means is that the coupling itself becomes driven by the environment.

6.1.1 Body symmetry

In Chapter 3, the significance of body plan symmetry was highlighted. And, since symmetry is inherently part of the body morphology, any change in the body will (i) effect the distribution of this symmetry and (ii) perpetuate change in neural architecture.

Now clearly, the symmetry of an animal influences its behaviour and therefore its chances of survival. Some of the theories presented in Chapter 3 for example, posit that elongation came about out of a need for directional movement. Often, this elongation presents the organism with bilateral symmetry. At the same time, the symmetry of an organism will be very niche-specific. A jellyfish's radial symmetry for example, lends perfectly to its passive, floating lifestyle. An eel on the other hand needs to locomote *with direction* via a utilisation of undulatory locomotion and its bilateral body plan facilitates this. In Evo-Critter, symmetry is represented using a notion of active motor symmetry (see Section 5.2.3). It is expected that this will emerge in a way that is fully bilateral (see Fig. 5.5) since this is shown to be optimal [20]. However, the question remains as to how the couplings existing between all of these different components – the motor symmetry, the body morphology, and the neural architecture – should become characterised during evolution. Although the abstraction level imparted by Evo-Critter cannot offer a full explanation, it is hoped that the experiments presented in this chapter will highlight their significance.

6.2 Emergent couplings

This section identifies three types of coupling existing between the nervous system and body plan morphology of a given animal, couplings that have been modeled to a greater or lesser extent in the Evo-Critter system. They are identified as follows:

- **Environmental**. For any animal, the interaction between the neural system and the body plan morphology is constrained by the environment. If component A changes due to a selection force, then pressure on component B will force it to 're-adapt' (in an evolutionary sense), to fit more optimally with component A. In this way, we can think of components A and B as being *environmentally coupled.* For the jellyfish, the environment enforces a large surface area which perpetuates a 'drifting' lifestyle. Consequently, the nerve net is 'forced' to re-adapt to this large surface area by becoming highly distributed. The nerve net and body plan morphology of the jellyfish (and for other given animals) can be said to be coupled via the environment.

- **Genetic.** These entail genetic interdependencies. In the model genotype (Fig. 5.8), both segment length and nervous system genes (positions, bias values, time constants, etc.) are genetically coupled to the number of body segments. Genes can therefore affect one another, so we can think of this as a type of gene regulation.

- **Implicit.** These reflect developmental abstractions. For example in Evo-Critter, the neural architectural distribution within a particular body segment is constrained by the length of the segment. When it increases, the distribution expands; when it decreases, the distribution compresses. This idea serves to characterise developmental plasticity which is crucial in theories of evolutionary development.

In many traditional artificial life models of biological organisms, addressing the above couplings is difficult since the nervous system is typically viewed as separate from the body. Both the body plan morphology and nervous system architecture are often implemented as architecturally static components which remain fixed throughout the evolutionary process (see Fig. 6.1a). In contrast, as depicted in Fig. 6.1b, a model such as Evo-Critter can capture the essence of the above couplings more appropriately, since it permits abstract levels of dynamic interoperability to exist between all major components.

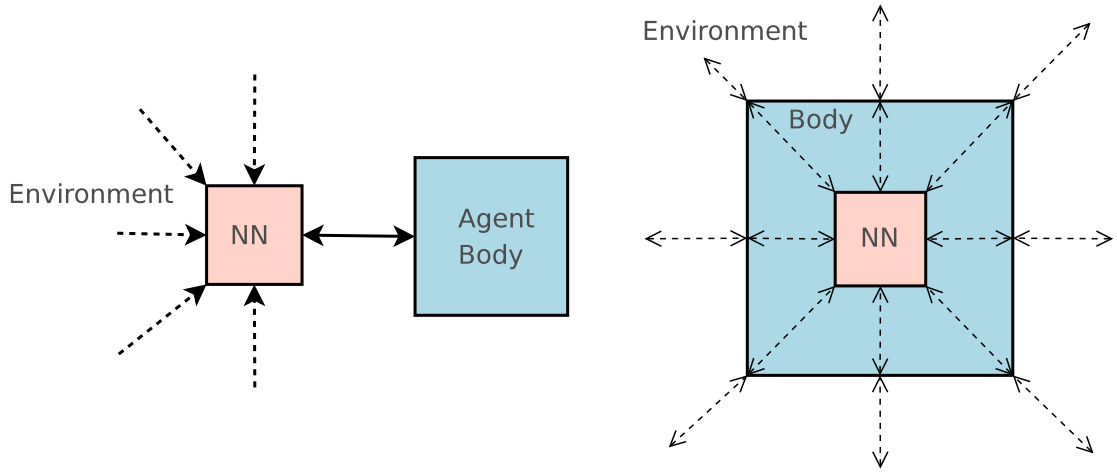

(a) Traditional (b) Realistic

Figure 6.1: **(a)** A diagram highlighting how agents in a traditional artificial life framework are constructed. The nervous system is typically static and separate from the body; **(b)** A more realistic view in which the agent's nervous system is coupled to its body; dynamic couplings are underpinned by forces existing between the body and nervous system. Dotted arrows represent forces and pressures interacting between different components.

6.3 Experimental setup

The goal of this chapter is to shed light on how the coupling between body plan morphology and nervous system should evolve when different components of the body plan morphology are constrained. Evo-Critter is used as the research tool; 4 sets of 50 differently seeded experiments were conducted; each placed a different level of constraint on the evolutionary process, as described:

1. **evo-ALL.** In this experimental setup, the full genotype as presented in Fig. 5.8 was evolved. The underlying motivation was to explore how the full system of interacting components on all levels of coupling – *environmental*, *genetic* and *implicit* – would interact on an evolutionary timescale, and, the effect that these couplings would have on individual fitness. The setup further provided a 'benchmark' that the experimental results from the other three setups could be compared to.

2. **evo-NOBCBL.** In this experimental setup, all parameters except for the number of body segments and the length-factors of each segment (refer to Eq. 5.3), were evolved ('no block count, no block length evolution' – historically, segments were also referred

to as 'blocks'). Given the evo-ALL results, how is fitness found to be altered when the segmentation characteristics are constrained?

3. **evo-NOBC.** In this experimental setup, all parameters except for the number of body segments were evolved ('no block count evolution'). What impact does segment count have on the fitness of an agent? The motivation for asking this question stems from Fig. 5.8, in which dependencies between different gene groupings introduce 'regulation'; i.e. the number of segments regulates the length of the genotype since for each additional segment, additional neurons and additional segment length genes are incorporated. By turning this aspect off entirely and then comparing the results to the evo-ALL simulations, we can find out whether such regulation has a positive or negative effect.

4. **evo-NOBL.** In this setup, all parameters except for the length-factor of each segment were evolved ('no block length evolution'). Together with the results of evo-ALL and evo-NOBCBL, we can ask how changes in fitness are characterised by changes in segment length.

The aim of the latter two experiments was to characterise, by counter-example, how changes in segmentation properties (which we may equate to body morphology), affect fitness. Fitness was given by the distance of the agent's head from a predefined target; specifically, $20.0 - d(animat, target)$, since the target was placed 20 units away from the head of the animat. Therefore fitter agents were those that could cover more distance between the starting location and the target (see Fig. 6.2).

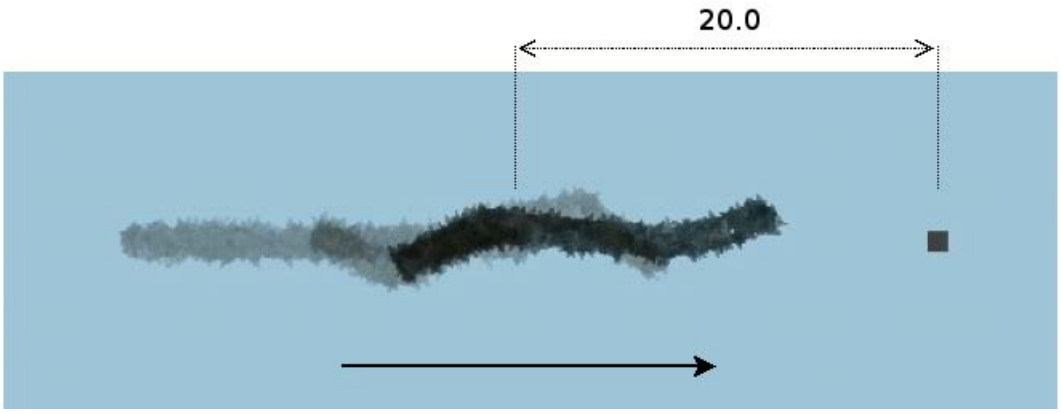

Figure 6.2: The simulation environment showing the target that the animat must locomote towards. The arrow indicates direction, the square indicates the target.

The population size was set to 80, the crossover rate was set to 0.2, and the mutation rate was set to 0.01. The other properties of the evolutionary process were as described in Section 5.3.

6.4 General findings

In this section, an overview of the main findings is given. More specific findings follow in Section 6.5. Throughout the results, median recordings are preferred over mean recordings. This is to firstly ensure that outliers are mitigated; secondly, generating median plots maintains consistency in the analysis since box-plots which generate median data are used extensively. Finally, note that 'evolution of segment lengths' should be interpreted as 'evolution of segment length-factors' (refer to Eq. 5.3 for clarification of what a segment length-factor is).

A visualisation of the behaviour of the best evo-ALL agent is provided in Fig. 6.3 and plots of fitness are given in Fig. 6.4. Comparisons between best fitness values at the end of evolution are given in Table. 6.1.

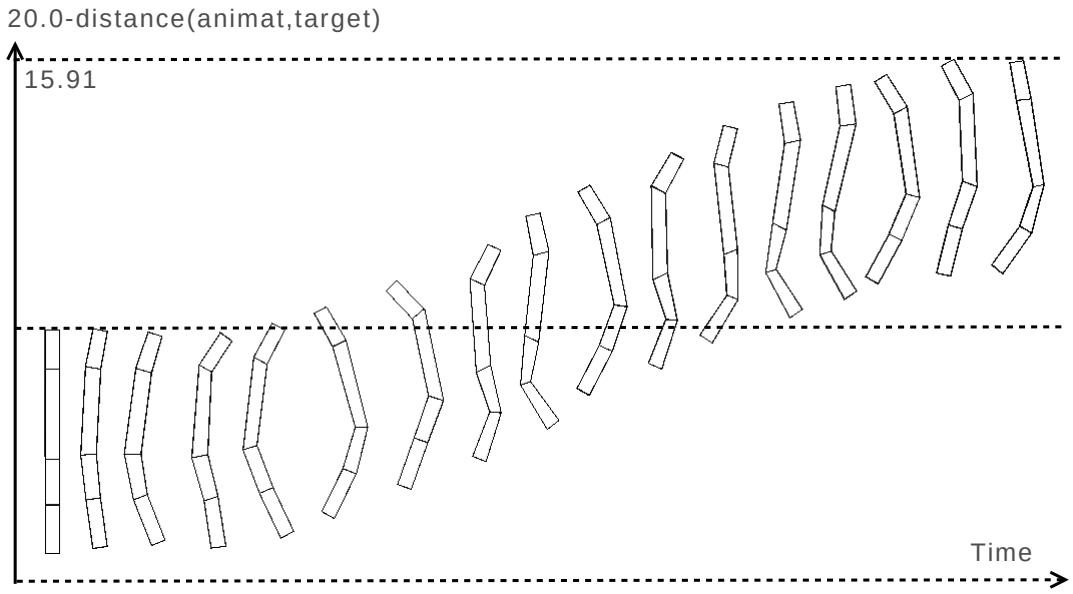

Figure 6.3: Animat behavioural sequences for the best animat from evo-ALL showing undulatory type locomotion in which a wave of propulsion passes down the length of the agent's body. Snapshots taken every 25 behavioural iterations.

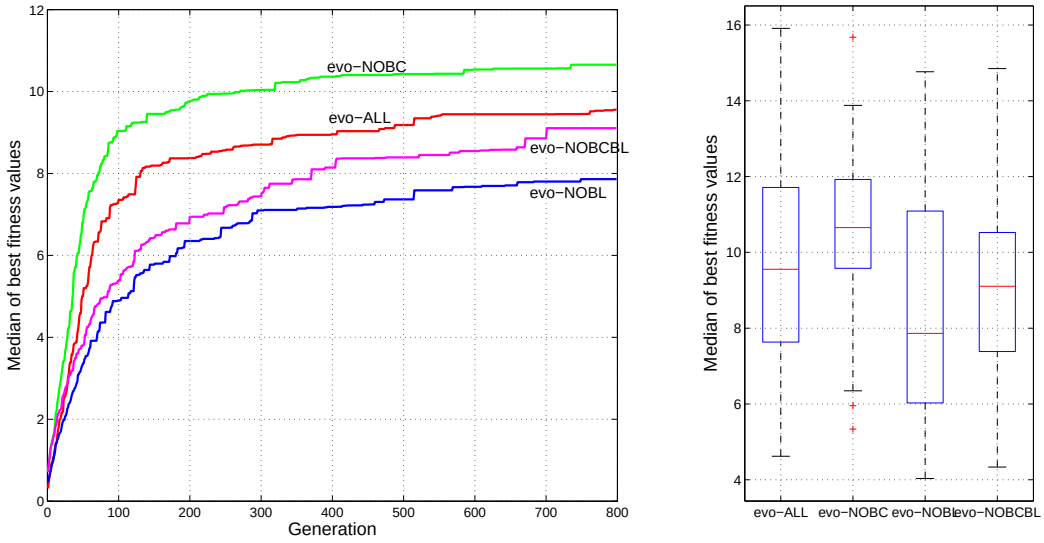

(a) (b)

Figure 6.4: (a) Medians over best individuals for each of the 4 sets of experiments (median readings are taken to prevent outlier artifacts); (b) a box plot of the fitness values at the end of evolution.

Comparison	evo-ALL	evo-NOBC	evo-NOBL	evo-NOBCBL
evo-ALL	-	0.0689	0.0393	0.4862
evo-NOBC	-	-	0.0003	0.025
evo-NOBL	-	-	-	0.1394

Table 6.1: Statistical p-values generated from comparisons in best agent fitness (ranksum test, 0.05 confidence level) at the end of evolution.

In terms of the plots, the results tell us that:

1. Fitness appears to be enhanced when evolution tunes the length of each segment.
2. Fitness appears to be degraded when evolution tunes the number of body segments.
3. General movement is undulatory. The movements of the fittest evo-ALL agent are visualized in Fig. 6.3.

Ranksum tests have been performed on the fitness data at a confidence level of 0.05. As shown by Table. 6.1, there are three significant differences: **(i)** evo-ALL vs. evo-NOBL;

(ii): evo-NOBC vs. evo-NOBL; **(iii)**: evo-NOBC vs. evo-NOBCBL. The least significantly different simulation sets are evo-ALL and evo-NOBCBL. From these findings, we can infer the following.

1. In terms of body morphology, when the length-factors of the individual segments are alone coevolved (i.e. evo-NOBC), fitness is enhanced. This indicates the positive effect that segment length has on the agent's fitness.

2. In terms of body morphology, when the number of segments is coevolved in addition to coevolving the length-factors (i.e. evo-ALL), fitness is degraded, meaning that evolving the number of segments is detrimental to the evolutionary process.

3. Evolving everything (i.e. evo-ALL) is better than evolving everything except for the segment length-factors (i.e. evo-NOBL). As with point 1, this again indicates the positive effect that segment length has on the agent's fitness.

4. Evolving everything (i.e. evo-ALL) is not significantly better than when none of the segmentation characteristics are evolved (evo-NOBCBL). We can think about this as follows: **Firstly**, we have observed from point 2 above that evolving the number of body segments can degrade fitness. **Secondly**, we have observed from points 1 and 3 above that evolving the segment length-factors can enhance fitness. **Therefore**, in interpreting this, we can say that for evo-ALL, evolving the segment length-factors enhances fitness but this fitness is then 'pulled down' because of the addition of also evolving the *number* of body segments.

Representations of the evolutionary fitness landscapes, for those simulations that yielded the fittest individuals, are visualised in Fig. 6.5.

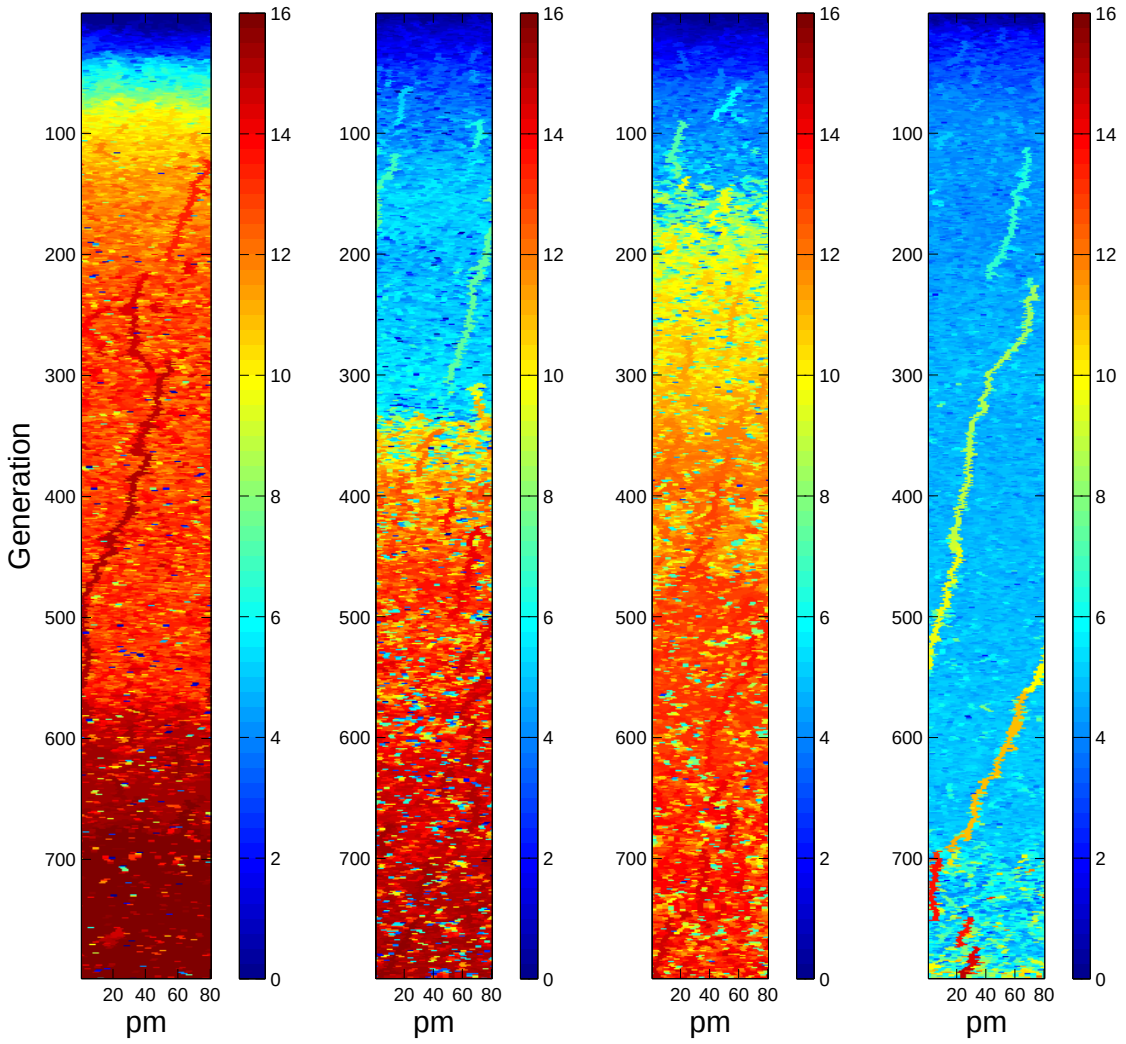

(a) evo-ALL (b) evo-NOBC (c) evo-NOBL (d) evo-NOBCBL

Figure 6.5: Evolutionary processes for best simulations highlighting changes in fitness, after selection has been applied. Note: pm=population member. Each pixel at a given generation is approximately one individual (subject to matlab formatting); colour represents fitness. Note: The visualisations are representative of fitness *after selection* has been applied, since this makes it easier to track the effects of selection pressure (refer to Section 5.3.1 for further clarification of the local selection scheme yielding these plots and for further clarification of the actual visualisation technique).

The case in which no segmentation characteristics were evolved (evo-NOBCBL) – Fig. 6.5d – is interesting since it shows a highly fit selection 'lineage' generated through evolutionary time (note, such paths can also be observed in the other subplots, but they are not as prominently visible). This path eventually leads to a fit 'descendant' (thus common ancestry is also identifiable). As further highlighted in Fig. 6.6, such fit individuals are shown to have been successively chosen over a very small field of the population. This demonstrates how, in the evo-NOBCBL simulations, evolution struggled to find fitness enhancing features.

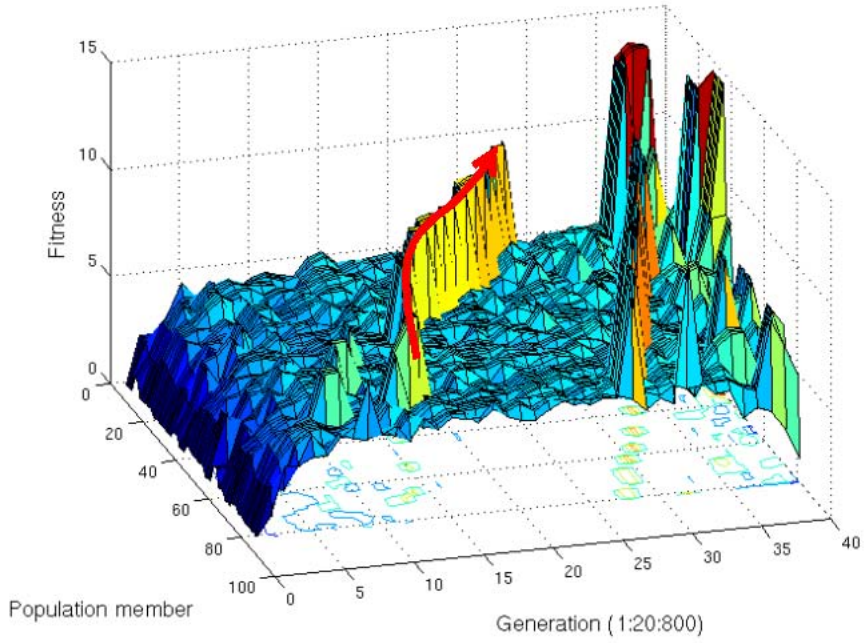

Figure 6.6: A visualisation of the changing population fitness for the best evo-NOBCBL simulation. Highlighted with the arrow is a highly fit selection 'lineage' (or optimal selection path); it highlights how fit individuals were successively chosen over a very small field of the population. The process is also visualised two-dimensionally in Fig. 6.5d.

In comparison and somewhat at the other extreme of what can happen, Fig. 6.5a shows distinctive 'bands of convergence' of ever increasing fitness emerging at different points of evolutionary time. For example, generations 0-80 (approx.) are marked by a blue-green region. A transition then yields a yellow-orange region until generation 550 (approx.) at which point, a transition to a dark-red region occurs. This succession in fitness increase is indicative of 'transitions' in features yielding ever fitter individuals across the whole population. In comparison to the last example, this exemplifies how fitter individuals are often more easily

sought, and further exemplifies how transitions can occur during the evolutionary process.

6.5 Specific findings

In this section, specific findings are addressed including motor symmetry, body segment characteristics (number of and respective lengths), neural architectures and neural dynamics. Also, where relevant, the emergence of a particular feature within a single simulation is explicitly visualised. This is in aid of attempting to understand the fitness changes visualised in Fig. 6.5.

6.5.1 Motor symmetry

For all experiments, the agent's motor symmetry was evolved (refer to "Motor symmetry" in Section 5.2.3). As indicated by Fig. 6.7, the most prevalent type of motor symmetry to have emerged in all cases was 0101 or 1010 (fully bilateral) which resulted in undulatory movements or those similar to *carangiform-* or *ostraciiform-type* fish movements.

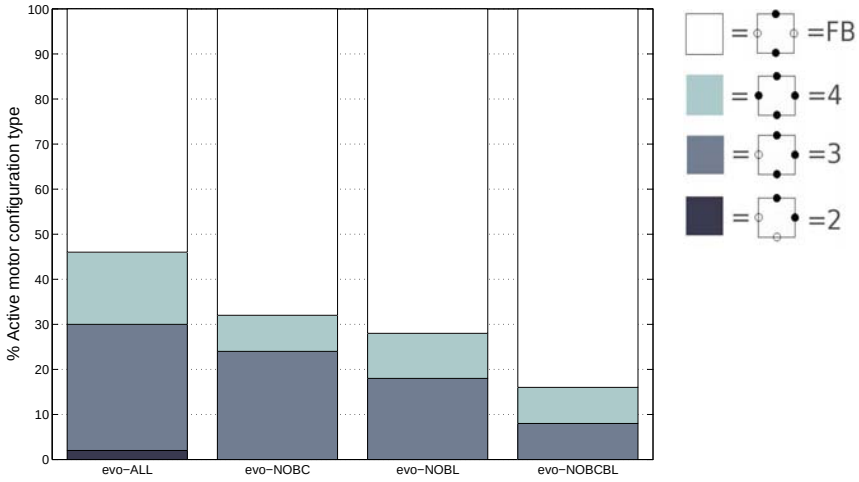

Figure 6.7: Percentages of motor symmetries to have emerged for the best individuals in each experiment type. **Note**: these readings are only approximately indicative of the motor symmetry part of the phenotype, since some 'active' motors may actually have emerged to be 'computationally dormant'. Not withstanding this fact, the results still capture evolution's tendency to prefer fully bilateral motor symmetries.

In total, 139/200 fittest individuals emerged to have this full bilateral motor symmetry (over 2/3 of all simulations). When we break down the fitness statistics of individuals having particular motor symmetries, we can further see that full bilateral symmetry generated the fittest of animat individuals, see Table 6.2.

Motor sym.	**evo-ALL**	**evo-NOBC**	**evo-NOBL**	**evo-NOBCBL**	
FB	15.911	15.675	14.767	14.848	***Best***
	10.914	10.896	9.337	9.712	***Average***
	5.243	7.320	5.513	4.337	***Worst***
4	10.709	7.995	9.706	5.629	***Best***
	7.411	6.760	5.815	5.266	***Average***
	4.621	5.338	4.740	4.961	***Worst***
3	15.871	13.879	13.078	8.126	***Best***
	8.826	10.387	6.113	6.884	***Average***
	6.058	5.956	4.034	4.871	***Worst***
2	6.306	n/a	n/a	n/a	***Best***
	6.306	n/a	n/a	n/a	***Average***
	6.306	n/a	n/a	n/a	***Worst***

Table 6.2: Fitness statistics for each motor symmetry type, for each experimental setup. Measurements are not shown for a single active motor configuration since no instances of this type arose. For the column 'Motor sym.', see legend in Fig. 6.7.

Although for undulatory locomotion a bilateral symmetry outcome is obvious, the actual evolutionary process undertaken during the simulation demonstrates rudimentary *symmetry making* or *breaking* since motors are actually considered in the model to be part of the bodyplan. Thus it signifies how evolution can and will hone in on particular body-symmetries given the niche of the evolving agent. For those cases where a full bilateral motor symmetry was not evolved, the animat either emerged to employ an alternative movement mechanism, as highlighted by the behavioural screen shots in Figs. 6.8 and 6.9, or a motor may not have been active at all, even when specified to be active by the genotype. This latter point is expanded upon below.

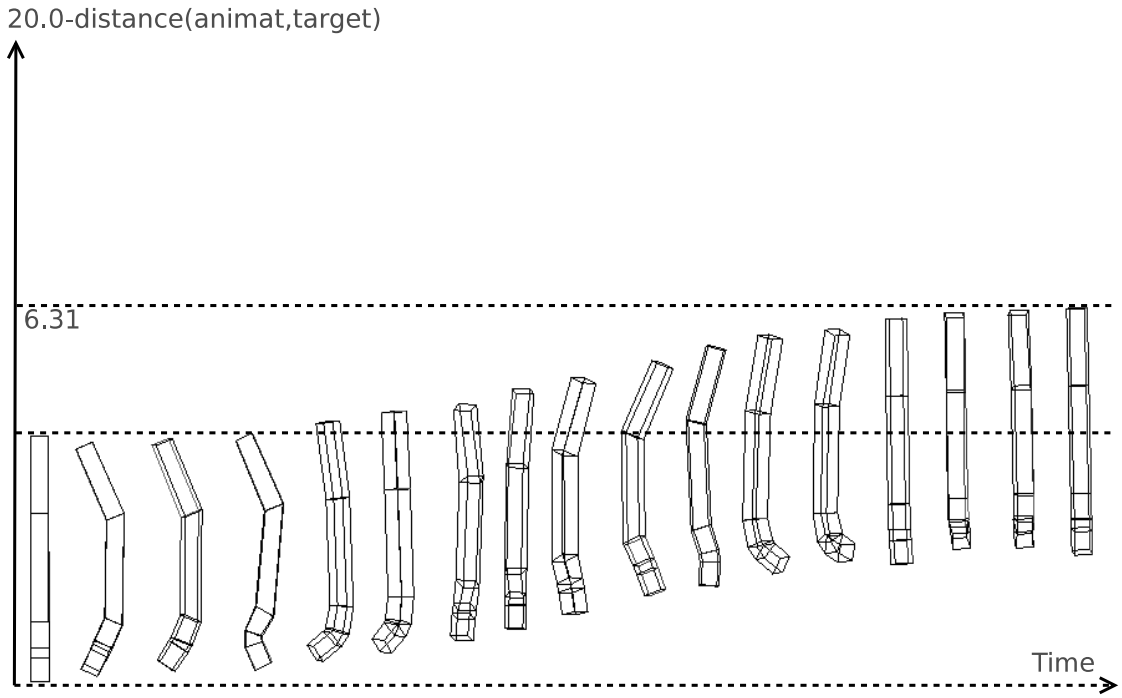

Figure 6.8: Animats to have emerged from evo-ALL with motor symmetries 1100. Seen to 'corkscrew' through time, spinning around the central axis.

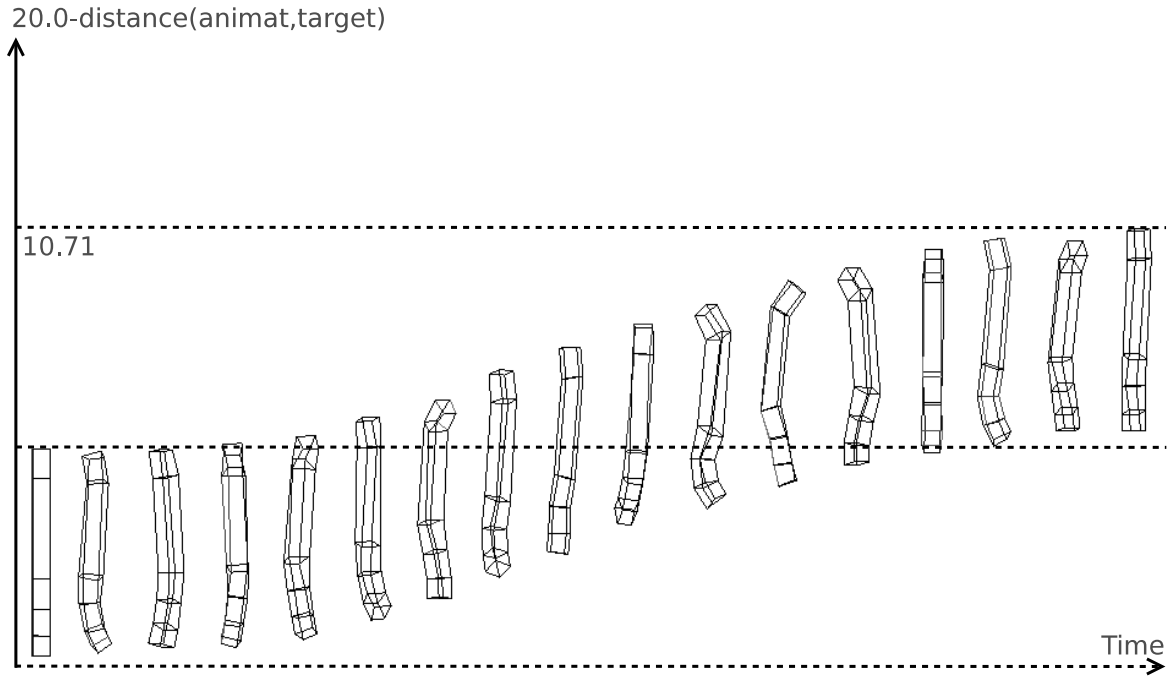

Figure 6.9: Animats to have emerged from evo-ALL with motor symmetry 1111. Again, seen to 'corkscrew' through time, spinning around the central axis.

Firstly, for those simulations that generated the fittest individuals, visualisations of the evolving motor symmetries are plotted in Fig. 6.10. A full bilateral motor symmetry arises early in all four examples, however, there are marked 'pockets' of individuals having a 0111 configuration, in particular from generation 700 to around generation 780 in evo-ALL and from generation 130 to 160 in evo-NOBL. These regions are indicative of evolutionary events such as a mutation and/or a recombination causing 0101 configurations to become 0111 configurations but with a minimal impact on population fitness. The following hypothesis attempts to shed light on this. In some instances, an 'active' side of the animat having motors that are genotypically established to play a part in movement may in fact consist of motors that remain 'computationally dormant'. That is to say, even though they could play a part in movement, they actually generate zero activity. Consequently, such motors have no bearing on movement behaviour. This has been confirmed by taking an individual from the grey region of Fig. 6.10a with motor symmetry 1101 and setting the first integer to 0 (i.e., the genotype was fixed from 1101 to 0101); this made it impossible for represented motors to have any active role in movement. If important, this change would have drastically degraded fitness, however, the result suggested otherwise, given an actual fitness impact of zero. In other words, only two out of the three 'active' animat faces ever had computationally active motors. Importantly, this tells us that more individuals may have emerged to be bilaterally symmetric than the genotype specifications alone (Fig. 6.7 and Table 6.2) are able to indicate. Note therefore that the readings only give an approximate indication of the symmetry phenotype.

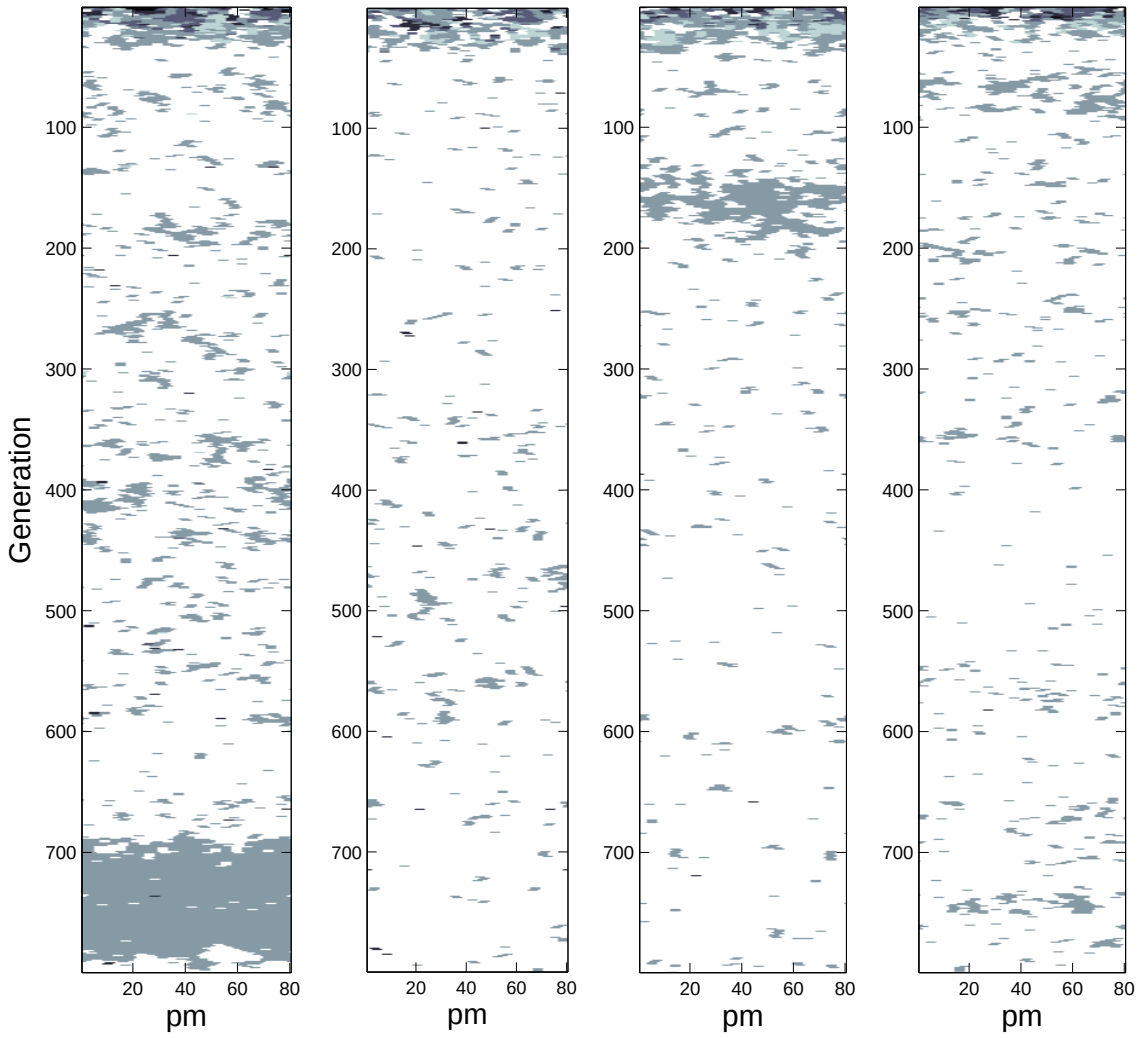

(a) evo-ALL (b) evo-NOBC (c) evo-NOBL (d) evo-NOBCBL

Figure 6.10: Each graphic represents how evolution tuned the motor symmetry for each best simulation. The 'best simulations' are those that generated the fittest individuals for the different setups. Note: pm=population member. The level of grey represents the type of motor symmetry to have emerged. 'White' represents those population members that have full bilateral symmetry. The flecks of light grey throughout are individuals having a '3' or '4' type motor symmetry (refer to legend in Fig. 6.7).

6.5.2 Effect of evolving the number of body segments

Fig. 6.11 tells us that a body segment count of ≈ 5 is optimal (note data has not been plotted for evo-NOBC and evo-NOBCBL, since the number of segments is fixed to 5 in these two cases). In order to check the importance of this, 30 additional simulations were conducted in which the agents were fixed to having 10 body segments (i.e. more than normal). In this case, the performance was found to be significantly worse than in the original evo-NOBC (5-segmented) setup when performing a ranksum test, see Fig. 6.12. Nevertheless, the fittest individual to emerge had a fitness of 10.61 (rounded to two decimal places), which is higher than many of the 5-segmented individuals. The agent is further able to undertake partial undulatory movement, see Fig. 6.13.

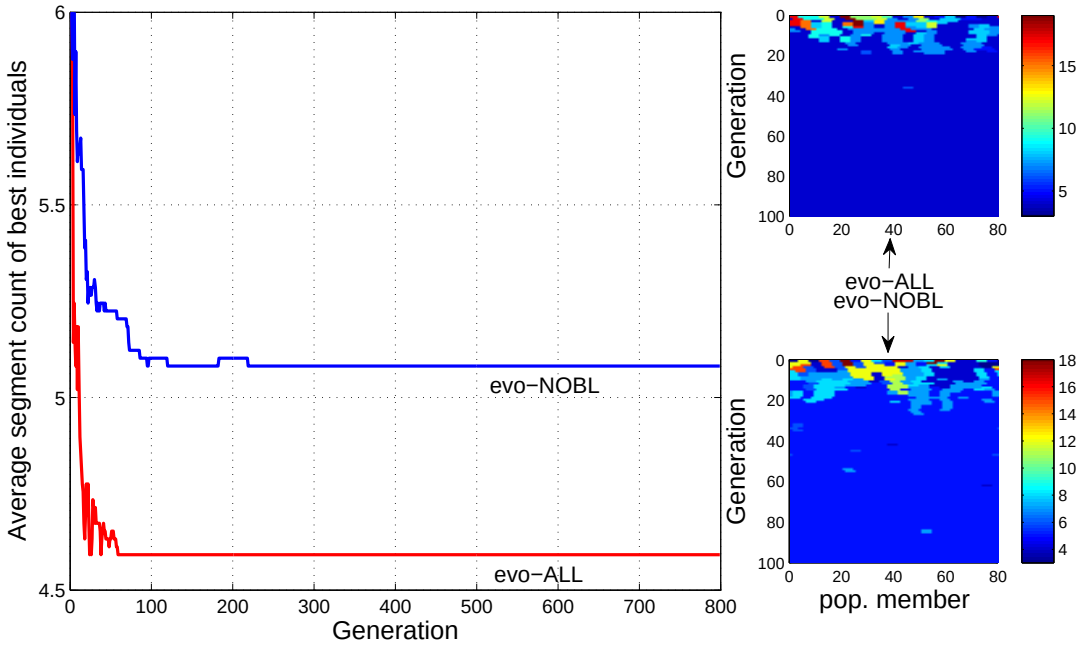

Figure 6.11: *(left):* Averages of best segment counts for evo-ALL and evo-NOBL; *(right):* Evolutionary emergence of segment count for best simulations, first 100 generations (y-axis is generation, x-axis is population member). Both show quick convergence to 4 and 5 body segments respectively.

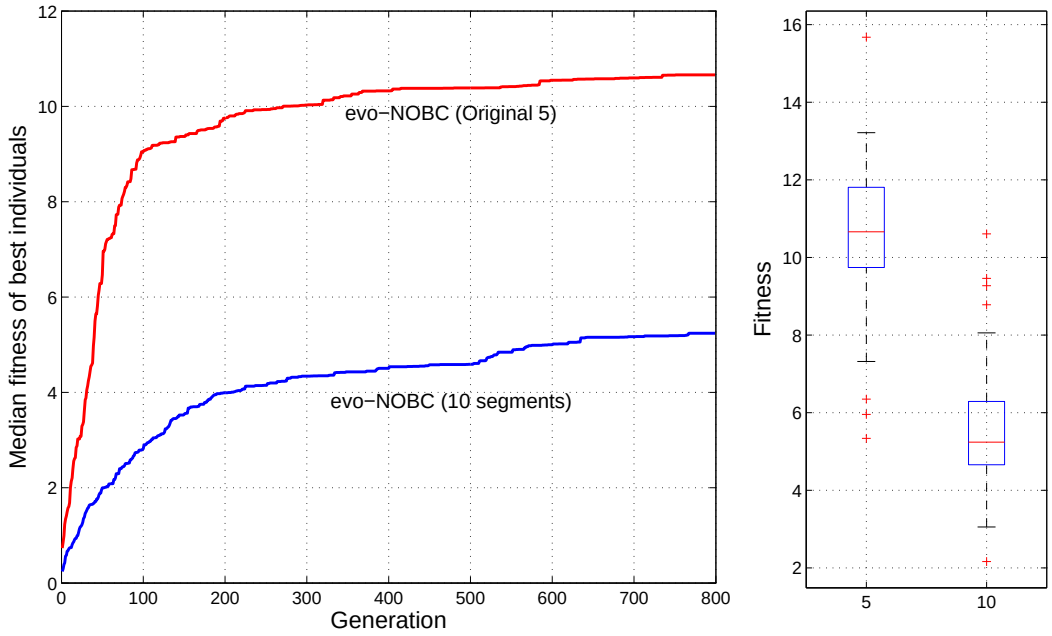

Figure 6.12: A comparison in fitness between the original 5-segment evo-NOBC simulations and the newer 10-segment evo-NOBC simulations during (left) and after (right) evolution.

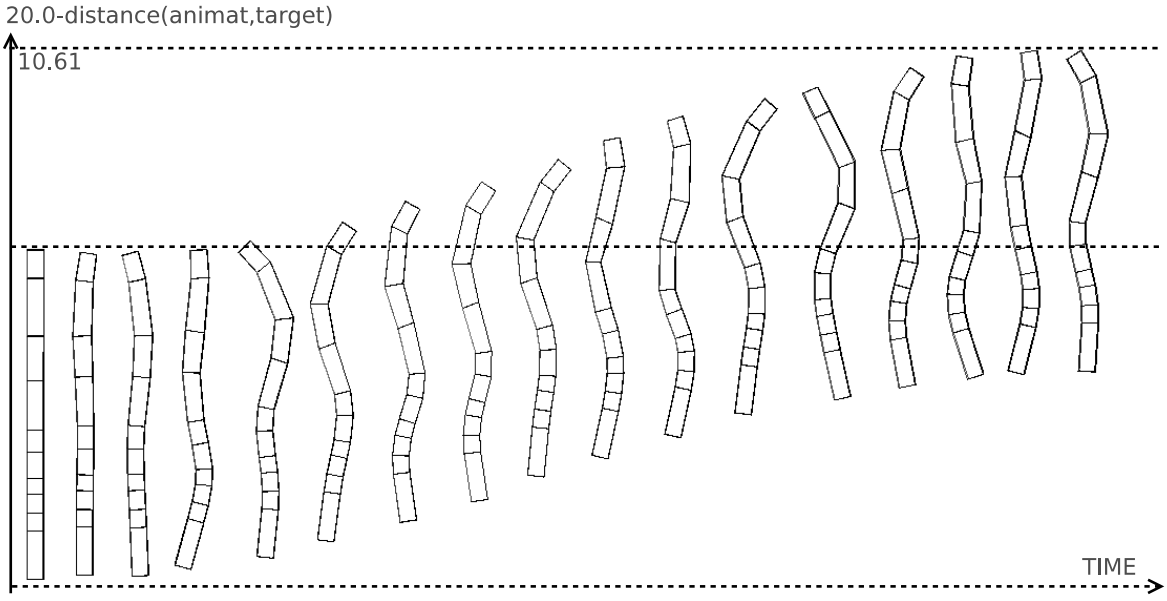

Figure 6.13: Undulatory movement shown for the best animat to have emerged in one of the evo-NOBC (10 segments) simulations (every 25 behavioural iterations).

Generally, the above results indicate some difficulty in evolution finding successful controllers for agents having many (≈ 10) body segments. This corroborates the finding that evolution hones in on a relatively small number of body segments. The actual reasoning for this difficulty is however less clear. A couple of hypotheses attempt to explain it:

- **Hypothesis 1:** An animat with more body segments is heavier since there are more point masses to be moved around. Therefore, evolution converges on fewer segments in order to reduce mass. But this seems unlikely given that an individual with a relatively decent fitness (10.61) was seen to emerge, so technically, it is possible for the extra mass to be moved around.

- **Hypothesis 2:** The undulatory wave necessary for movement is essentially built out of segmented central pattern generators (one per segment) meaning that it should take longer to propagate in agents having more body segments. This is problematic since the evaluation period is time-limited meaning that it could terminate before the agent is allowed to properly engage in undulatory locomotion. In line with this, we should find that for the many-segmented agents, the neural activities have longer wavelengths (and therefore lower frequency) since this would indicate less regular motor actuation and reflect the longer period of time it takes to propagate the undulatory wave. To evaluate this hypothesis, measures 'oscillatory count', and 'oscillatory period' are plotted in Fig. 6.14[1]

Statistically, a ranksum test indicates a higher oscillatory count for the 5-segmented agents (Fig. 6.14a), but there is no statistical difference in the oscillatory period (Fig. 6.14b). Therefore, for the 10-segmented agents, the lower oscillatory count does not cause a proportionate change in the oscillatory period. In other words, the agents are not actually engaging in any proper neural activity; the neural activities are just lesser.

Thus, for many-segmented agents, evolution evidently struggles to find neural controllers that are capable of yielding the correct oscillatory dynamics. This is further visualised for the best '10-segment' simulation in which a very narrow optimal selection lineage is correlated to a very narrow optimal level of neural dynamic. See Fig. 6.15. This narrowness highlights

[1] Oscillatory count is defined as the number of times that a neuron's activation changes from a positive state to a negative state or from a negative state to a positive state; oscillatory period is the time taken between a pair of oscillations. These definitions are more formally defined in Section 5.4 (Eqs. 5.17, 5.18 and 5.19).

a fitness landscape in which finding the optimal solution is like trying to find a needle in a haystack.

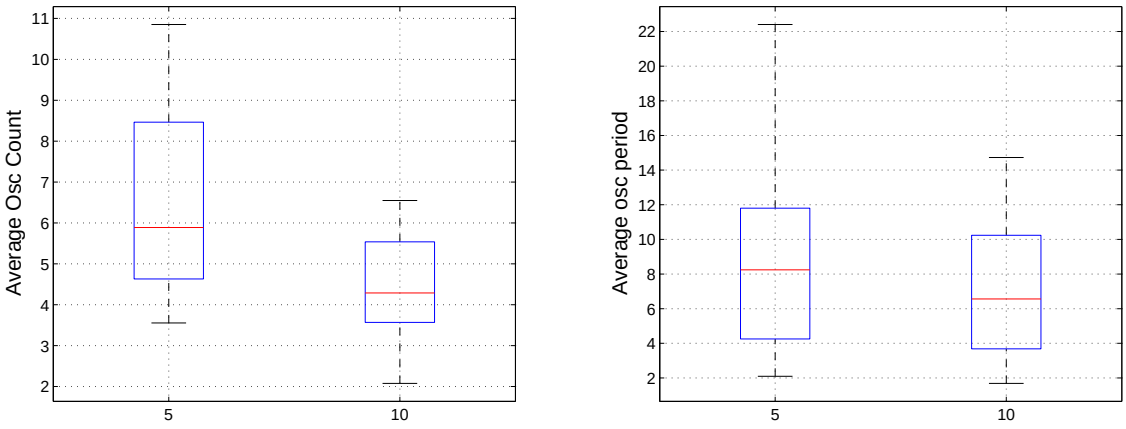

(a) Oscillatory count ('frequency')

(b) Oscillatory period ('wavelength')

Figure 6.14: A comparison of neural activity statistics for 5- and 10-segmented agents.

6.5.3 Effect of evolving segment lengths

In our "General Findings" (Section 6.4), we noted the positive effect that segment length has on agent fitness. From Figs. 6.16 and 6.17, we can elucidate these findings, noting that:

1. Segment length-factor 2 is 'maximised' to around 2.0. This results in segment 2 becoming the longest of body segments.

2. Segment length-factor 5 is 'minimised'. This results in segment 5 becoming the shortest of all body segments.

3. All other segment length-factors are optimised to around $<= 1.0$.

Having noticed evolution's tendency to maximise segment length-factor 2, we can look at the emergence of this property alone. Thus, the evolutionary emergence of this single feature for the very best individuals has been plotted in the smaller right-hand subplots of Figs. 6.16 and 6.17. As shown, convergence on a high value (≈ 2.0) occurs early (within 30 or so generations; only the values for the first 100 generations are plotted since there are no latter changes). Given this and the above three points, we are thus presented with a deepening picture of how segmentation within Evo-Critter becomes characterised and how such patterning affects fitness.

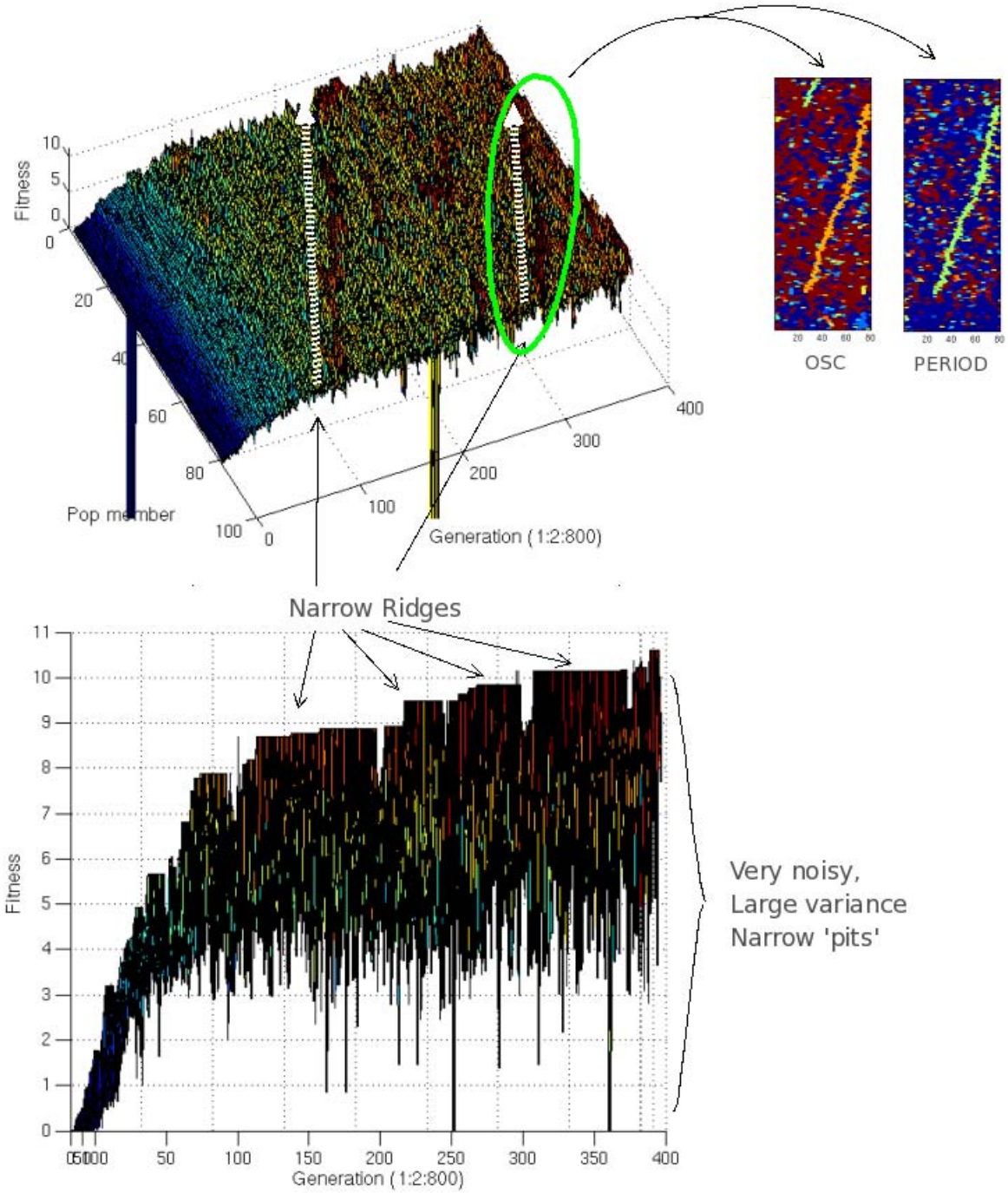

Figure 6.15: A visualisation of how fitness changes for the evolution of the best 10-segmented agent simulation as shown from two different angles. Three features are highlighted: (a) very narrow 'paths' of high fitness (marked with arrows); (b) these paths equate to optimal levels of neural activity (indicated by the top right snippets which are visualisations of 'oscillation count' and 'oscillation period' for the area circled); (c) as highlighted by the lower plot, deep 'pits' of low fitness indicate local optima in the fitness landscape.

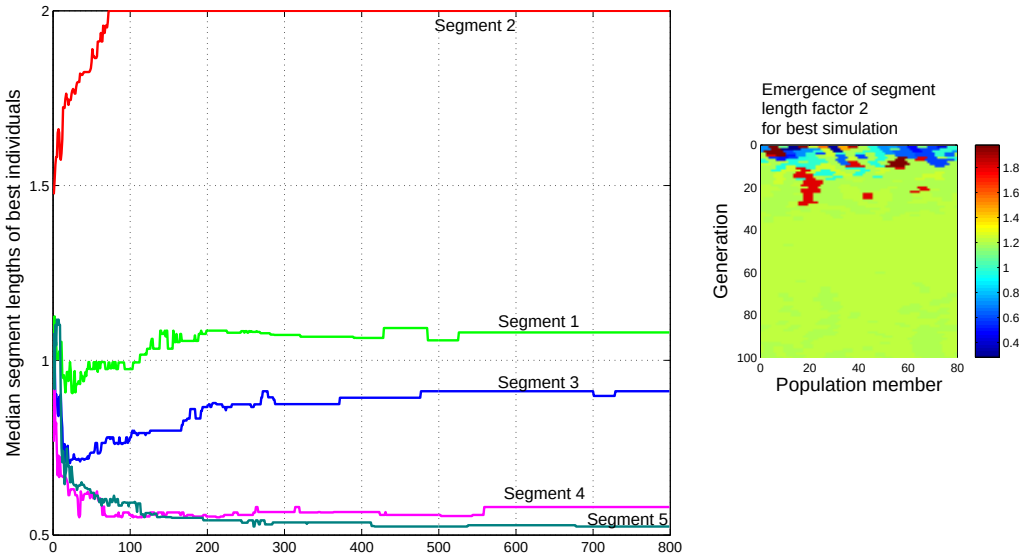

Figure 6.16: Medians of best individual segment lengths for evo-NOBC. The evolutionary emergence of segment length-factor 2 is further plotted to the right of the line graph. Only the first 100 generations are shown, since convergence is quick.

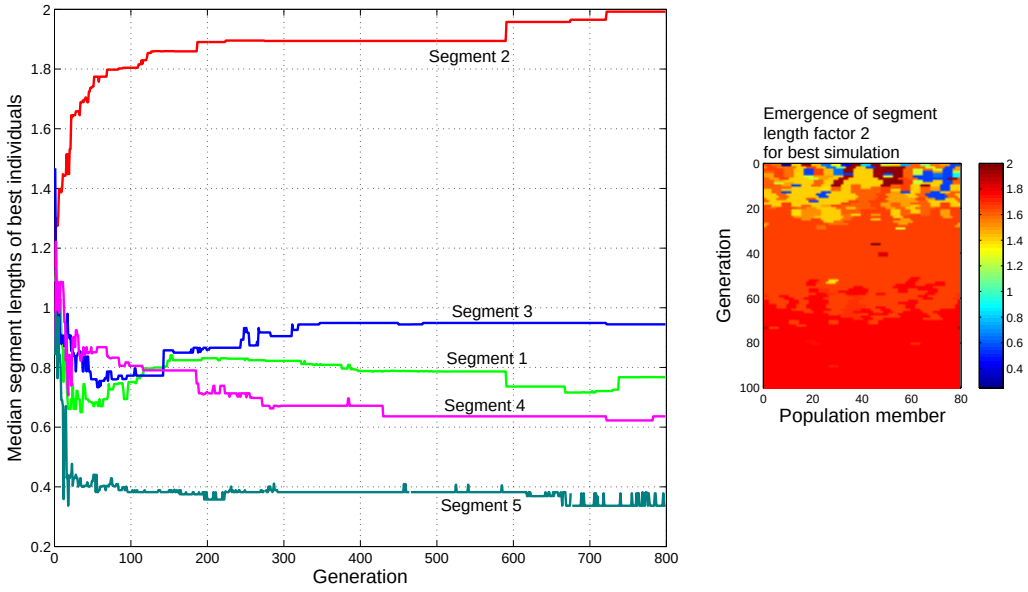

Figure 6.17: Medians of best individual segment lengths for evo-ALL. The evolutionary emergence of segment length-factor 2 is further plotted to the right of the line graph. Again, only the first 100 generations are shown, since convergence is quick.

Let us now analyse how segment length might be having an effect on agent fitness. Three hypotheses are explored below:

1. **Hypothesis 1: Water force**. Varying the length of a body segment affects its surface area. This alters the interaction of the surrounding 'water' (refer to the A term in Eq. 5.9). Hypothetically, it is possible that this is 'pressuring' the segment length patterning to evolve in a particular way. In order to test this hypothesis, the evo-NOBC experiments have been repeated 30 times (for significance testing), but this time, the A term in Eq. 5.9 of the water force model has been omitted, so that the force, $\mathbf{w}$, exerted by the water on a given face of a given body segment, becomes $\mathbf{w} = \mathbf{f}cd$. This eradicates any possibility that the area of a segment (which is larger when the segment is longer) can affect the force exerted by the water[2]. When comparing the median fitness of the first 30 individuals of the original evo-NOBC experiments and the median fitness of the 30 evo-NOBC_wa (without area) experiments, both at the end of evolution

   evo–NOBC = 10.661 (to 3 decimal places)
   evo–NOBC_wa = 12.635 (to 3 decimal places)

   ranksum tests indicate significant differences (at the 0.001 level). This indicates that, given the water force model, area has a significant physical effect on the fitness of the agent. The fact that fitness is 'better' in the unrealistic evo-NOBC_wa case is not surprising given that the area ('A') term in Eq. 5.9 would ordinarily see an increase in the water's drag; by removing it, the drag is artificially lessened and the agent can swim further. However, in terms of the lengths of the individual segments, when compared with the original evo-NOBC results, no differences are seen to emerge in the general patternings. This suggests that water force is not responsible for the observed segment length patternings.

2. **Hypothesis 2: Agent kinematics.** Varying the length of a body segment will change the natural resting length of each constituent spring. This will alter the physical spring properties, due to alterations in their tensile and compressive strengths, etc. These changes will impact on agent kinematics, dictating how efficient the agent will be able to locomote. Thus it is hypothetically possible that the segment length patternings observed emerged in order to facilitate optimal movement. In fact, this is highly likely

[2]Note of course, that when we do this, any notion of physical realism is destroyed.

given our findings so far: **firstly**, the finding that the simulations incorporating segment length evolution alone (evo-NOBC) yielded significantly better swimmers than any of the others; **secondly**, the conclusion that the area term used in the water force model is not an implicated factor. Thus, the only other possibility is neural distribution. So, let us take a moment and explore this third possibility before deciding one way or the other.

3. **Hypothesis 3: Neural distribution.** Varying the length of a body segment constrains the geometrical 'spread' of the resident neurons (lengthening increases the spread; shortening compresses the spread – see Eq. 5.10). It is therefore possible that the general segment length patternings observed are actually helping to establish the optimal neural spread and therefore the optimal neural architectures necessary for optimal CPG dynamics. However, if all a good Evo-Critter needed was an optimal neural architecture, then it should be possible for evolution to find those optimal neuron structural parameters that can yield fit individuals without also incorporating the length-factor model. However, this would appear difficult given the simulations in which the lengths of the individual segments were not evolved, in which the fitnesses were typically lower (refer to "General Findings" above – Section 6.4). In other words, evolution of neural morphology parameters alone could not yield individuals as fit as those in which the lengths of the segments were evolved. Also, an additional experiment in which the effect of Eq. 5.10 was turned off, but one in which the segment length-factors were still evolved, was found to have no significant bearing on fitness (results not shown). This rules out the neural distribution as a 'force' in shaping the observed segment length patternings.

Therefore, only the second hypothesis is reasonable. Thus in conclusion, we can argue that the segment length patternings observed for the original experiments emerged to facilitate and bring about optimal agent kinematics.

6.5.4 Effect on neural architecture

In Fig. 6.18, the neural architectures for the best individuals to have emerged are visualised. There are **several observations** to be made. **Firstly,** there are no connections between the sub-network architectures (one sub-network per body segment). This indicates a preference for fully decentralised, computationally independent sub-networks. Moreover,

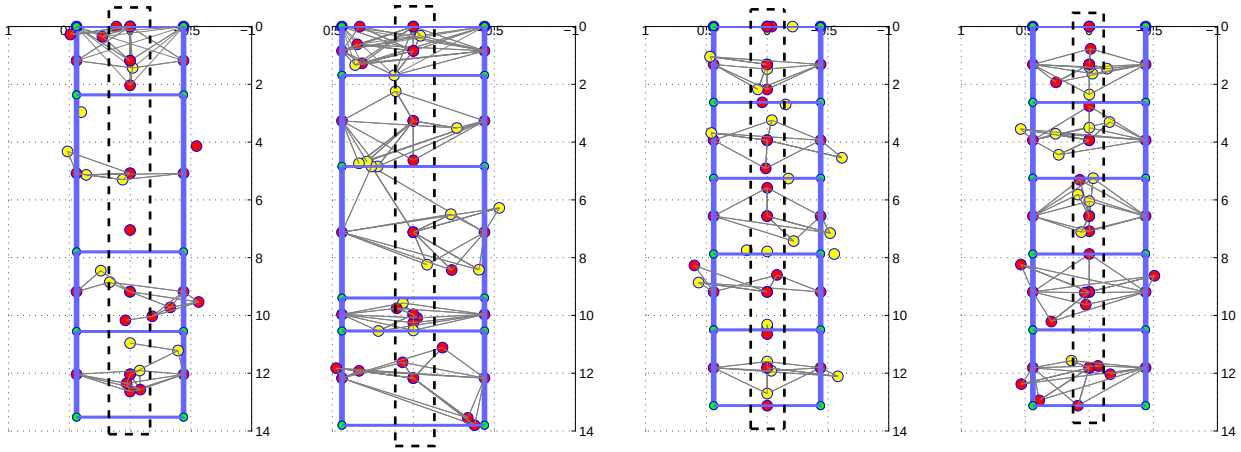

(a) evo-ALL (b) evo-NOBC (c) evo-NOBL (d) evo-NOBCBL

Figure 6.18: Best of the best neural architectures. In all architectures, there was a general tendency for neurons to arrange themselves (via evolution of positional information) around a central axis of the agent. These arrangements are highlighted with dashed rectangles.

when connections are artificially added to such agents, fitness decreases in proportion to the number added (results not shown). **Secondly**, in all cases, few connections were established from the sensory neurons. In instances where connections did emerge, it seems doubtful that the sensory neurons were actually employed, since a simple test in which the target object was removed from the environment subsequent to the evolutionary process found that agents could still successfully locomote. Thus, most agents (if not all) evolved without a true sensory system. The distribution of sensory information is explored more fully in the following chapter. **Thirdly,** the neural architectures typically emerged such that 'functional neurons' – those that became connected within the individual neural circuits – arranged themselves around a 'central axis'. This tendency is highlighted for the four architectures presented in Fig. 6.18

We can also observe differences in wire length, with evo-ALL agents evolving to have shorter connections than agents from the other simulations, see Fig. 6.19 and Table. 6.3. The most significantly different are **(i)** evo-ALL and evo-NOBC and **(ii)** evo-ALL and evo-NOBCBL. The least significantly different are evo-NOBC and evo-NOBCBL. These differences are interesting for the fact that they do not tie in with the statistical differences in fitness (Table. 6.3), in which **(i)** evo-ALL and evo-NOBL, **(ii)** evo-NOBC and evo-NOBL and **(iii)** evo-NOBC and evo-NOBCBL were all deemed significantly different at the same

0.05 confidence level. Thus specific differences in fitness are not reflected by differences in wire length. However it would seem that generally, connectivity has a tendency to emerge minimally in all cases and more so in evo-ALL.

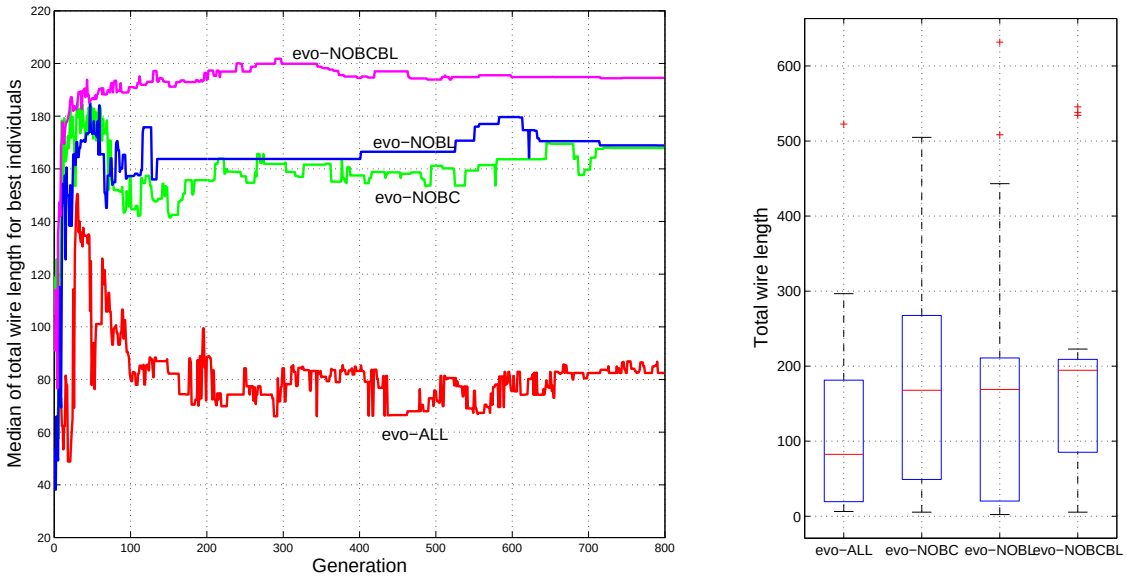

(a) (b)

Figure 6.19: Total wire lengths for the best individuals (a) during evolution and (b) subsequent to evolution.

Comparison	evo-ALL	evo-NOBC	evo-NOBL	evo-NOBCBL
evo-ALL	-	0.0072	0.1725	0.0018
evo-NOBC	-	-	0.1840	0.8590
evo-NOBL	-	-	-	0.2190

Table 6.3: Statistical p-values generated from comparisons in best agent wire length (ranksum test, 0.05 confidence level) at the end of evolution.

6.5.5 Neural and motor activities

Evaluating the neural and motor dynamics allows us to establish which of the four types of agent (evo-ALL, evo-NOBCBL, evo-NOBC, evo-NOBL) evolved to become the most 'computationally active'. These evaluations are based on measures, 'oscillation count' and 'motor

contraction count'. Refer to Section 5.4 for definitions. The measures are then averaged over all neurons. Statistics of oscillation count and motor contraction count ('motor activity'), derived from the behaviours of all agents, are plotted in Figs. 6.20a and 6.20b. Further, the neural activities of the best agents are plotted in Figs. 6.21 and 6.22. The main discoveries are itemised below:

- With regards to Tables. 6.4 and 6.5, we can clearly observe statistical differences in comparisons **(i)** evo-ALL vs. evo-NOBL, **(ii)** evo-ALL vs. evo-NOBCBL, **(iii)** evo-NOBC vs. evo-NOBL and **(iv)** evo-NOBC vs. evo-NOBCBL**.** Except for the comparison **evo-ALL vs. evo-NOBCBL,** these differences correspond to differences in fitness (refer to Table. 6.1).

- Since we have already observed above (Section 6.5.4) that differences in neural wire length *do not* strictly correspond to differences in fitness, it follows that differences in neural wire length (i.e. connectivity) are not responsible for the observed differences in neural dynamics. Thus the differences that we observe in neural dynamics must be due to other architectural properties, for example, the extent to which neurons align themselves around the central axis of the agent and/or computational properties, for example, whether or not neurons are inhibitory, their time-constants, and their bias values.

- With regards to Fig. 6.20a, we can observe that neural activity is statistically greater in simulations evo-NOBL and evo-NOBCBL than in evo-NOBC and evo-ALL. Also, with regards to Figs. 6.21 and 6.22, we can observe that actually, neural activity is minimal in all types of agent, given the limited number of neural circuits exhibiting at least *some* neural activity, but less prominently so in the evo-NOBL and evo-NOBCBL agents. This signifies that for agents in which the lengths of the segments are not evolved, movement kinematics become constrained to the extent that neural activity has to compensate. This consolidates the hypothesis that segment lengths are evolved to facilitate optimal agent kinematics as originally considered in Section 6.5.3.

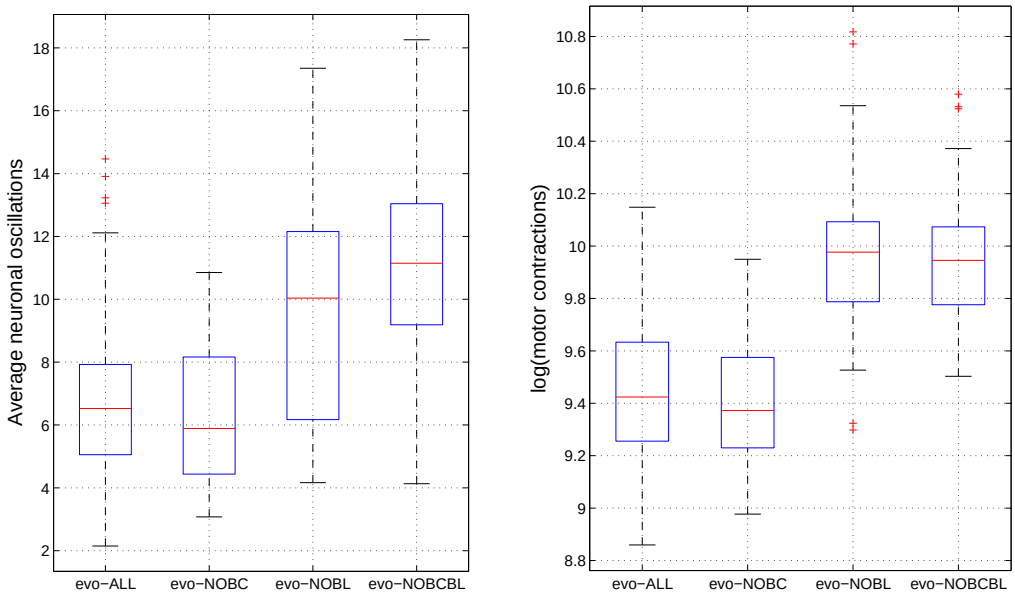

(a) (b)

Figure 6.20: (a) A box plot of neural activity for best individuals at the end of evolution; (b) A box plot of motor activity for best individuals at the end of evolution (note: a logarithmic scale is used in order to put the values into a sensible range).

Comparison	evo-ALL	evo-NOBC	evo-NOBL	evo-NOBCBL
evo-ALL	-	0.3919	0	0
evo-NOBC	-	-	0	0
evo-NOBL	-	-	-	0.0259

Table 6.4: Statistical p-values generated from comparisons in best agent neuronal oscillation counts (ranksum test, 0.05 confidence level) at the end of evolution.

Comparison	evo-ALL	evo-NOBC	evo-NOBL	evo-NOBCBL
evo-ALL	-	0.8229	0	0
evo-NOBC	-	-	0	0
evo-NOBL	-	-	-	0.8646

Table 6.5: Statistical p-values generated from comparisons in best agent motor contraction counts (ranksum test, 0.05 confidence level) at the end of evolution.

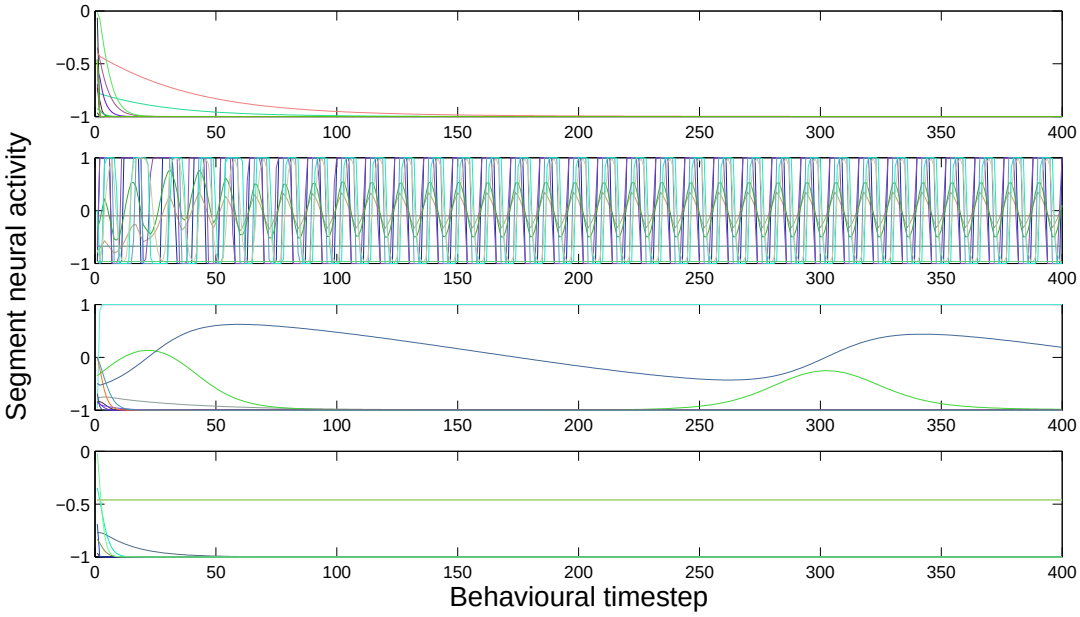

(a) evo-ALL

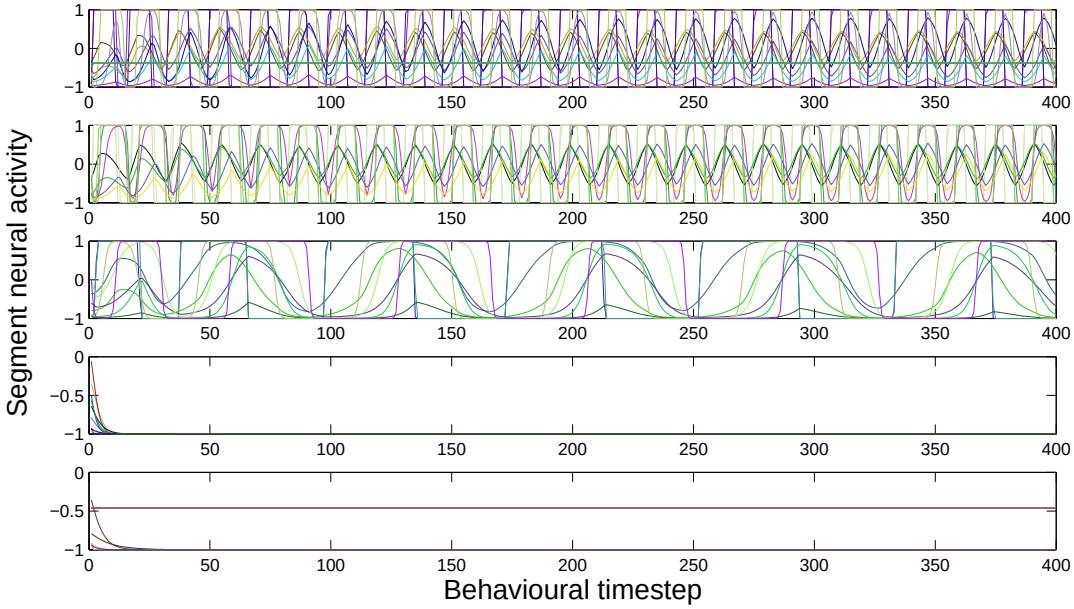

(b) evo-NOBCBL

Figure 6.21: Neural activities of the very best individuals from simulations evo-ALL and evo-NOBCBL. Each horizontal bar represents the neural activity in one body segment (the fittest evo-ALL agent emerged to have only 4 body segments).

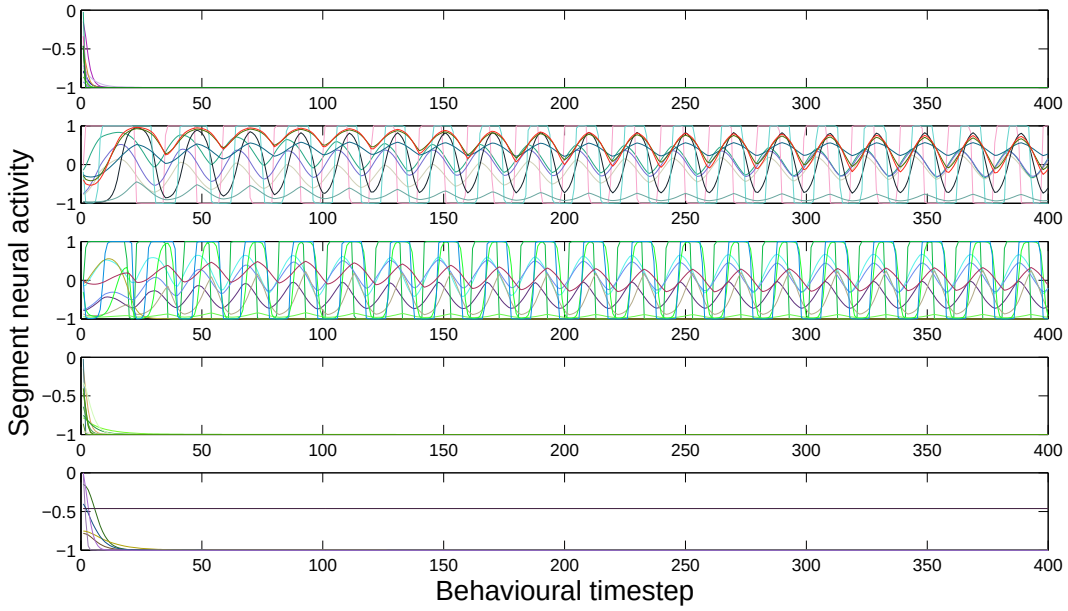

(a) evo-NOBC

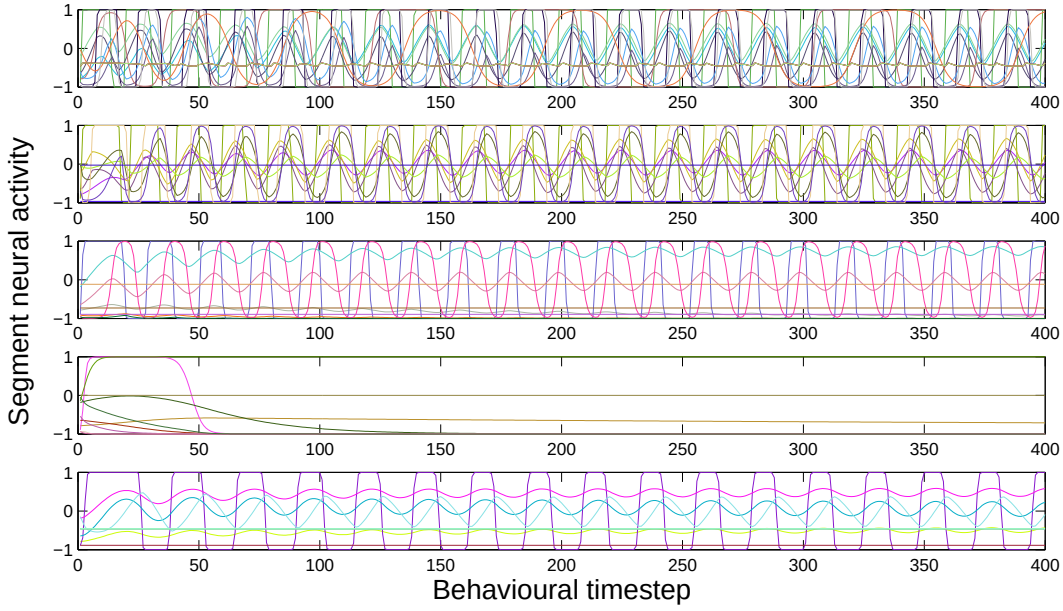

(b) evo-NOBL

Figure 6.22: Neural activities of the very best individuals from simulations evo-NOBC and evo-NOBL. Each horizontal bar represents the neural activity in one body segment.

6.6 Discussion

The results presented in this chapter pave the way in understanding how, for the evolution of a given animal or agent, neural organisation is constrained by the body plan morphology. Successful animal or agent behaviour will only emerge if these two components interact appropriately. It is further evolution's job to tune this coupling. In terms of this, let us begin by clarifying the main properties of the model:

1. There are two main components: the body plan morphology and the nervous system architecture.

2. Selection pressure can exert force on either component.

3. The two components are coupled together but this coupling is non-linear.

4. The actual strength of the coupling is also subject to selection forces.

Thus we can imagine how the two components are linked together via a two-headed arrow, with each head pointing towards a particular component. The level of evolutionary pressure exerted on a given component can be thought of as the width of the arrow head: the greater the width, the larger the pressure. Furthermore, the line connecting the two arrow heads can be thought of as a non-linear link representative of the coupling (see Fig. 6.23). We can then envisage how it is possible for evolution to exert pressure on both components, and on the link itself. Moreover, since it was demonstrated that the fitness landscape is often rough, and that evolution will often end up selecting in favour of a very narrow range of individuals (recall Fig. 6.6), it is likely that different combinations and levels of pressure will emerge throughout the evolutionary process (e.g., scenarios (A), (B), (C) and (D) in Fig. 6.23). In some cases, pressures on the different components, and on the coupling will all be equivalent (scenario A) but this is very unlikely given the complexity of the fitness landscape.

Thus before any evolutionary process has begun (i.e., immediately after random initialisation), all agent types will be subject to the equivalent pressures of scenario (A). Then, as the evolutionary process proceeds forward, the pressures change depending on the pre-existing constraints of the agent. For example, in terms of those agents not endowed with segment length evolution (which were demonstrated to be of significantly worse fitness than all other agent types) we might argue that scenarios (C) and (D) will happen more often given minimal flexibility in the evolvability of the body plan morphology, but greater flexibility in the

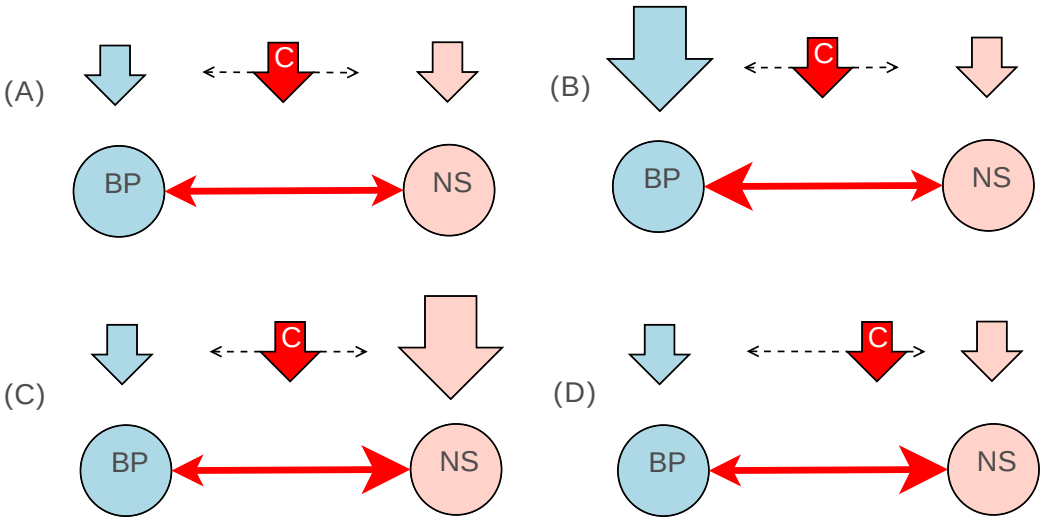

Figure 6.23: A diagram visualising several evolutionary selection forces: (i) force on body plan morphology (labeled BP), (ii) force on the nervous system architecture (labeled NS) and (iii) force on the coupling itself. The two-headed arrow connecting BP and NS represents a non-linear coupling. The width of an arrow head indicates the level of 'weighting' placed on the importance of a particular feature. The large vertical arrows represent environmental selection pressures (except for the middle red arrow, size represents the level of pressure). (A) through (D) represent possible combinations and levels of different types of selection pressure: (A) all pressures are 'equal'; (B) more pressure is placed on the body plan morphology; (C) more pressure is placed on the nervous system architecture; (D) pressure on the coupling results in a higher level of change in the nervous system architecture than in the body plan morphology. Changes along the coupling are complex (as demoted by 'C').

evolvability of nervous system organisation. On the other hand, scenario (B) is likely to more often occur for those agents that are endowed with segment length coevolution since they have greater flexibility in what parts of their body plan characteristics can be evolved.

Thus, we can conjecture that depending on the type of constraint in the body plan morphology – or viewed differently, depending on the level of permitted flexibility – various levels of 'pressure' pre-exist. In other words, based on the constraints set *a priori,* evolution's search for optimal behaviour is easier or harder from the outset. In terms of segmentation characteristics, we can argue the following:

1. when the lengths of the segments are tuned by evolving the segment length-factors, then based on the better behavioural fitness values that we observed, the pressures existing within the framework are favourable from the outset. When the segment length-factors are not evolved, the pressures are less favourable, however, a combination of different types of pressure then results in statistically greater neural activity with the result that

reasonable agent behaviour is still attainable.

2. when the number of body segments is evolved or fixed to a non-optimal value, the evolutionary selection pressures are 'finely balanced' when striving to attain or maintain fitness; we can observe this in terms of the narrow paths of optimal selection as visualised in Figs. 6.5d, 6.6 and 6.15.

Having assessed the evolution of the body segmentation characteristics, we were led in Section 6.5.3 to the conclusion that a particular combination of segments each having a specific length, will facilitate agent movements because of better spring properties. This means that a tuning of the body plan morphology alone can have a very significant impact on fitness (or, in terms of tuning the number of body segments, a very detrimental impact), and this is before we even consider the computational effort made by the nervous system. In other words, much of the movement control can actually be offloaded to the dynamics of body morphology; but, in terms of Evo-Critter, the level of this offloading is potentiated or restricted depending on the constraints that we impose. The process of an animal offloading control to its body morphology is often referred to as *morphological computation* [98]. We will revisit this idea in the following chapter when we analyse how *computational process* is distributed between body plan morphology and the nervous system in agents endowed with sensory feedback.

We can extend the notion of morphological computation to an *event distribution framework*. We can define this framework in terms of signals propagating through the animal as it interacts with its environment. Thus it basically reflects how computational events trigger effector cells, or how the effector cells trigger parts of the nervous system whilst providing feedback. A description of the global process might be as follows: a signal arriving at an animal's sensor is propagated to the rest of the neural system which leads to the eventual actuation of a particular effector. This culminates in certain environment-changing behaviour (since all behaviour, no matter how marginal, will induce change in the environment). Finally, this 'behavioural loop' is closed when the changes are accordingly detected by the agent's sensory system. Now, in an animal or agent in which the coupling between its nervous system and body plan morphology is tightly integrated, the computational dynamics of one component will significantly impact on the dynamics of the coupled component. And this is expected to alter the efficiency of event distribution and therefore the ability of the agent to undertake correct behaviour.

In terms of the simulation results, in cases where segment lengths were not evolved, the body was subsequently observed to lack in its ability to react appropriately to the nervous system signals since the nervous system was observed to try and compensate – as it were, to try and get the signals through to the body plan morphology – by generating higher levels of neural activity. In this respect, the level of information process and thus, the distribution of computational process was altered. In situations in which the neural activity might be constrained by a need to minimise energy loss, this could be disadvantageous (since greater neural activity would require greater energy consumption). The idea of computational process distribution is investigated in the following chapter, and an investigation of energy as an additional constraining factor within the coupled neural-body system is investigated in chapter 8.

6.7 Conclusion

The contributions of this chapter are as follows. Firstly, an investigation of how the body plan morphology of an undulatory agent constrains the emergence of its neural architecture, the commensurate changes to neural dynamics and the effect on behaviour, has been provided. The work has demonstrated, using the Evo-Critter framework, that behaviour is affected by how the neural control system and body plan morphology become coupled together and that during certain evolutionary periods, varying pressures placed on different aspects of this coupling ensure that optimal behaviour can continue to emerge. Specifically, the contributions are as follows:

1. A demonstration of how segmentation characteristics impact on behavioural fitness: when the lengths of the body segments are coevolved, fitness is enhanced; on the other hand, when the number of body segments is coevolved, fitness is degraded. These findings contribute to an understanding of how segmentation characteristics in an undulatory agent affect behavioural fitness.

2. A demonstration that for agents endowed with a larger number of body segments, reaching reasonable behavioural fitness levels is harder; this was understood to be due to a 'lower level' of neural dynamics and moreover, due to the difficulty that evolution has in finding a 'needle in a haystack' solution. Hence the understanding that attaining optimal neural dynamics (and therefore optimal behaviour) in many-segmented agents

is difficult, is strengthened.

3. A demonstration that the coevolution of segmentation characteristics (or a lack thereof) has a direct influence on the emergence of motor symmetry. Thus, the findings contribute to how symmetry emerges during the evolutionary process.

4. The understanding that a particular combination of segments each having a specific length, emerges in order to provide optimal agent kinematics and further, that this combination has no bearing on the need to optimise neural architecture. Thus optimal behaviour is largely due to the body plan characteristics alone.

5. A demonstration that neural architectures emerge in a minimal fashion; that the total wire length is lower when all agent parameters are coevolved. Thus, in terms of evolutionary selection pressure, the emergence of neural architecture is shown to depend on the presence and subsequent evolutionary tuning of certain body morphology characteristics.

6. The finding that for agents whose segment lengths were not coevolved, neural activity is far higher; this demonstrates how the neural system has to dynamically compensate for the lack of kinematic flexibility.

These findings are significant because they bring to bear the rich couplings present between the nervous system, the body plan morphology, the symmetrical properties of the motors, and the environment. They highlight the impact that body plan morphology has on the emerging neural control system and the commensurate effect on neural dynamics. Moreover, the findings identify the 'how' of this impact. They demonstrate that much of the behavioural process can be offloaded to the body plan morphology, and crucially, that this can result in the emergence of minimal neural architecture. We can speculate that similar mechanisms are at play in nature.

Chapter 7

Proprioceptive Feedback and the Distribution of Computational Process

Synopsis

In the preceding chapter, it was demonstrated how for an undulatory agent, the coupling between body plan morphology and nervous system architecture emerges to potentiate optimal swimming behaviour. In the discussion, it was considered how this behaviour might be interpreted in terms of an *event based framework* in which the passive processes of the body interact with the computational processes of the nervous system; i.e. both components were observed to be dynamically coupled. In order to broach this within Evo-Critter, a notion of proprioceptive feedback has been incorporated, so that body kinematics can also influence the dynamics of the nervous system. Of course in the current model, the nervous system already affects the body kinematics due to effector actuation. With such an addition, it is expected that in terms of connectivity, the distribution of sensory information will emerge in a different way, since this will determine how the different processes (body kinematics and nervous system activities) become dynamically coupled; but the way in which this emergence should progress is less clear – the aim of this chapter is to find out. Specifically, we will investigate how such feedback **(i)** affects the distribution of sensory information, **(ii)** affects the balance of computational process between the nervous system and body plan morphology and **(iii)** affects the nervous system architecture. We will also examine proprioceptive feedback in the context of robust behaviour. Several of the findings outlined in this chapter are presented in [57].

The layout of this chapter is as follows: Firstly, in Section 7.1, background on proprioceptive feedback mechanisms is presented. Secondly, the changes that were made to the Evo-Critter model, in order that proprioceptive feedback could be incorporated, are outlined in Section 7.2. An experimental overview is provided in Section 7.3, and the results are presented in Section 7.4. An analysis of how the proprioceptive feedback mechanism affects the coupling between body kinematics and neural dynamics is provided in Section 7.4.1. Finally, a short discussion together with conclusions is provided in Section 7.5.

7.1 Background on proprioceptive feedback

The state of a given animal's external environment or niche is presented to the animal via its sensory system. This generates informational cues regarding for example, predator or prey items, allowing the animal's nervous system to invoke either pervasive or evasive behaviours. Typically over time, the animal is able to learn and adapt[1]. Higher animals also employ proprioceptive mechanisms enabling them to detect the current state of the locomoting body; these basically serve as feedback mechanisms for the underlying neural circuits. Previous studies have shown that central pattern generators (CPGs) responsible for the periodic movement control are all affected and constrained by such feedback, e.g. [89]. Other studies have highlighted how feedback can help undulatory organisms surpass a 'speed barrier' [47]. The necessity of proprioception in the peristaltic movements of *drosophila* larvae has also been established, without which, locomotion is seen to be significantly degraded [113]. In undulatory organisms, proprioceptive mechanisms are typically built around 'stretch receptors' located within the animal's body wall [43]: during movement, parts of the body undergo distension which, via the proprioceptive mechanisms, can then be detected and fed back to the nervous system. Thus, together with the sensory events emanating from the vision system, the sensory information that should propagate throughout the nervous system is richly dynamic; how this information is distributed and processed will ultimately effect the behaviour of the agent, therefore, the interconnectivity within the nervous system will need to be such that adequate distribution of this information can be facilitated.

We will pick up on the point of proprioceptive feedback, how it influences the 'flow' of information throughout the nervous system, and further, how this impacts on the dynamic

[1]Although note, for Evo-Critter, behaviour should only be considered in reactive 'Braitenberg vehicle' terms [22].

coupling between the passive dynamics of the agent kinematics and the computational dynamics of the nervous system. Thus, in the experiments that follow later, a comparison is made between two core simulations: one in which the agent is endowed with sensory feedback, and a second in which it is not. In both, the animat has an abstract visual system which it may or may not utilise depending on how the neural circuits become interconnected. As in the preceding chapter, the goal is for the evolved Evo-Critter agent to swim forwards towards a predefined target.

7.2 Simulation environment

The Evo-Critter framework was used for all of the experiments outlined in this chapter, but crucially, two additions/changes were made to the model in order that proprioceptive mechanisms could be incorporated: **(i)** an addition of the proprioceptive feedback mechanism itself and **(ii)** a change to the neuron model. These alterations are described as follows:

Proprioceptive mechanism The proprioceptive mechanism is based on a notion of stretch receptor activity, for example, that found in the leech [43]. Also, like the vision system outlined in Section 5.2.3, it is exponentiated, taking the amount of spring distension as input which, in order to maintain consistency in the way sensory information is processed, is then exponentiated to yield an input current, I_M,

$$I_M = \exp(\Delta d) \tag{7.1}$$

where Δd is the level of spring distension. The current I_M is then fed directly into the associated effector neuron. Thus, the higher the level of spring distension, the greater the level of feedback.

Change to the neuron model The neuron model introduced in Section 5.2.3 makes it possible for a neuron to exhibit some activity even when its membrane potential is zero. In terms of understanding the influence that proprioceptive feedback has on neural connectivity, this becomes problematic. To understand why, let us first recall Eq. 5.15,

$$a_i = \tanh(u_i - \beta_i)$$

The problem is basically this: because of the bias value, it is possible for a neuron to exhibit activity even when the membrane potential is 0. Thus neural activity within a collection of neurons could 'spontaneously' emerge even in the absence of any external input – the bias could trigger the neural dynamics. Now in terms of studying the effect of proprioceptive feedback in which we wish to focus on how connectivity should become distributed, this is problematic, since the need for connectivity from external devices such as effectors and sensors is inherently impacted upon. To counter this problem, the activation function is changed to the following formulation:

$$a_i = \begin{cases} \tanh(u_i - \beta_i) & |u_i| > 0 \\ 0 & \text{otherwise} \end{cases} \tag{7.2}$$

By making this change, actuators will only come 'alive' when triggered by one of three events: input from a pre-synaptic neuron, input from a sensory neuron, or, input from the proprioceptive system. It therefore prevents the above implementational artifact and allows connectivity to emerge in a way that reflects the effect of proprioceptive feedback.

7.3 Experimental overview

7.3.1 Research questions

Experiments were conducted to address the following questions:

1. How does proprioceptive feedback affect fitness?
2. What is the importance of having a correct proprioceptive mechanism?
3. How is the feedback mechanism together with the wire length related to optimal neural dynamics?
4. What impact does proprioceptive feedback have on the emergence of neural architecture?
5. How does feedback affect the dynamic coupling between the body plan morphology and the neural dynamics?

6. Does a feedback mechanism facilitate an agent's robustness to environmental perturbation?

7. Does a feedback mechanism facilitate an agent's robustness to neuronal perturbation?

Questions 1-4 are addressed in Section 7.4. Note some of question 3 is further addressed in Section 7.4.1 as is the whole of question 5; question 6 is addressed in Section 7.4.2, and question 7 is addressed in Section 7.4.3.

7.3.2 Methodology

Two sets of 40 experiments were conducted (for statistical significance) with each individual simulation being allowed to run for 800 generations. In the first setup, the animat was endowed with proprioceptive feedback. In the second, it was not. In both, the animat was required to swim forwards in order to reach a pre-defined target. The fitness function was simply $f = 20.0 - d_{target,animat}$ (i.e. the same environment as described in the last chapter). This setup was simple enough in order to explore how sensory information becomes distributed when the animat is endowed with particular feedback mechanisms. From this point on, agents that were evolved with proprioceptive feedback shall be referred to as 'with-agents' and agents evolved without proprioceptive feedback shall be referred to as 'without-agents'.

7.4 Results

In Fig. 7.1, we can see that with-agents performed significantly better than without-agents. We can secondly observe that a higher number of connections were required in without-agents, Fig. 7.2. A higher number of connections equates to higher connectivity between neurons in *adjacent* neural circuits, higher connectivity within *individual* neural circuits, and the presence of some connections from the *sensory neurons* located in the head of the animat. This is also reflected by differences in total wire length, Fig 7.3. Representative neural architectures are given in Fig. 7.4.

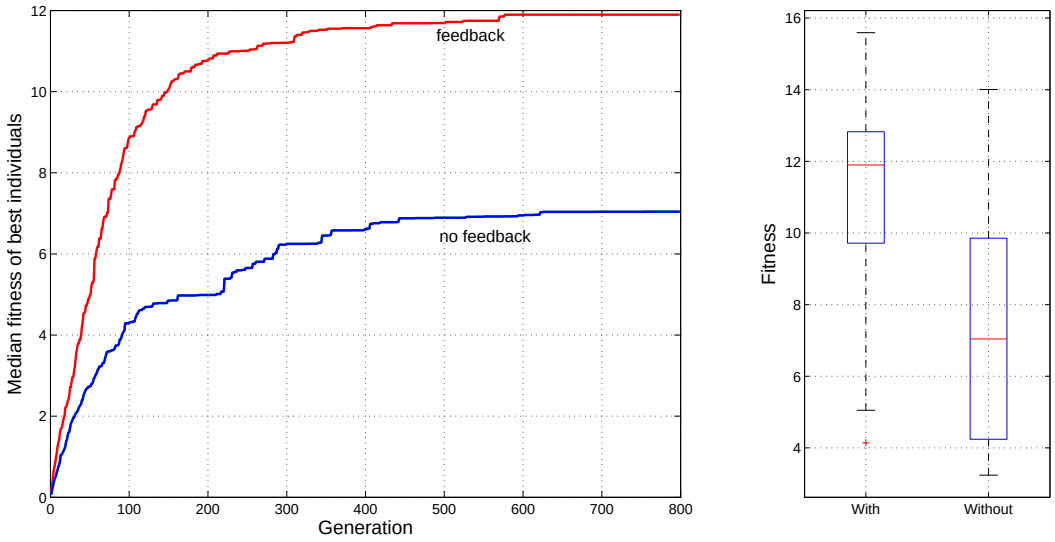

Figure 7.1: A comparison of median fitness through evolution calculated over all best individuals and subsequent box-plot after evolution. Differences significant at a 0.05 confidence level. Agents with feedback are shown to have emerged with significantly greater fitness.

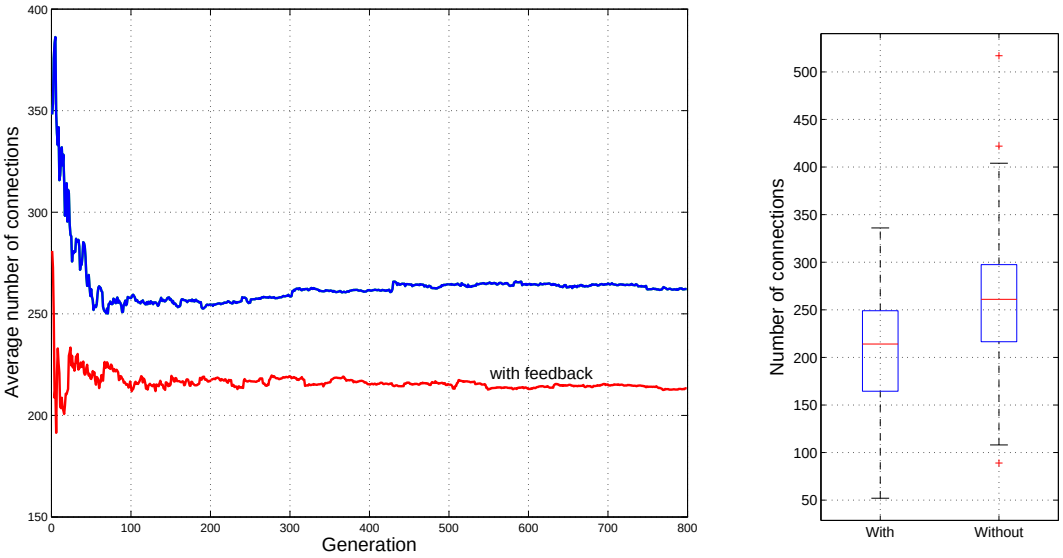

Figure 7.2: A comparison of mean connectivity levels calculated over all best individuals, and, subsequent box-plot after evolution. Differences are significant at a 0.05 confidence level. Agents with feedback are shown to have emerged with significantly sparser neural connectivity.

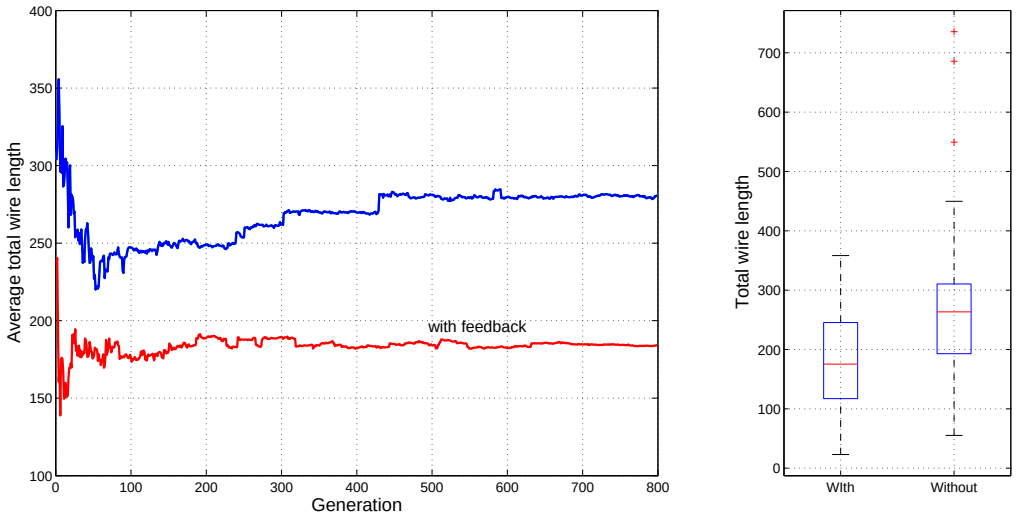

Figure 7.3: A comparison of mean total wire length calculated over all best individuals, and subsequent box-plot after evolution. Differences are significant at a 0.05 confidence level. Agents with feedback are shown to have emerged with less wire.

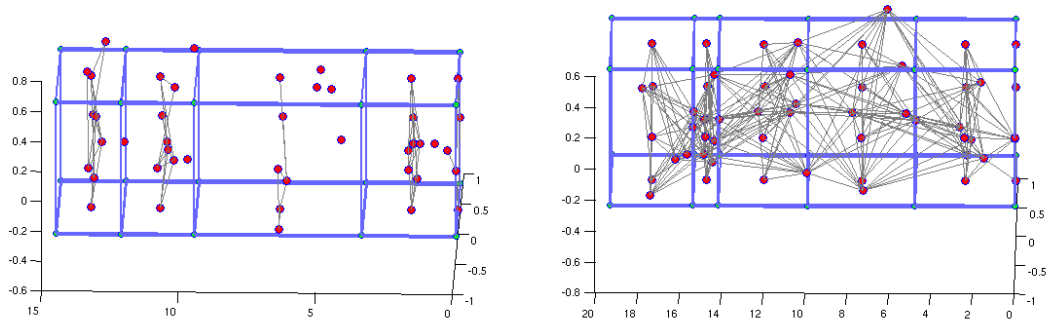

(a) With-agent (b) Without-agent

Figure 7.4: Example neural architectures to have emerged in both cases. We can see that in 7.4a, the neural architecture has emerged with sparse neural connectivity. By comparison, in 7.4b, the connectivity emerged to be far denser.

In Fig. 7.5, it is further shown how for several simulations, the evolutionary process exhibited 'paths' or 'lineages' of optimal selection. These equate to highly fit individuals which have been selected due to their optimal properties; and, given the above findings, these properties are likely to have been the wire length and connectivity level. We can further see in Fig. 7.6 that for each agent type, a selection 'path' emerging in the wire length space corresponds to selection 'paths' in the neural dynamics space, both of which then correspond to a path of high fitness, in the fitness space. This suggests that in the generation of optimal

behaviour, optimal wire length precludes optimal neural dynamics.

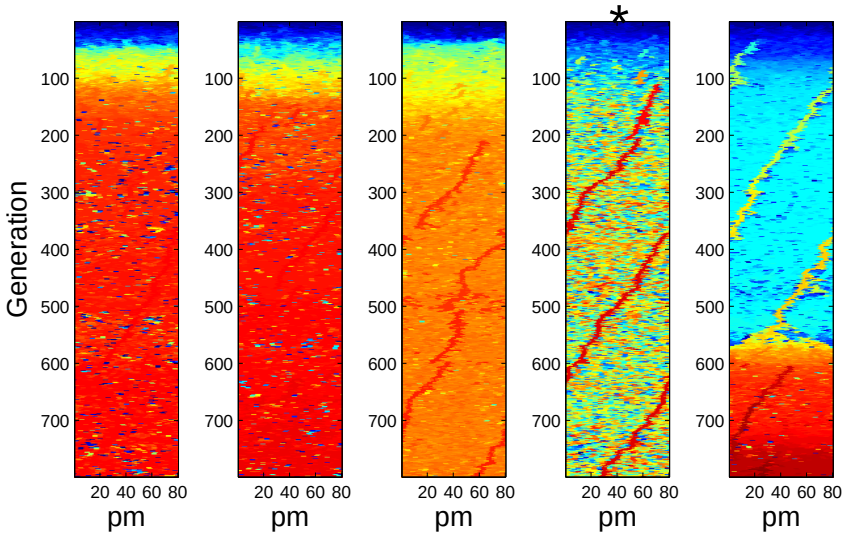

(a) With

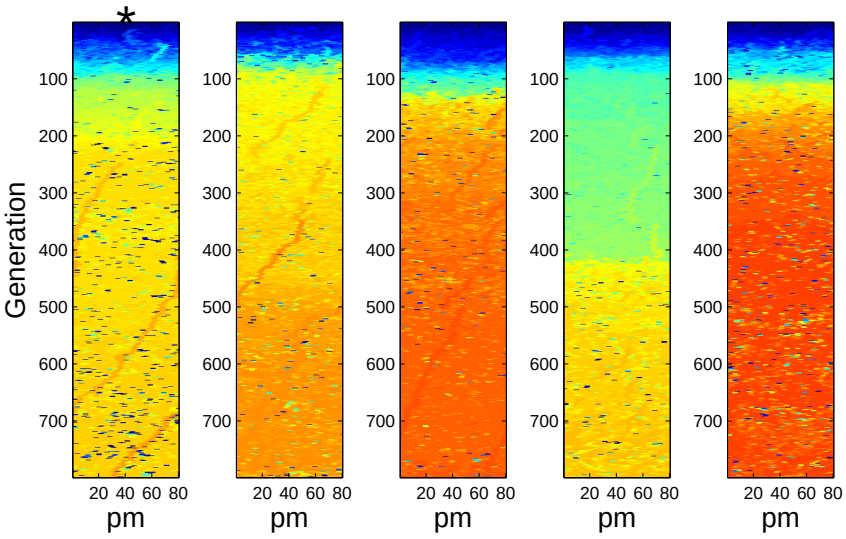

(b) Without

Figure 7.5: Representations of population fitness emerging for each of 5 simulations from each setup; note: pm=population member (total of 80 population members in each). Colour represents fitness with deep red being fittest and dark blue being least fit. Of interest are 'paths of selection' which can be clearly observed in strips 3-5 of 7.5a and to a lesser extent in strips 1 and 2 of 7.5b. Those marked with asterisks are compared to neural dynamics and wire length in Fig. 7.6.

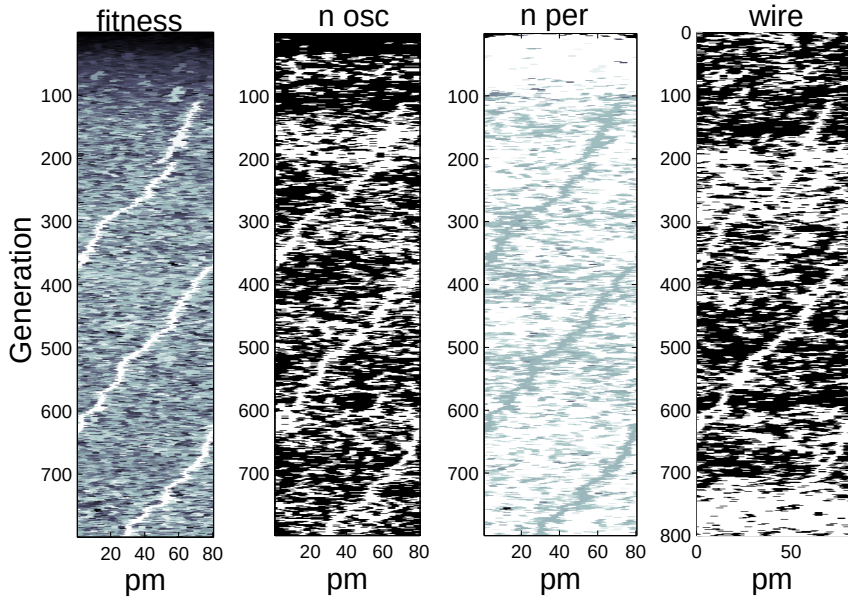

(a) With

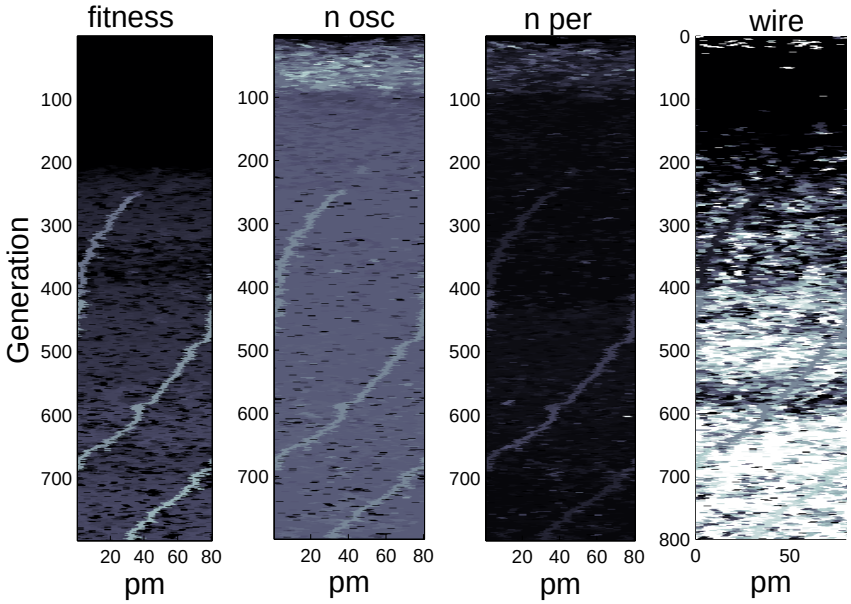

(b) Without

Figure 7.6: For each of the visualisations marked with asterisks in Fig. 7.5, visualisations are given of the corresponding neural dynamics (neuronal oscillation and neuronal period) and total wire length. Note they have been highlighted to show the 'selection tracks'. The neural dynamics definitions are provided in Section 5.4.

Although it is clear that the proprioceptive feedback model benefits agent behaviour, it is difficult to know whether the feedback provided is actually serving to modulate the

neural dynamics – as would be the case in true proprioception – or whether the feedback is just triggering the network to reach a particular attractor state. In order to test this, a set of simulations took the 40 best with-agents and replaced the feedback mechanism with varying levels of noise. This worked by substituting the input current for a real value generated from the uniform range [-n,n]. The smallest and largest chosen noise ranges were [-0.2,0.2] and [-2,2] respectively. The results of having done this are plotted in Fig. 7.7 and visualisations comparing behaviour are provided in Fig. 7.8. We can see that all noise levels effect performance, with higher levels of noise having the most negative impact. Thus, when the proprioceptive feedback is artificially 'broken' the whole behavioural process is degraded, therefore, we can infer that the 'un-broken' proprioception model is working as it should be – by regulating the dynamics of the nervous system. However, as we shall come to understand in the following section, the proprioceptive feedback mechanism actually underpins something far more complex – that of a rich dynamic coupling existing between the agent kinematics and nervous system dynamics.

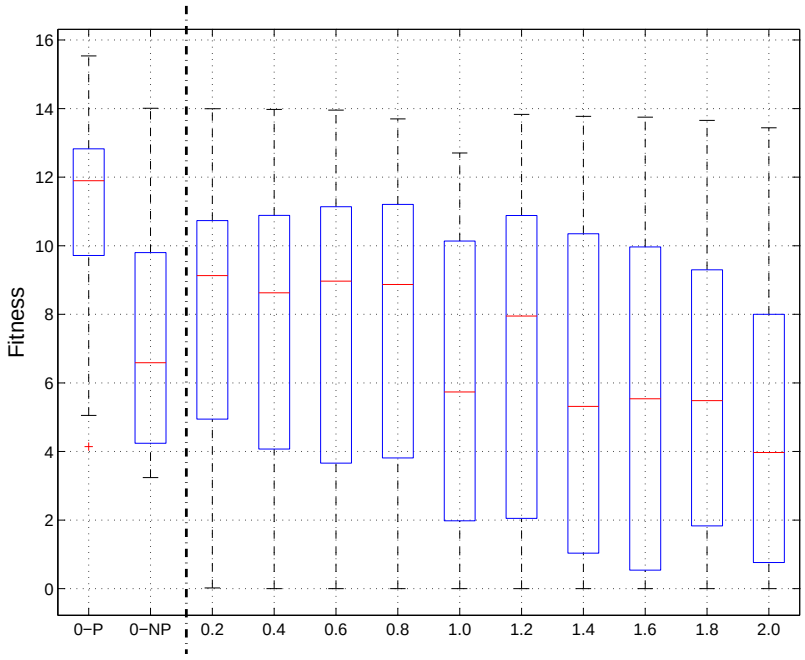

Figure 7.7: A boxplot showing how fitness is effected when uniform noise, represented by the x-axis, is used to replace the proprioceptive feedback mechanism. The '0-P' and '0-NP' cases left of the vertical line are representative of fitness values for the normal with-agents and without-agents. Those to the right are representative of the noise-effected agents.

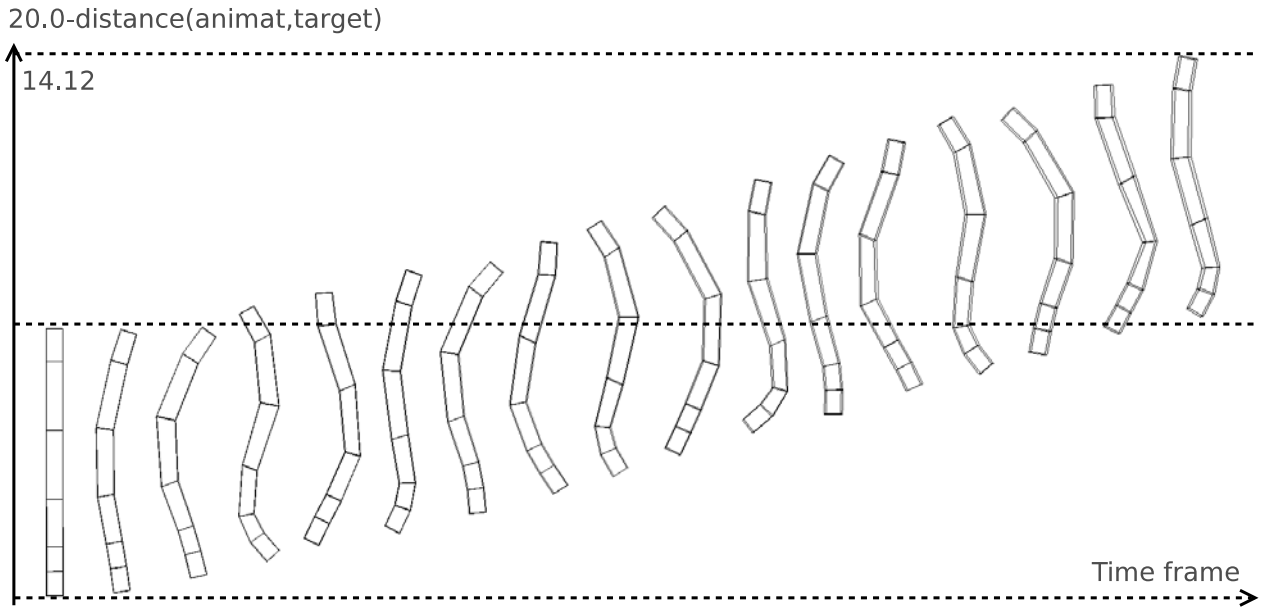

(a) Normal

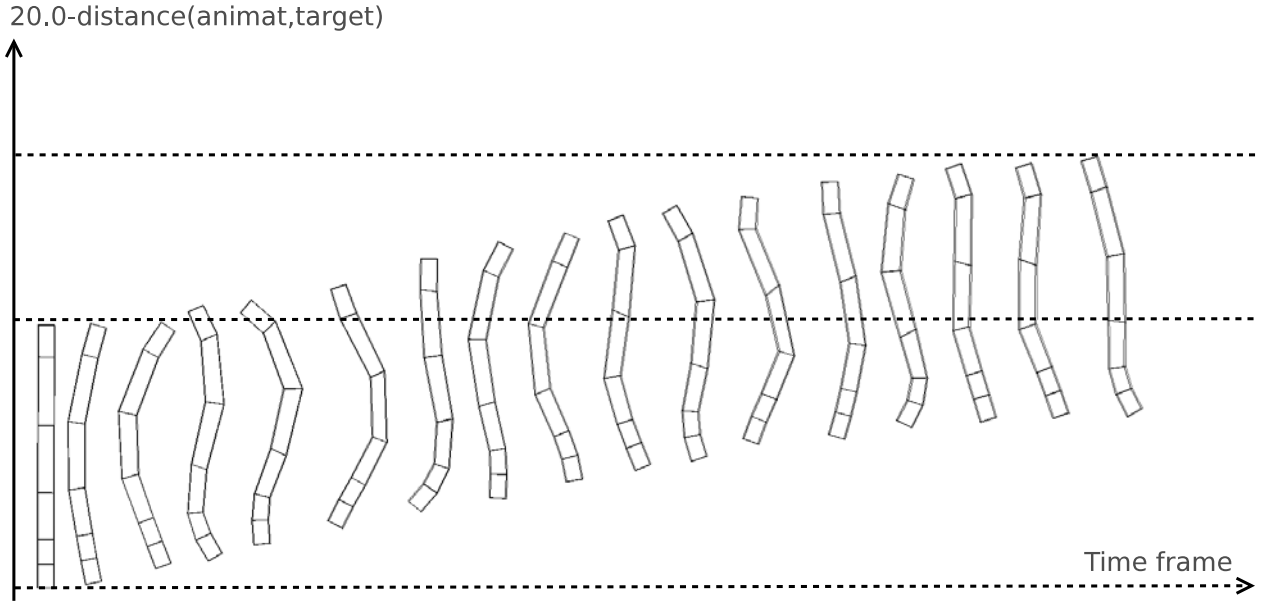

(b) With 0.8 uniform noise

Figure 7.8: Movement visualisations for a normal with-agent and a with-agent in which noise has replaced the feedback mechanism. As shown, the noise-effected with-agent's performance is degraded; it is unable to swim as far forward as the normal with-agent.

7.4.1 Kinematic–neural dynamic coupling

In the prior section, we discovered that noisy feedback has a drastic effect on the agent's kinematics. We ended on the remark that the proprioceptive feedback mechanism is somehow having a 'regulatory effect' on the neural control system. To investigate this further, we need to analyse both the movements of the body – the agent kinematics – for which we can look at the spring dynamics, and, the dynamics of the neural system. Both sets of dynamics underpin behaviour; both are richly coupled.

Measuring agent kinematics In terms of analysing the agent kinematics, we can record and average individual levels of spring distension. For a given spring, distension is given as,

$$d_s(t) = d_{\text{current}}(t) - d_{\text{rest}}(t) \tag{7.3}$$

where, at a given time t, $d_{\text{current}}(t)$ and $d_{\text{rest}}(t)$ are the current and natural spring lengths respectively. When we plot these distensions the overall kinematics of the locomoting agent can be visualised, see Fig. 7.9. These individual readings can then be averaged,

$$D_b(t) = \sum_{s=1}^{4} d_{s(t)} \tag{7.4}$$

$$A(t) = \frac{1}{B+4} \sum_{b=1}^{B} D_b(t) \tag{7.5}$$

Thus, Eq. 7.4 accumulates the spring distensions occurring in a segment to yield $D_b(t)$. This is repeated for all body segments and the results are accumulated and then averaged to yield $A(t)$, Eq. 7.5. There are 8000 time steps in total, yielding an eventual vector of noisy $A(t)$ values. To remove the noise and make the vectors more amenable to analysis, they are filtered using a Savitzky-Golay Filter [125], chosen arbitrarily for its ability to remove noise,

$$\chi = \phi\left(\langle A(1), A(2), \ldots, A(8000)\rangle\right) \tag{7.6}$$

where χ is the filtered vector and $\phi(x)$ is the filter function.

The effect of a depleted feedback mechanism on kinematics Now, in order to assess the importance of having a correct level of proprioceptive feedback – so that we may shed

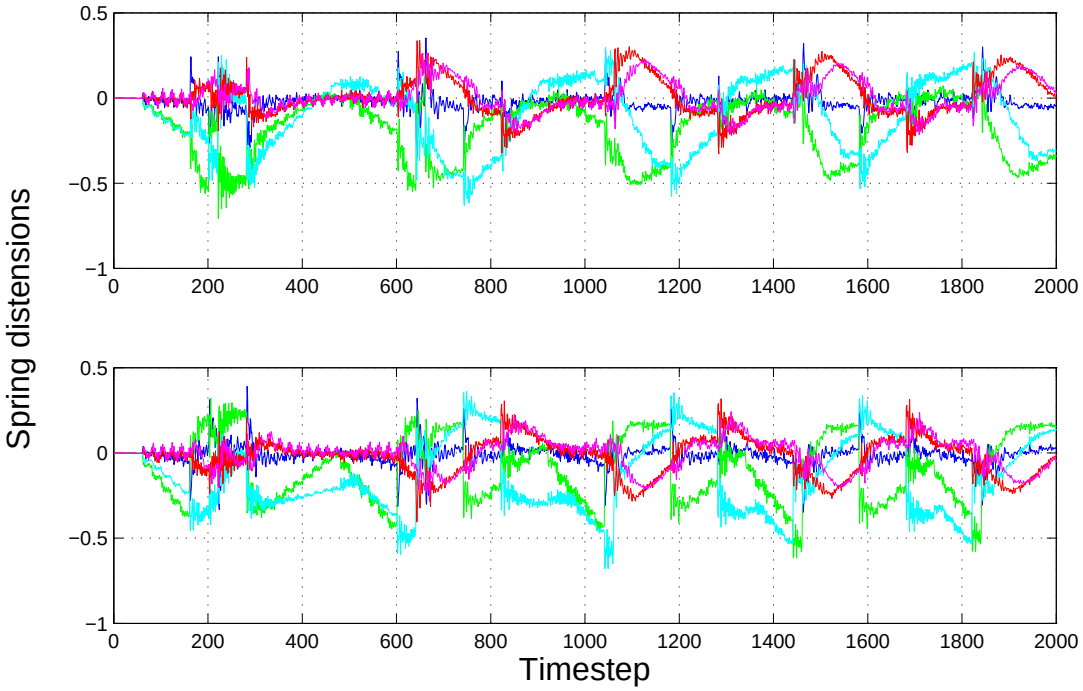

Figure 7.9: Kinematics (spring distensions) generated by a locomoting individual having proprioceptive feedback. The top subplot is the left half of the agent, the lower subplot the right half. A given colour represents a motor in a given segment. There are 5 segments in total for this agent. y-axis is level of distension, x axis is time (there are 8000 steps in total, only the first 3000 are shown). Note that only those motors determined to have had an active role in movement are plotted.

light on what we already know about it – we can observe what impact the scaling down of the feedback current has on agent kinematics. We can scale it down by basically applying a scalar, ϵ, to the feedback model,

$$I_M = \exp(\Delta d\epsilon) \tag{7.7}$$

When we do this, as shown in Fig. 7.10, the phase of the kinematic is somewhat altered. Thus we can validate our developing notion that correct feedback is necessary if our with-agents are to maintain correct – in-phase – movement dynamics.

A comparison of movement kinematics When we further compare the filtered kinematics produced by each type of agent, Fig. 7.11, we can see how the spring compressions for case 'with' are greater than for case 'without'. In case 'with', the average spring compression is consistently greater (as indicated by more negative value). This means that over

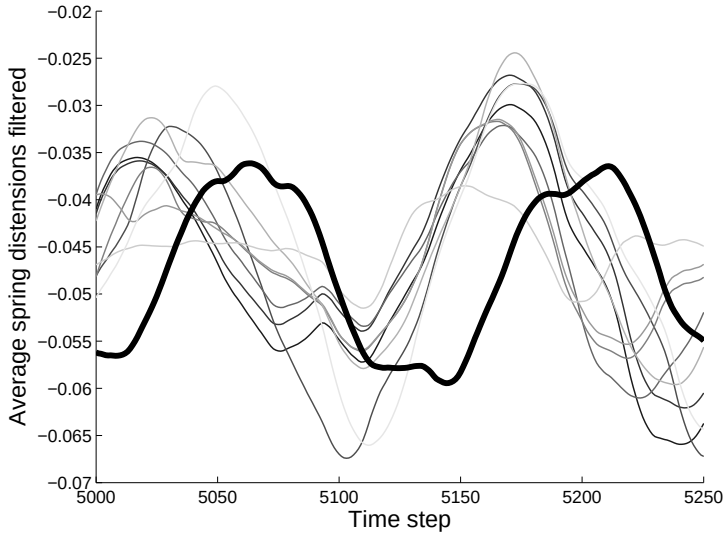

Figure 7.10: A section of the filtered agent transients for the locomoting proprioceptive agent whose broader kinematics are plotted in Fig. 7.9. The thick black line represents the filtered average transient with the normal feedback mechanism whilst the thinner grey plots are the result of the normal feedback mechanism having been multiplied by scalars $< 0.1, 0.2, \ldots, 0.9 >$.

behavioural time, the springs have a larger amount of potential energy that can be utilised during movement. Also, the larger standard deviation of the 'with' kinematic entails a greater oscillatory amplitude, thus, more kinetic energy is exhibited by the with-agents during the behavioural process.

The effect of feedback on motor activity Given that the with-agents demonstrably have higher fitness than the without-agents and that in terms of kinematic movements they are shown to have larger oscillatory amplitude, the feedback mechanism must be positively impacting on the output power of the motor system. To understand how, we can **(i)** observe the activity of one consistently active motor neuron and **(ii)** observe the proprioceptive activity – the current – that is fed back from the spring to the motor. Note that the level of proprioceptive feedback reflects the level of spring distension; thus we can make similar measurements for the non-proprioceptive variant by plotting the level of spring distension. Doing the above yields the results plotted in Fig. 7.12. The results tell us that:

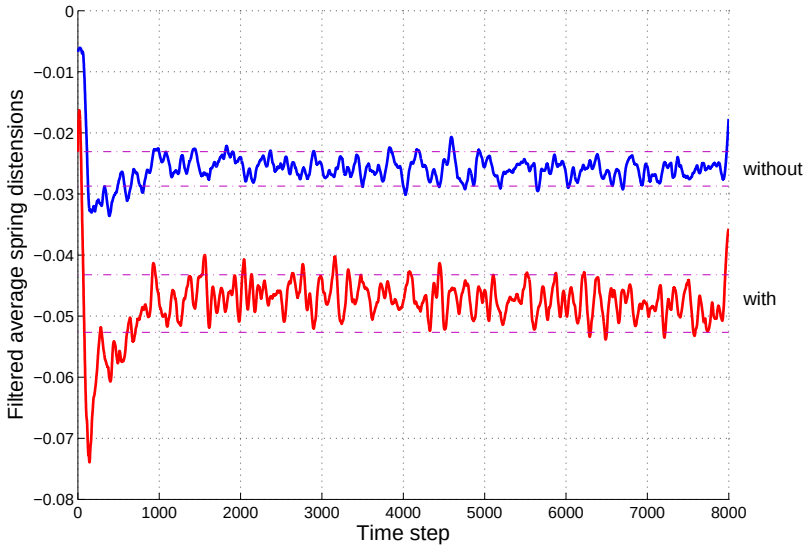

Figure 7.11: Averages of the filtered agent kinematics. Note: The more negative the value, the greater the spring compression. Results significant at a 0.05 level. The purple dashed lines represent the standard deviations. As shown, with-agents have more negative spring distension which corresponds to greater spring compression. A larger standard deviation also entails a greater oscillatory amplitude i.e. greater levels of kinetic energy.

- In both cases, the feedback or spring distension level is in antiphase with the motor activity. This is to be expected since positive motor activity results in corresponding spring compression (negative spring distension).

- In the 'with' case, as indicated by the cubic interpolations (solid purple lines in Fig. 7.12a), a rise in the average spring feedback sees a fall in the average neural activity until a point of stabilisation is reached. Therefore, to begin with, the spring dynamic 'dampens' the neural activity via the feedback mechanism, until both become locked into a pattern of stable coupling. No such pattern can be observed in the 'without' case.

- In the 'with' case, the antiphase troughs in the neural activity are significantly deeper than in the 'without' case. Thus when the agent is endowed with feedback, the neural oscillations are of a higher amplitude suggesting greater levels of motor activity.

- As shown by the green dashed line in Fig. 7.12a, when the feedback mechanism is depleted, the motor activity undertakes a shift in phase (we have already noted this effect

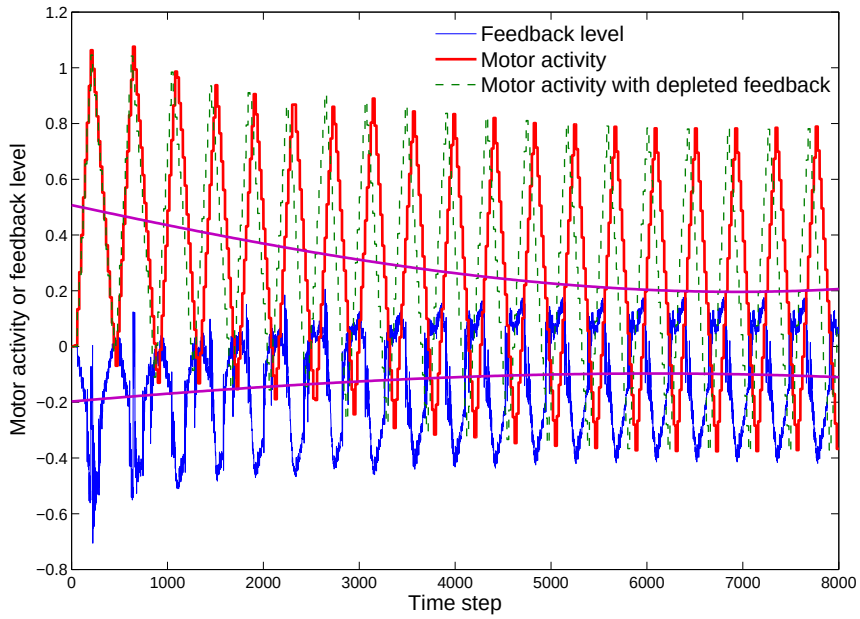

(a) With-agent

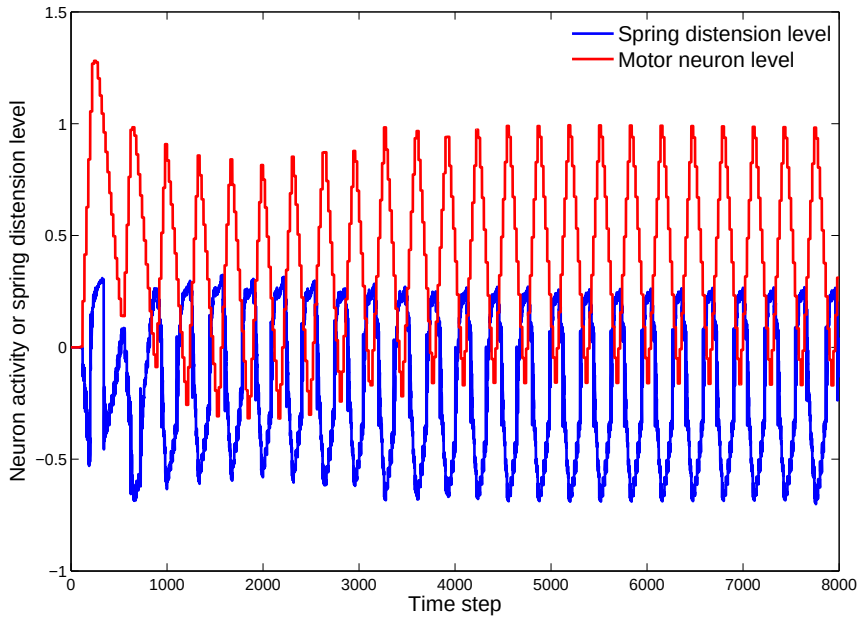

(b) Without-agent

Figure 7.12: Comparison of motor and proprioceptive feedback/spring distension levels for with- and without-agents. The purple plots in (a) reflect cubic interpolations. As shown in (a), a rise in the feedback level sees a fall in the average motor activity until a point of stability is reached. There are no such patterns in (b) however.

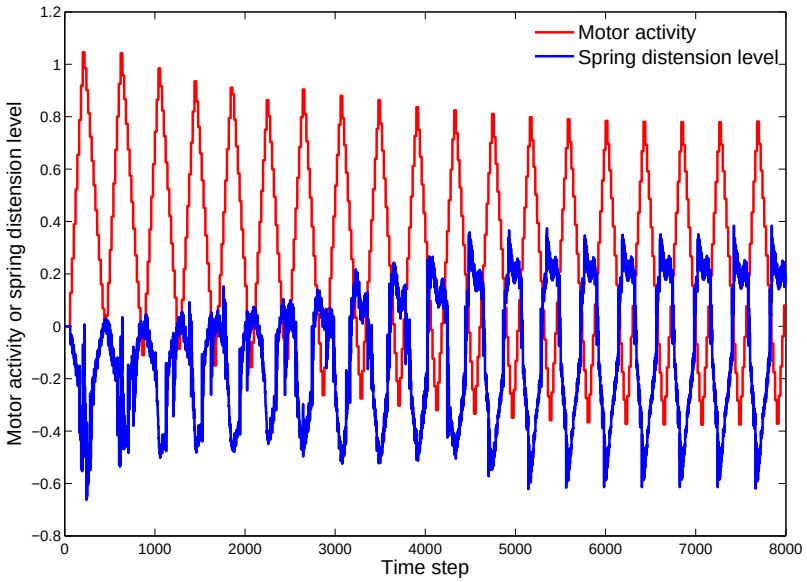

Figure 7.13: Spring distension overlaid with motor activity when the sensory feedback has been scaled to 0.01 of its original value. The result is a left phase shift in motor activity (as highlighted by the dashed plot in Fig. 7.12a), a commensurate left phase shift in the spring distension pattern and in comparison to Fig. 7.12a, a drastic increase in the spring distension amplitude.

in terms of kinematics, Fig. 7.10), and with regards to Fig. 7.13, it further increases the amplitude of the oscillating spring. Thus the feedback mechanism evidently modulates the phase of the motor unit which has the commensurate effect of maintaining correct spring dynamics.

Comparing neural activity Fig. 7.14 compares the average motor neuron activity patterns generated through behavioural time. As we can see, activation in the 'with' case is far more negative than in the 'without' case. As we noted in the above analysis of a single motor neuron, this is to be expected since spring compression provides negative input current via the feedback mechanism. Therefore, when the agent is endowed with proprioceptive feedback, the *body* has more of a 'regulatory' effect on the computational processes taking place within the nervous system. The coupling between the body and neural controller is made stronger. In practice, this means that neural oscillations are capable of driving and being driven by the kinematic oscillations of the body; and this ensures that correct CPG dynamics within the individual neural circuits can be maintained. Consequently, the overall behavioural process is consolidated. Without the feedback mechanism however, the neural

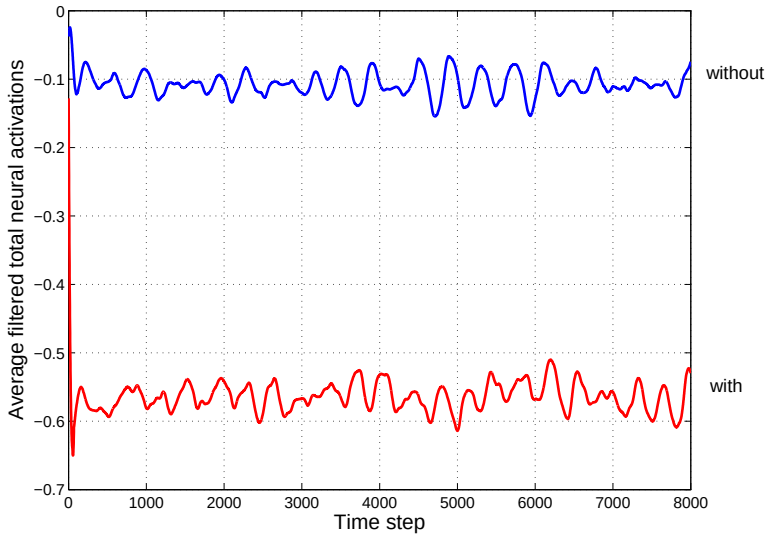

Figure 7.14: Averages of the filtered motor neuron activations from the locomoting agents generated in each setup. Results significantly different at a 0.05 level. As shown, activity in the with-agents is more negative than in the without-agents. This is to be expected, given the greater level of spring compression, which, via the proprioceptive mechanism, provides negative feedback current to the neural system.

circuits lack input current and the neural oscillations cannot come about as effectively. The body-motor coupling is diagrammatically summarised in Fig. 7.15.

In the following section, we investigate how the above described dynamic coupling is essential in maintaining robust behaviour.

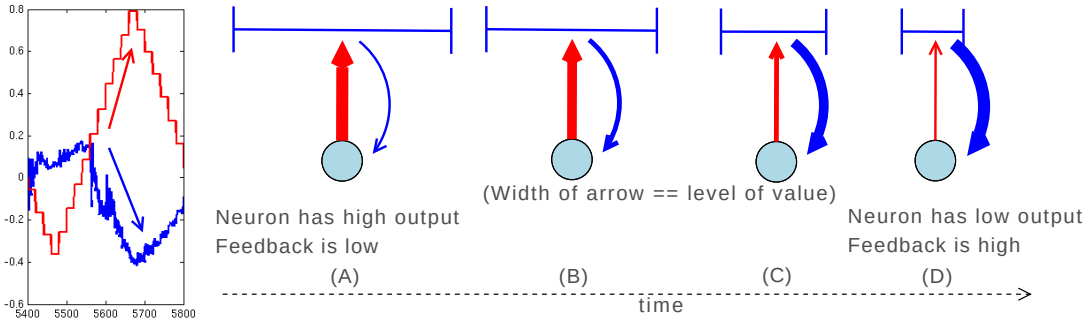

Figure 7.15: A depiction of how motor neuron dynamics are driven by spring distensions: when neural output is high (A) the spring is compressed (B-D), resulting in progressively greater feedback current and therefore progressively lesser motor activity; the spring will then resume to its natural resting length before the cycle is allowed to repeat.

7.4.2 Robustness to the environment

It has been suggested in [38] that the feedback mechanisms in lamprey enable it to more easily locomote when the environment is perturbed, for example, in the presence of water current. In order to examine this in the Evo-Critter model, a further experiment was conducted in which a simulation of water current was incorporated. This works by applying a side-on force to the agent as it undertakes undulatory behaviour. The process of doing this and the resulting effect is visualised in Fig. 7.16.

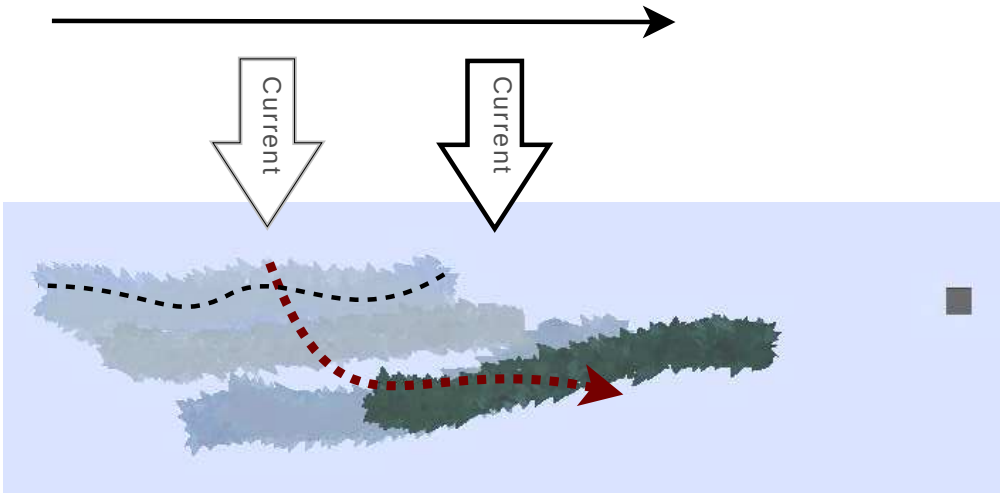

Figure 7.16: A visualisation showing how the environment perturbation model works. As the agent swims forward, virtual water current is enforced which has the effect of knocking the agent slightly off course.

As shown by Fig. 7.17a, which plots the changes in fitness with different levels of 'water current', it is found that the with-agents are significantly better able to maintain their swimming behaviour. Interestingly, for the 0.25 level of water current, a large number of changes to the without-agent fitness levels are unexpectedly better; yet, we can further interpret this in the light that the with-agents are better able to maintain their original behavioural dynamic. Furthermore, Fig. 7.17b shows us the commensurate changes in neural dynamics. We can observe that in the with-agents, these are better maintained; this again demonstrates the robustness of the with-agents to environmental perturbation.

Whilst sensory feedback has already been shown by Ekeberg [38] and others to mitigate the effect of environmental perturbation, the actual reasoning behind this was less clear. The above results suggest that feedback enhances robustness to perturbations in the environment, which in light of the analysis in Section 7.4.1, is because of the way in which proprioceptive

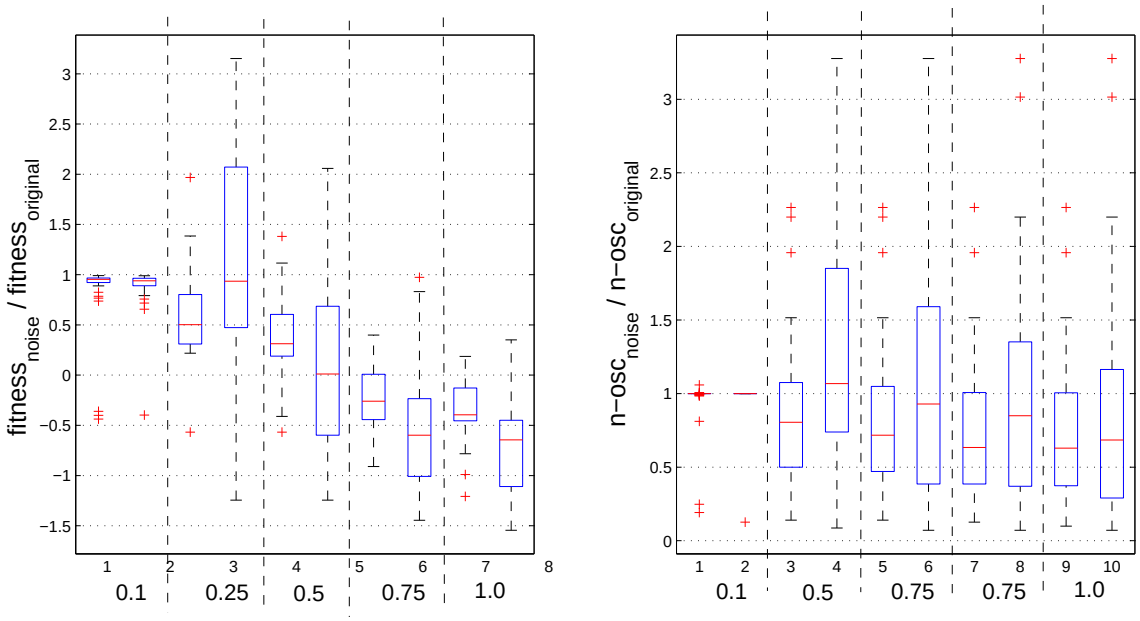

(a) Change in fitness

(b) Change in number of neural oscillations

Figure 7.17: (a) A box-plot showing the effect of water current on fitness; (b) the commensurate changes in neural oscillations. For both plots, in between each vertical dashed line, the left bar represents the change for the with-agents, the right bar for the without-agents. We can interpret the results as follows: the greater the difference in value from 0, the greater the change. For perturbation levels 0.25, 0.5, 0.75, and 1.0, the changes in fitness are shown to be significantly different.

feedback entails a stronger coupling between body kinematics and neural dynamics. We can thus come to understand that the stronger environmental robustness is actually due to this stronger coupling; i.e., the ability of the nervous system to both drive and be driven by the body kinematics enables the agent to perform robustly in the face of noisy conditions.

7.4.3 Robustness to neuronal perturbation

In Section 7.4, we came to understand that the wire length and the level of connectivity both have a significant impact on the behaviour of the agent. Crucially, with regards to the connectivity function (Eq. 5.12), this tells us that the geometrical neuron locations must have emerged in a way that facilitates connection formation.

Fig. 7.18 shows two dimensional visualisations of the median neuronal x,y coordinate positions before and after evolution. Importantly, we can infer from the emergence of the

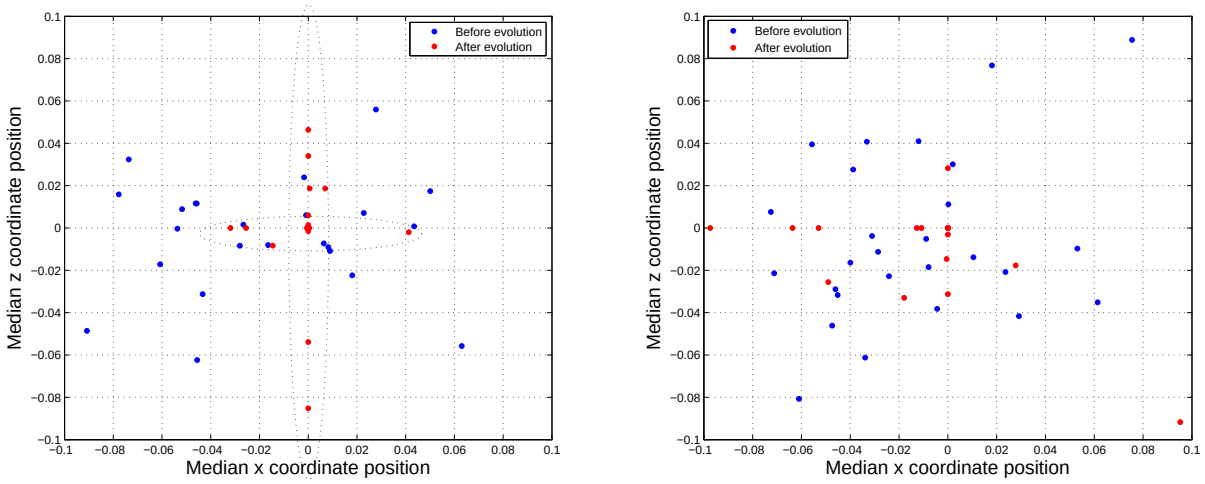

(a) With-agent

(b) Without-agent

Figure 7.18: Two dimensional visualisations of the neural architectures show regularity to have emerged through time, as highlighted in (a) by the two ellipses.

'cross-hair' arrangements a degree of structural regularity. Now, what we can do is perturb this regularity and observe (i) how the level of connectivity is altered and (ii) any changes in agent behaviour. This will indicate how robust a particular agent is to neuronal perturbation. A neuron's position is perturbed by adding a small amount of noise ([-0.5, 0.5] or [-1.0,1.0]) to its x and z coordinates (the y coordinate position is maintained).

Fig. 7.19a shows how, in the presence of such perturbation, the fitness of each type of agent is affected. Figs. 7.19b and 7.19c further elucidate the commensurate changes in connectivity. Our observations are as follows:

- In terms of fitness, in the presence of neural perturbation, some without-agents generate zero behaviour – this equates to agents entirely lacking an ability to move (as indicated by thickened black lines). In contrast, none of the with-agents were led to have zero behaviour. However, all levels of perturbation led to significant decreases in fitness for both types of agent.

- With regards to Fig. 7.19b, it would first appear that fitness is not resulting in a commensurate change in connectivity, however, when we actually compare the change ratios as in Fig. 7.19c, the changes become observably significant.

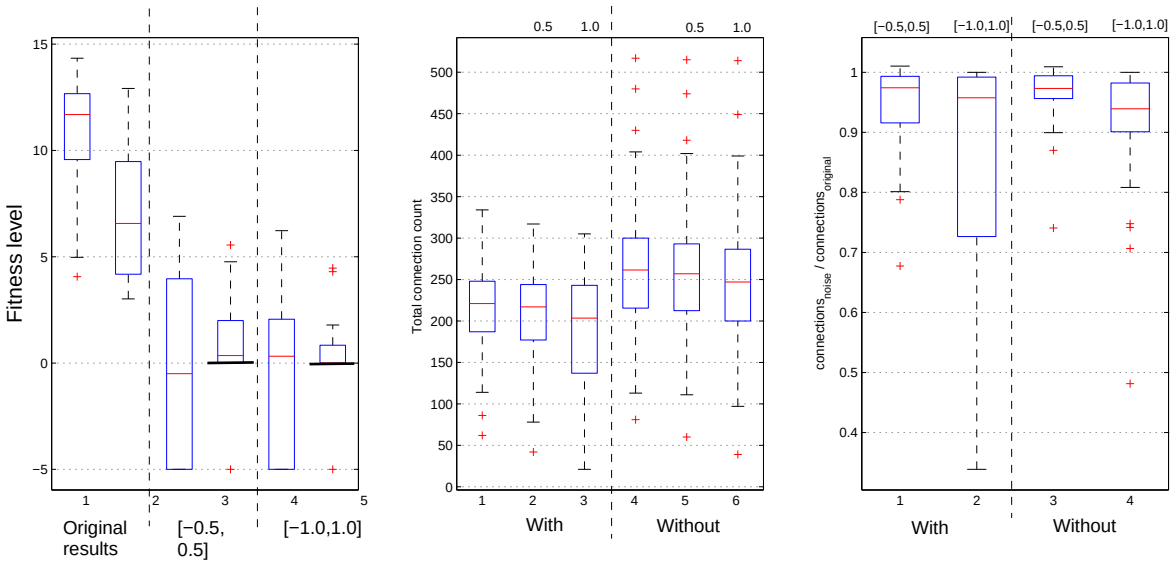

(a) (b) (c)

Figure 7.19: **(a)** The effect of perturbing neuron positions on the fitness of each agent type. As marked by the black horizontal lines, in the presence of neuronal perturbation, some without-agents generated zero movement; **(b)** the commensurate effect on connectivity level in which no differences are apparent; **(c)** ratios indicating the connectivity change magnitudes; these are shown to be statistically different.

- Change in interneuronal pair distances will also affect the connection weights existing between any unbroken connections; given the model defined in Eq. 5.11, interneuronal weight values are established according to the distance between them; perturbing the neuron positions will thus alter such distances and therefore the weight values.

In the case that neuronal perturbation led to many of the without-agents exhibiting zero fitness, we can infer that essential connection motifs were broken which prevented them from engaging in any activity. We cannot say that this was due to the weights having been altered and that connections were in fact not broken, because this would have endowed the agent with *some* movement activity (although of course, connection weights of unbroken connections would have still been modified). In contrast, the fact that with-agents were still able to generate some activity and therefore undertake some movement suggests that even when the connectivity decrease is large, as in the case of the [-1.0,1.0] range of perturbation (Fig. 7.19c), the importance of neural connection motifs in generating behavioural process, when a proprioceptive mechanism exists, is less crucial.

7.5 Discussion and Conclusions

We have observed that proprioception advances the animat's ability to locomote forwards. Also, that replacing the proprioceptive mechanism with noise can degrade performance. This firstly suggests that the system is not robust to high levels of this type of noise; secondly, that correct proprioception has a fitness enhancing or at least a modulating effect on the neural dynamics given that any level of noise is seen to degrade performance.

We secondly observed that for the setup with feedback, the individual neural circuits often emerge in a completely decoupled fashion. When we artificially add connections to these neural circuits, the behavioural mechanisms are degraded (results omitted for brevity), thus, we can infer that 'inter-circuit' connectivity is minimised in order that interference between the circuits can be reduced. We further found that connectivity in general evolves to become sparser, whilst connectivity in without-agents evolves to become far denser. This indicates how information distribution within the agent depends on the presence (or a lack) of a feedback mechanism.

An analysis of the dynamic coupling existing between the body kinematics and the computational dynamics of the neural controller was further undertaken. It was found that for agents endowed with feedback, both components are led to dynamically 'drive' each other; this has the effect of facilitating correct oscillatory dynamics. To validate this idea, we artificially lowered the feedback mechanism which led to a distortion in the dynamic coupling and a commensurate decrease in fitness.

We then extended the importance of having a proprioceptive mechanism in the context of behavioural robustness, finding that in the face of environmental perturbation, agents endowed with feedback are **(i)** better able to maintain the dynamics of their neural control mechanisms which **(ii)** allows them to more easily surpass such noisy regions. It was then suggested how, given the feedback mechanism, this is due to the stronger dynamic coupling between the body kinematics and neural dynamics.

Finally, we looked at how regularity within the neural architecture facilitates correct connection formation, finding that for the without-agents, when the individual neuron positions are perturbed, connectivity formation is distorted and fitness is lowered. However, crucially, we found that in the without-agents, destruction of neural circuitry became more problematic given the result that many were led to having zero behaviour. Thus we observed how neuronal connectivity has greater importance in the without-agents. In contrast, we found

that with-agents were always able to generate *some* modicum of behaviour, even after significant connectivity decrease. This suggested to us that in agents having sensory feedback, the requirement for neural circuitry is minimal (which indeed we can see in our initial results); and, in the face of minimal neural circuitry, fitness is maintained by the proprioceptive feedback mechanism which evidently consolidates the body's ability to undertake much of the computational process – this exemplifies morphological computation [98].

In conclusion, the contributions of this chapter are as follows:

- Proprioceptive feedback is shown to have a positive impact on behavioural fitness.
- Optimal fitness is governed by optimal neural dynamics which is largely governed by an optimal wire length.
- Wire length is shown to be different in each type of agent (with or without feedback); thus information is distributed differently in each type of agent.
- In agents having feedback, the body plan morphology is shown to have a regulatory effect on the neural dynamics.
- A feedback mechanism provides greater robustness to environmental perturbation which is argued to be due to a strengthening of the dynamic coupling between the body kinematics and neural dynamics.
- Regularity in the neural architecture emerges during the evolutionary process.
- The argument that the denser amount of wire found to emerge in agents not endowed with feedback is necessary, given the finding that a perturbation of neuronal regularity which leads to a disruption in connectivity, results in zero behaviour generation.

Part III

Energy as a constraining resource

Chapter 8

Energy: A Constraining Resource in the Coevolution of Body and Brain

Synopsis

In the preceding chapters, results indicate how the morphology and nervous system of an undulatory agent coevolve to bring about optimal swimming behaviour. Over the course of several simulations, we observed how the body plan morphology becomes characterised and places constraint on the evolution of the nervous system architecture. However, as we noted in Chapter 3, when we think about nervous system evolution, we also need to think in terms of energy efficiency, which, given such factors as wire-length and metabolism, is also a major constraint in the evolutionary process. Thus in this chapter, we address the final question posited in the introduction, repeated here for convenience:

Question: *What effect does energy constraint have on the evolution of both nervous system and the body plan morphology of an organism?* **Guiding principle:** In nature, an organism will ultimately die if it has no energy to survive. An energy conserving framework is therefore added to models developed earlier on, and considers how energy is lost due to the activity of the neural and motor systems and how evolution strives to minimise this, but whilst endowing the organism with maximum functional advantage. The need to conserve energy places a variety of constraints on the coupled body plan morphology and neural system. By varying the energy constraint, changes in the neural architecture and/or body plan characteristics can be observed and progressively understood.

In tackling the above question, this chapter presents two pieces of work:

1. Section 8.1 presents a very abstract model of a freshwater Hydra (entirely different to the Evo-Critter framework) which is endowed with a spiking neural network the architecture of which is evolved to **(i)** minimise energy loss due to spiking activity (and is proportional to connection length), and **(ii)** maximise energy gain via a 'food-catching' behaviour. The animat's body morphology is fixed to be radially symmetric and the optimisation process becomes purely about the neural system. The main contribution is a novel framework that explores how energy places constraint on the evolution of primitive neural organisation via interaction with the environment. This work is reported in [59, 58].

2. In Section 8.2 the Evo-Critter framework is extended to also incorporate a notion of energy loss. Thus the importance of energy as a constraining factor on the emergence of neural architecture *and* body morphology is more fully encompassed. The main contribution is a demonstration of how, during evolution, the nervous system should become organised and architecturally coupled to the body symmetry and other morphological components, when it is constrained by both the agent's segmentation characteristics and a need to minimise energy loss.

8.1 The Evolutionary Emergence of Neural Organisation in a Radially Symmetric Agent

8.1.1 Overview of research

The role of efficient information processing in organising nervous systems is investigated. For this purpose, a computational model termed the *Hydramat Simulation Environment*, so named since it simulates certain structural aspects of fresh water Hydra, has been developed. In simulation, the evolution of neural organisation in architectures that remain static throughout their lifetimes and neural architectures that are perturbed by small random amounts are compared. It is found that (a) efficient information processing directly contributes to the structural organisation of a model nervous system and (b) lifetime architectural perturbations can facilitate novel architectural features.

8.1.2 Hypotheses

In the following experiments, we explore the influence that energy conservation has on neural organisation and the additional effect that *noise* has on this process. In order to do this, a model of a radially symmetric organism which loosely resembles the freshwater *Hydra* termed 'Hydramat' is simulated and evolved in a virtual environment. The focus is on how the nervous system should configure itself around a fixed radially symmetric body plan. **The hypothesis** is threefold: the neural architecture of a radially symmetric agent will arrange itself such that **(i)** the agent is afforded maximal functional benefit and **(ii)** the agent is afforded the ability to conserve energy and **(iii)** structural innovations are benefited from lifetime architectural perturbations.

8.1.3 Biological basis and previous work

The simulated agent proposed in this work is based on observations of the nervous system of the genus *Hydra*, since crucially, they are phylogenetically the first to have a nervous system that resembles major principles of nervous systems in later organisms [81, 116]. The actual simulation environment to be outlined in Section 8.1.4 is heavily inspired by Albert [1], who devised a simple model for the Hydra and its nervous system (also see Chapters 3 and 4). From a systems biology approach, the model is further inspired by the work of Niv et al. [91], who looked at the foraging behavior of honey-bees and Florian [42], who employed biologically inspired neural networks for agent control.

8.1.4 The Hydramat Simulation Environment

The Hydramat is modeled on a tube and has a nervous system consisting of the following types of cell (also see Fig. 8.1).

Sensory neurons These are computational neuron units that remain fixed at the top of the Hydramat tube. They detect falling food particles. When a piece of food is dropped, the sensory cell that the piece of food is closest to is the one that 'spikes', providing input to the rest of the spiking neural network. The other sensory cells remain dormant.

Effector neurons Each effector neuron, of which there are always 8, is used to 'wobble' the animat in one of eight directions, so that a food particle can be 'caught', see Fig. 8.2. Note

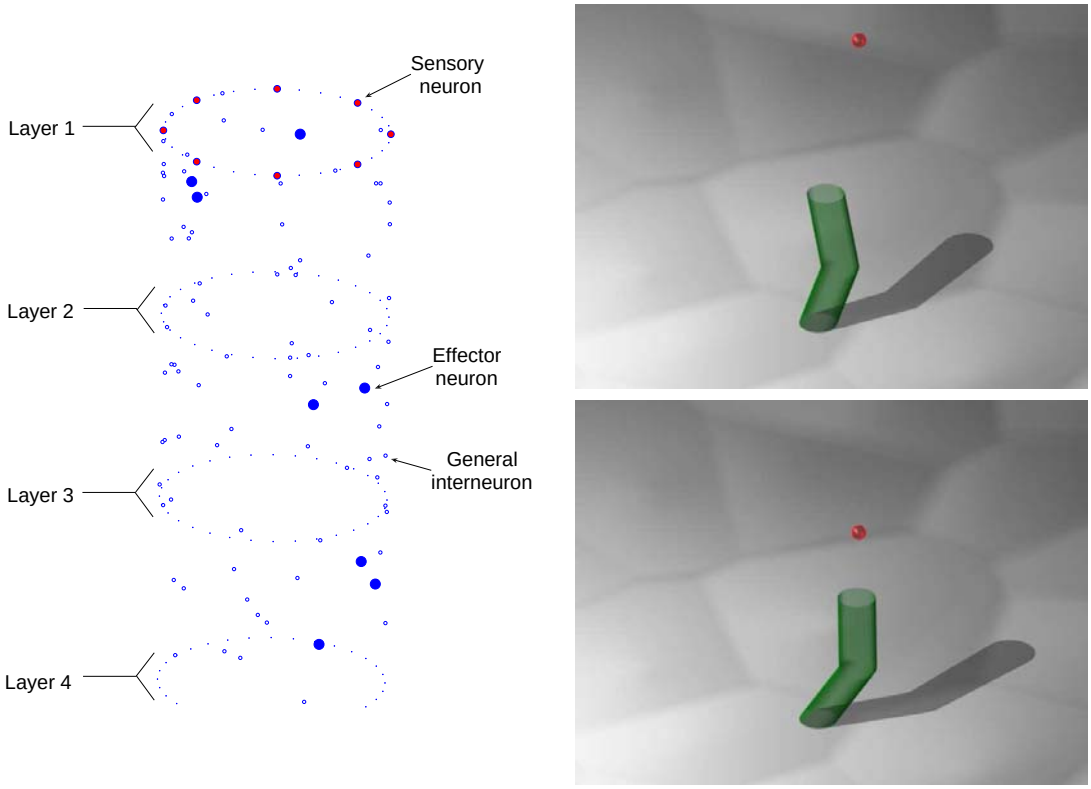

Figure 8.1: *Left:* A visualisation of the Hydramat showing a neural cell distribution; *Right:* Two snapshots of the simulation environment. The sphere represents a food particle.

that a food particle is deemed caught when it comes to within a small distance threshold of the top of the Hydramat. The effector cell that ends up firing the most is the one that brings about movement whilst the others remain dormant. A firing rate is therefore observed within a short time-frame (10 updates to the simulation environment) to decide the behavior.

General interneurons Additional neuron units residing within the 'skin' of the Hydramat. The Euclidean locations of both the interneurons and the effector neurons are evolved throughout a process of simulated evolution and this is the crucial way in which the architecture of the nervous system is evolved. These localities are constrained to reside within the skin of the Hydramat, since this is the case in Hydra.

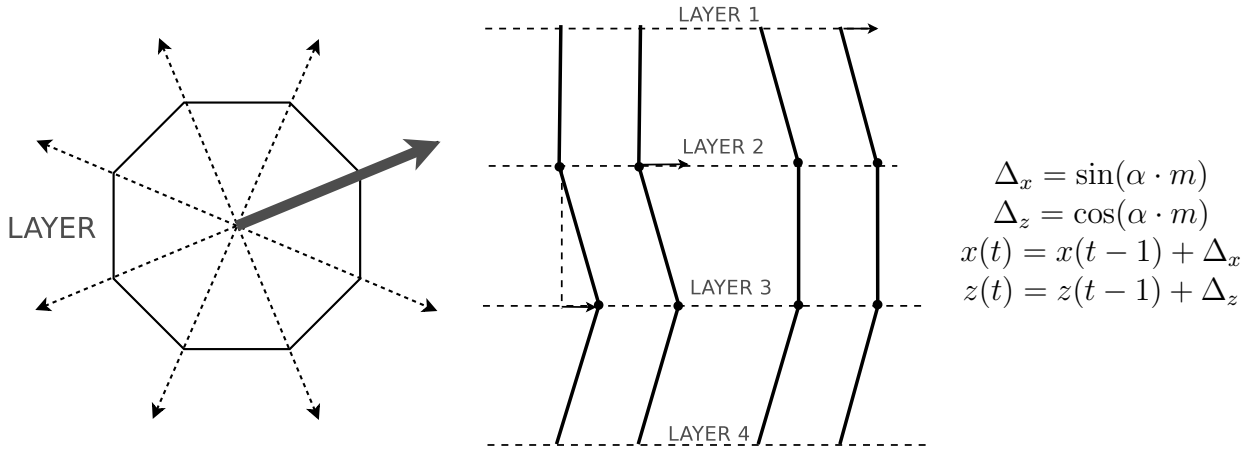

Figure 8.2: The movement mechanism of a Hydramat layer. A chosen direction of movement has been highlighted for a layer (left-hand diagram). The way in which the Hydramat aligns itself following a movement is also depicted (right-hand diagram). The value m is a predefined constant and defines movement magnitude. The value α represents the angle of the directional movement shown in the left-hand diagram.

8.1.4.1 Movement dynamics

The Hydramat 'wobbles' to catch a piece of food by moving its third layer, see Figs. 8.1 and 8.2. The other layers passively align themselves to this moving layer. The amount by which a contracting layer moves due to a spiking effector neuron is predefined by a movement magnitude (m), which was always set to 0.8 (see equations in Fig. 8.2). The other layers iteratively align themselves in proportion to the amount by which layer 3 changed position during such a movement update (Eqs. 8.1, 8.2 and 8.3). In this respect the passively updating layers observe very simple spring-like dynamics:

$$f_a = dc_a \tag{8.1}$$

$$f_b = -dc_b \tag{8.2}$$

$$F = f_a + f_b \tag{8.3}$$

Note that f_b is employed as a kind of relaxation 'force', causing the tube to resume to a resting upright state. The parameters c_a and c_b are predefined constants set to 0.2 and 0.01 respectively.

8.1.4.2 Hydramat Nervous System

An integrate and fire spiking neural network The Neuro Simulation Toolkit NEST [44] is used to build a simple integrate and fire (iaf) model for the Hydramat nervous system. A change in membrane potential of a neuron is given by the following differential equation

$$\tau_i \frac{du_i}{dt} = -u_i + RI_i(t) \tag{8.4}$$

where I_i is input current and R is resistance. The multiplicative effect is typically equivalent to the accumulated strength of all incoming presynaptic activity i.e., an accumulation of weight values representing the connection strengths multiplied by functions of when presynaptic neurons fired prior to the current 'time step' ($\sum_j^N w_{ji} k(t - F_j)$). The value τ_i, is the membrane time constant of the neuron.

Neuron positioning and synaptic efficacy In the model, the distance between a pair of neurons (i and j) determines the connection strength of the connection between them if such a connection exists. The formula

$$w_{ji} = \frac{\xi}{d_{ji}} \tag{8.5}$$

is used to derive this value, where d_{ji} is the Euclidean distance between neurons i and j and the value $\xi = 16$ has been empirically set to ensure that w_{ji} has the potential to be significantly large. The maximum value of d_{ji} is given by the bounds of the Hydramat's geometrical properties. In the experiments, the length of the cylindrical Hydramat and its diameter were always set to 6.0 and ~ 1.6 respectively. Therefore, the theoretical ranges of d_{ji} and w_{ji} were $[0, \sim 6.23]$ and $[\sim 0.64, > \xi]$ respectively; the smaller the distance between a pair of neurons, the larger the weight value between them, if a connection exists between them.

Neuron positioning and connectivity A second aspect of the nervous system model is that the connectivity between any pair of neurons is determined using a Cauchy probability distribution of the form

$$P_{ji} = \frac{1}{\pi \cdot \lambda_i \cdot \left[\left(\frac{d_{ji}}{\lambda_i} \right)^2 + 1 \right]}. \tag{8.6}$$

The value of λ_i governs the width and height of the distribution. If the value is small, the shape will be tall and narrow. If it is large, the shape will be short and wide. Each particular neuron-type pair has its own value. Since in the model there are three neuron types (sensory (S), effector (E) and interneuron (I)), we have six types of connectivity as the connectivity relation between two neurons is not symmetric. A connection from S to E does not equate to a connection from E to S, i.e., $SE \neq ES$. The model actually employs 6+1 λ scalars: one for each of the different connectivities, and a further one since interneurons are permitted to connect to other interneurons. Except for the interneurons, a particular type of neuron is never connected to a neuron of the same type.

Finally note that the setup includes an artificial constraint that prevents connections bisecting the Hydramat cylinder. This is to ensure that connections remain within the 'skin' of the Hydramat like it is in real hydra. If a pair of neurons are angled more than 20° away from each other, the connection probability is set to zero.

Lifetime architectural perturbations In order to assess whether there is an advantage in perturbing the neuronal architecture throughout the lifetime of the Hydramat, the neurons are made to move stochastically by small random amounts. The motivation for doing so stems from Hydra, in which the neural cells undergo constant movements (e.g. [14]). At each update of the simulation, a neuron's position changes with a probability of 0.05, by an amount drawn from a normal distribution having an expectation of zero. For the neuron's y coordinate gene, the variance of this distribution is set to 0.1 and for the neuron's angle, 10.0. If during such a movement the neuron moves outside of the Hydramat's bounds, it is replaced with a neuron occupying the position of the original neuron before any lifetime movements were undertaken.

8.1.4.3 Measuring efficiency

In the Hydramat neural model, a single spike is considered as a single unit of information transmission, which is associated with an energy cost, e_j, of the spiking neuron

$$e_j = \sum_{i=1}^{C} \frac{d_{ij}}{d_{max}} S_{loss} \tag{8.7}$$

where d_{ij} is the distance between two neurons and S_{loss} is the maximum possible energy that will be lost (0.1) when the connection length is d_{max}. Energy is also accumulated whenever

the Hydramat catches a food particle. In the simulations, this value was set to $F_{gain} = 40.0$. To keep things simple, the energy that could be lost due to movement is not considered in this work.

8.1.4.4 Evolutionary process

A simple evolutionary algorithm is used to evolve the neuron positions and connectivity parameters. Typically we have 8 sensory neurons, 8 effector neurons and 84 interneurons. So we have 92 neuron positions to evolve (since the sensory neurons are fixed) and the 7 lambda connectivity parameters. Binary tournament selection, discrete recombination and a Gaussian mutation with an adaptive standard deviation (σ) are further employed. The selection scheme randomly selects pairs of individuals and then selects the fitter of the two until a new population is established; discrete recombination exchanges gene values between two offspring candidates selected randomly from the offspring population. The adaptation process relies on the setting of two strategy parameters, $\tau_0 = 1.0/\sqrt{2.0 * D}$ and $\tau_1 = 1.0/\sqrt{2.0 * \sqrt{D}}$ where D represents the dimensionality of the vector being evolved. These values have been shown to be optimal in a process of self-adaptation [7]. The σ values are adapted as follows

$$\sigma_i \leftarrow \sigma_i * \exp\left(N(0, \tau_0) + N_i(0, \tau_1)\right).$$

Both genes representing the spatial positioning vectors and those representing the connectivity parameters are subsequently normally mutated by applying the corresponding σ value.

8.1.4.5 Experiment overview

A very simple 'food catching' task has been devised to explore the hypothesis. In Fig. 8.3, a bird's-eye perspective of the environment is depicted. At the center of the environment resides the Hydramat, whose task is to catch each of the eight pieces of food depicted as filled circles (one at a time). The performance (fitness) measure is the amount of energy that can be retained. Each Hydramat population member starts with 200 units of energy and units are gained whenever a piece of food is caught and lost whenever a neuron spikes, if energy efficiency is considered. In order to ensure that the spiking neural network truly evolves to react to the food stimuli, the order in which the food pieces are dropped is randomly shuffled at the turn of each population member.

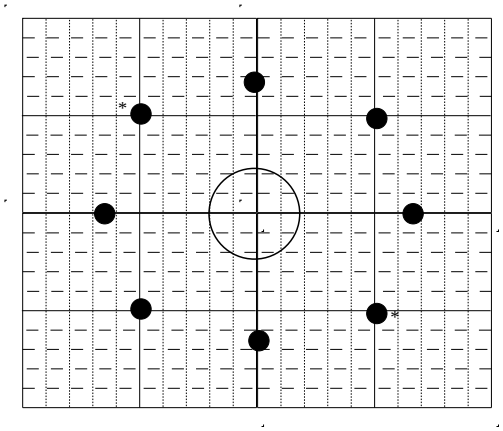

Figure 8.3: The 8-food-task environment from a bird's-eye perspective. Each of the 8 pieces of food, represented as an outer filled circle, is equidistant from the center of the Hydramat, located at the center of the diagram.

8.1.5 Summary of Hydramat results

Four sets of experiments have been performed to investigate two things:

1. **The influence of energy efficiency**. As a methodology, the energetic cost of function is novel. Its incorporation is entirely essential if we are to identify how neural organisation is constrained by a need to minimise energy loss.

2. **The effect of lifetime architectural perturbations on neural organisation**. Investigating this effect will shed light on why the most primitive of nervous systems – those belonging to members of the Genus Hydra – is endowed with lifetime tissue movements. We can ask: are these movements necessary for the emergence of novel neural architectures?

The four experimental setups were as follows:

1. **Architectural perturbations with energy efficiency** taken into account.

2. **No architectural perturbation with energy efficiency** taken into account.

3. **Architectural perturbations without energy efficiency** taken into account.

4. **No architectural perturbations without energy efficiency** taken into account.

Fig. 8.4 shows the energy conserved in the four experimental setups. We can see that evolution progresses steadily in all experiments and when energy consumption due to spikes

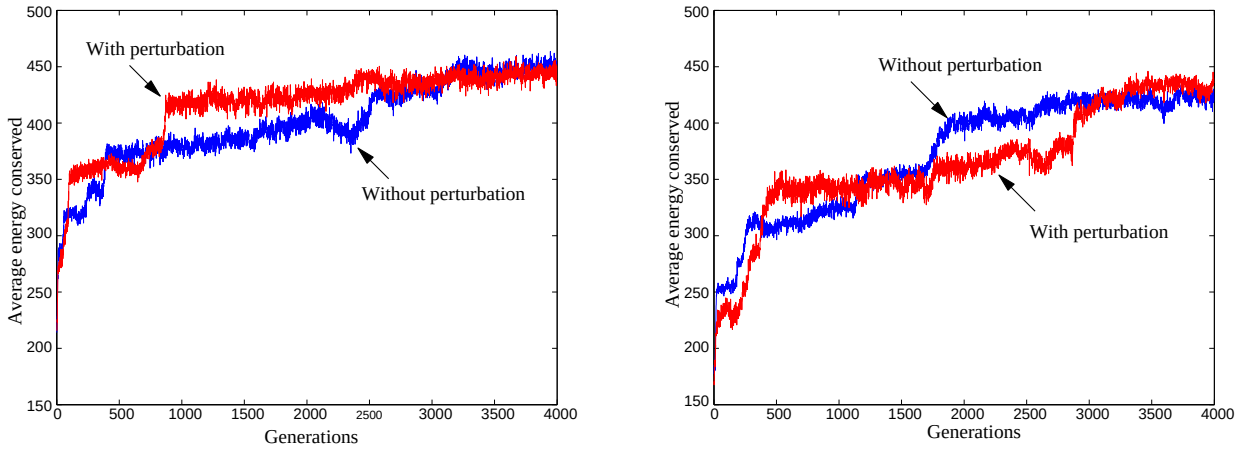

(a) (b)

Figure 8.4: Energy conserved as evolution proceeds (a) without energy efficiency, and (b) with energy efficiency taken into account.

is not taken into account, energy conserved from food caught increases more rapidly. Fig. 8.5 presents the relationship between energy conserved and connectivity density. From the figure, we can conclude that minimising energy loss due to spikes effectively reduces the density of neural connectivity which however, becomes harder when lifetime architectural perturbations exist.

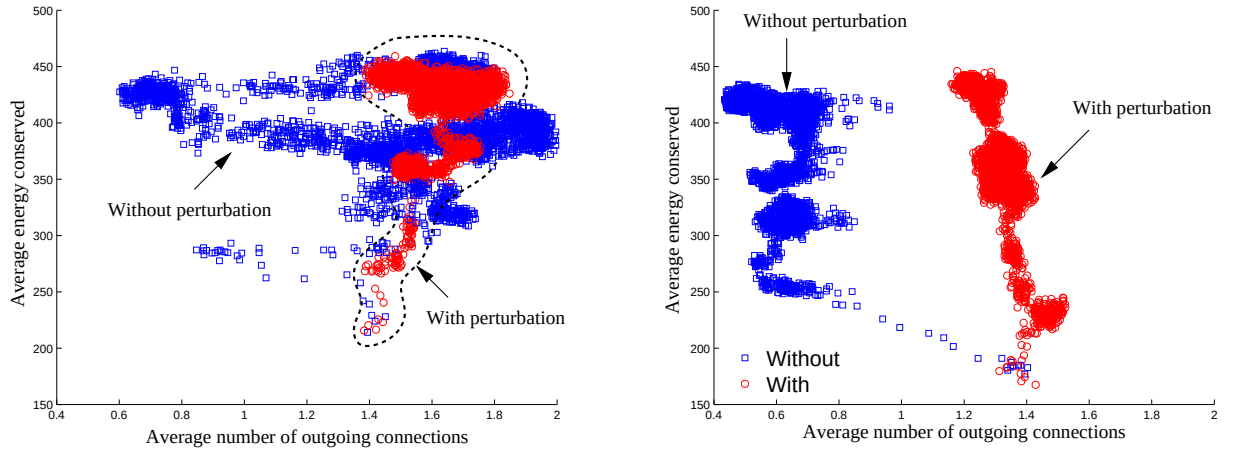

(a) (b)

Figure 8.5: Energy conserved versus the number of outgoing connections (averaged over the whole population) when energy loss due to spikes is (a) not considered and (b) considered.

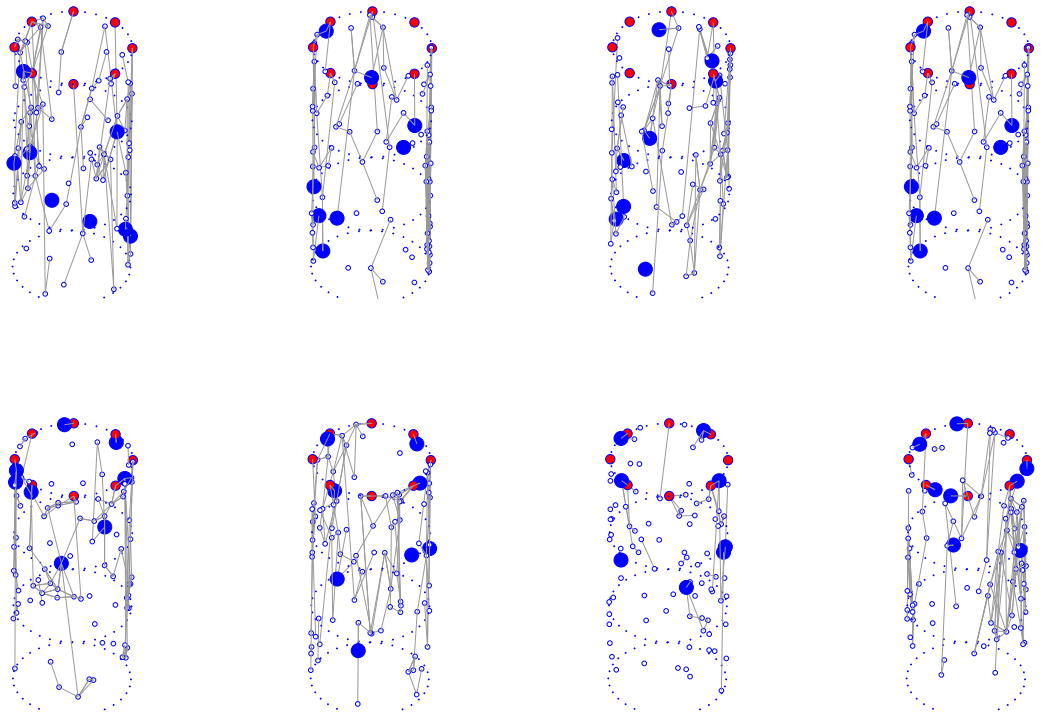

(a) (b) (c) (d)

Figure 8.6: Initial (*upper*) and optimised (*lower*) neural architectures of the four experiments indicate that effector neurons (larger filled circles) tend to move toward the sensory neurons (smaller filled circles). (a) energy efficiency not considered, no architectural perturbations; (b) energy efficiency not considered, with architectural perturbations; (c) energy efficiency considered, no architectural perturbations; and (d) energy efficiency considered, with architectural perturbations.

The optimised neural architectures in the four experiments are illustrated in Fig. 8.6. From these results, we can make the observation that effector neurons (enlarged filled circles) tend to aggregate around the sensory neurons (small filled circles). This suggests that functionally significant neurons have a tendency to become proximal to each other, which might be a functionally useful feature. Moreover, significance tests based on 30 runs when energy efficiency is considered indicate that lifetime perturbations increased the likelihood that effector neurons would move towards the top of the Hydramat to a significance of 0.005.

Two main findings seem to have emerged from our simulation results. First, energy has a direct impact on neural organisation. Second, lifetime neural perturbations can facilitate the emergence of biologically plausible structures.

8.2 Energy constraints in the Evo-Critter framework

In the first part of this chapter, experimental results demonstrated that for radially symmetric agents, energy conservation is a major driving force in the evolution of minimal neural architecture. It was observed how functionally significant neurons would aggregate around the sensory system in order that energy loss could be minimised. Also, this indirectly endowed the agent with the capacity to properly react to external stimuli, since the falling food particles would increase the agent's energy and therefore help in the energy conserving process. In light of this, energy was observed to be a constraining factor in how the neural architecture should emerge.

However, there are several caveats of the above study. One is the static nature of the agent's radial symmetry. This is problematic, since in reality, an organism's body plan morphology and its coupling to the nervous system is rich and highly complex, both in terms of the evolutionary process (Chapter 6) and in terms of the behavioural process (e.g. Chapter 7). Only in the sense that neurons are constrained to reside within the 'skin' of the Hydramat agent does its body plan have any kind of influence, therefore, in terms of our analysis, we are restricted in terms of what we can look at. However, by incorporating an energy conserving approach to Evo-Critter, we are provided with a more extensible framework, since it allows us to study how energy affects the evolution of all aspects – body plan morphology, body symmetry *and* neural control system – and the couplings between them.

8.2.1 Energy measure

In the Hydramat model, energy loss is associated with the spiking activity of the neural system. Each time the network spikes, energy is lost, but in proportion to the outgoing connection lengths. Since in the Evo-Critter framework an analogue neural network (i.e. a CTRNN) is used, this formulation of energy loss is no longer amenable. In the CTRNN, energy lost becomes the absolute value of the membrane potential u (see Eq. 5.14). This is accumulated over time. A single moment in time is the point at which the neuron's activation changes from a positive state to a negative state or from a negative state to a positive state; for clarity, this is termed 'oscillation' (see Eq 5.17). The membrane potential is read and accumulated at such point. This accumulation is then averaged over all oscillations f, to

yield a metabolic energy m:

$$m_i = \frac{1}{f}\sum_{k=1}^{f} |u_k| \tag{8.8}$$

Finally, the energy E, of the whole neural system is taken to be the average of all metabolic energies weighted with the total average wire length

$$E = \frac{1}{N}\sum_{i=0}^{N-1} m_i \cdot \frac{1}{C}\sum_{i=0}^{C-1} \text{length}(c_i) \tag{8.9}$$

Note that this formulation also includes motor neurons, therefore, energy lost due to physical movements are implicitly taken into account (recall that springs are actuated in proportion to the membrane potentials of the motor neurons, Section 5.2.3).

Fitness function Given the above formulation of energy, the fitness function is made to be multi-objective by firstly incorporating the original function which measures the distance of the animat from the target, which needs to be maximised, and secondly the energy accumulated, which needs to be minimised

$$f_1 = 20.0 - \text{distance(animat,target)} \tag{8.10}$$

$$f = a\hat{f}_1 - b\hat{E} \tag{8.11}$$

Therefore, E becomes a 'penalty', the value of which needs to be minimised. The values a and b are constants and determine the weighting of each term. This function is an example of an aggregate objective function of the type described in [31]. The advantage of using this approach is that different $a : b$ ratios can be compared. Note that this ratio is similar in principle to the energy gain : energy loss ratio employed in the Hydramat framework (see Section 8.1.4.3).

8.2.2 Experimental setup

From this point on, energy gain : energy loss will be termed *a:b*.

In order to assess the effect of energy in the Evo-Critter system, different *a:b* ratios were studied. For each particular ratio, 30 simulations were conducted for statistical significance.

Besides the different ratios, and the new fitness function defined in Eq. 8.11, the parameters and simulation setups were exactly the same as for the evo-ALL simulations presented in Chapter 6 (Section 6.3). The ratios chosen were 1:0 (i.e. the original evo-ALL experiments, with no energy loss considered), 0.9:0.1, 0.8:0.2, 0.7:0.3, 0.6:0.4 and 0.5:0.5.

8.2.2.1 Research questions

1. For different *a:b* ratios, how does energy minimisation affect behavioural fitness?
2. How is wire length effected?
3. How does the emergence of energy minimisation relate to the emergence of behavioural fitness?
4. Precisely, how does evolution minimise energy loss? Via a minimisation of connectivity? By bringing connected neurons closer together?
5. How do different *a:b* ratios effect the emergence of neural architecture? Are certain motifs and other connectivity patterns seen to emerge?
6. How do different *a:b* ratios affect segmentation characteristics and the emergence of symmetry?

8.2.3 Results

Fitness Fig. 8.7 shows how the median value of f_1 changed during evolution and the corresponding boxplot at the end of evolution, for all six ratios. We can see that in general, the more weighting applied to the energy loss objective, the less ability that the agent has in reaching the target. In other words, minimising energy loss conserves energy; the animat generates less neural activity and cannot swim as far. An interesting case is when only slight energy loss is incorporated (a ratio of 0.9:0.1, indicated by the red plot). This shows virtually equivalent value to the 1.0:0.0 (black plot) ratio. A ranksum test confirms 'equivalence' with the two sets becoming 'different' only at the 50% level. On the contrary, there *is* significant difference when the ratio 1.0:0.0 is compared to all others besides 0.9:0.1.

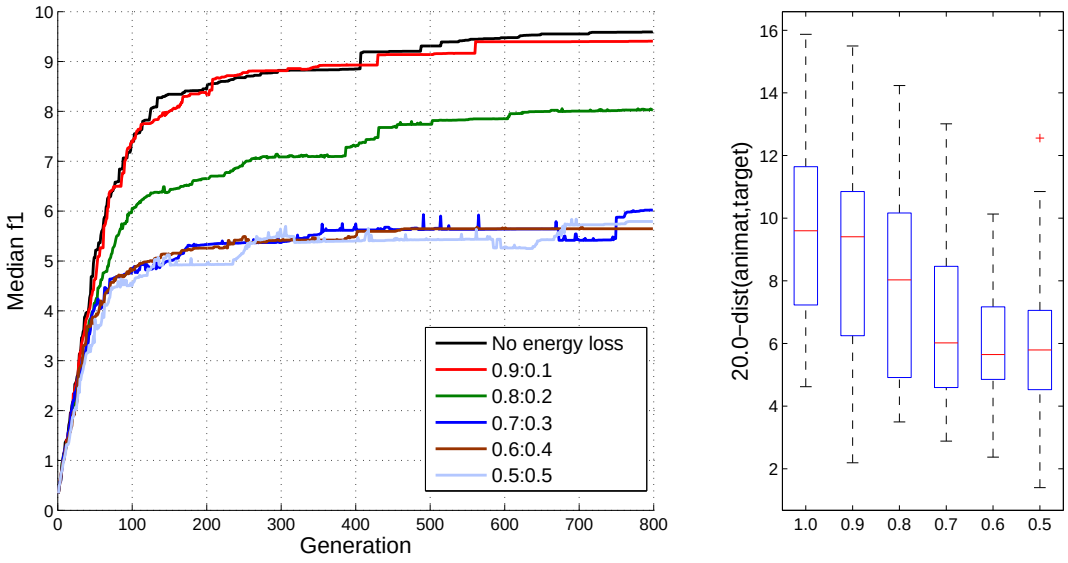

Figure 8.7: A comparison of f1, the value determining the distance of the agent from the target for the 6 different ratios, during, and after (boxplot) evolution.

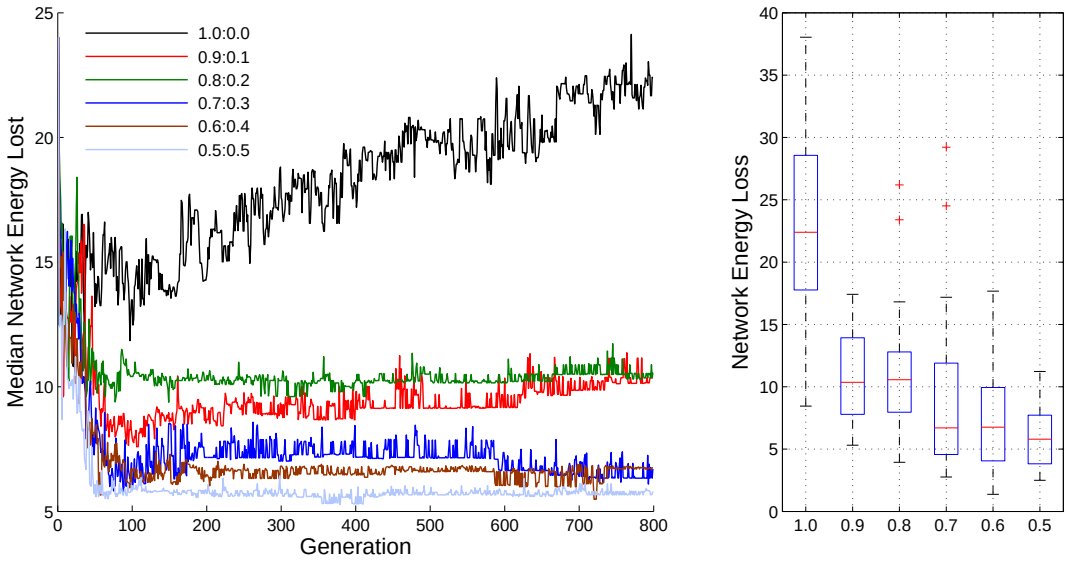

Figure 8.8: A comparison of the network energy lost for the 6 different ratios, during, and after (boxplot) evolution.

Network energy and wire length The above finding demonstrates that provided the energy constraint is small (0.9:0.1), its minimisation will not impact on the neural system's operational capacity. This is made clear in Fig. 8.8 (above), which shows the median loss of network energy for each ratio. Importantly, energy loss is significantly greater in the

1.0:0 case than in the 0.9:0.1 case (ranksum). Similarly, the total wire length, which one would expect to be minimised during the introduction of the energy loss term, is shown to be significantly greater in the 1.0:0.0 case since in this zero energy constraint, there was no energetic need for wire length minimisation (see Fig. 8.9).

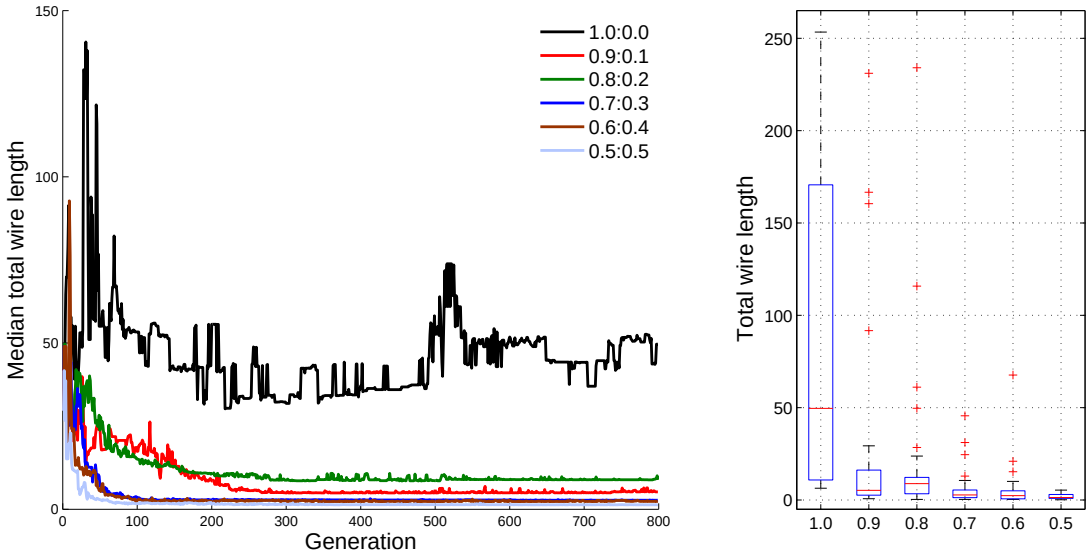

Figure 8.9: A comparison of total wire length for the 6 different ratios, during, and after (boxplot) evolution.

Visualisations showing the evolutionary emergence of fitness and levels of energy loss for representative individuals are given in Fig. 8.10. We can make the following observations:

- The higher the energy constraint, the lower the evolutionary emergence of behavioural fitness (ability to swim) and the greater the minimisation of network energy loss.
- In all cases, there are short periods immediately at the beginning of the evolutionary process in which energy loss is greatest. These periods further equate to least behavioural fitness. Thus to begin with, there is an inherent drive towards energy loss minimisation since this has the natural effect of also enhancing behavioural fitness. However, once behavioural fitness has reached a certain point, as indicated, the only way to enhance it even further is by increasing the energy expenditure. Such occurrences are marked with dashed horizontal lines in Fig. 8.10b.

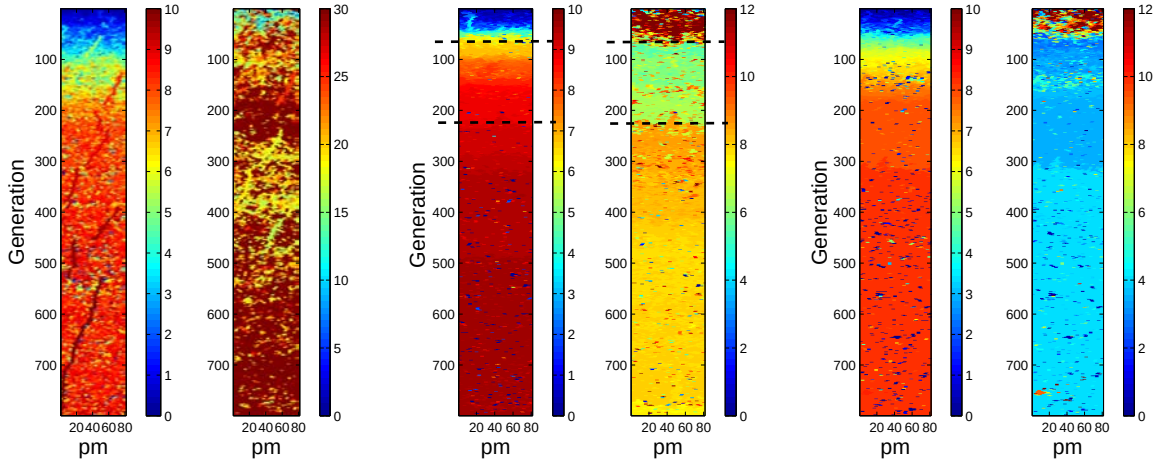

(a) 1.0:0.0 (b) 0.9:0.1 (c) 0.8:0.2

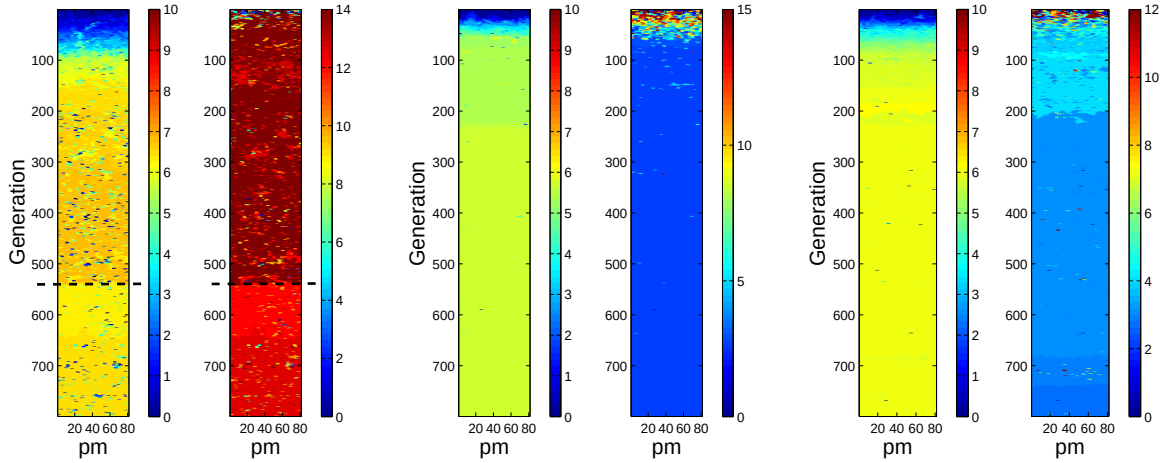

(d) 0.7:0.3 (e) 0.6:0.4 (f) 0.5:0.5

Figure 8.10: Visualisations of how evolutionary selection progressed for representative simulations. In each subplot, the left bar represents changes in behavioral fitness, the right bar changes in network energy loss; x-axis (pm) is population member (1-80). In subfigures b and d, dashed lines indicate how changes in energy loss reflect changes in behavioural fitness.

- In cases where the energy constraint is 'very' high, the drive towards behavioural fitness is less pressing. In such cases, points of transition within the evolutionary process are marked by reductions in energy loss and commensurate decreases in behavioural fitness. An occurrence of this is indicated by horizontal dashed lines in Fig. 8.10d.

Connectivity Wire length is related to connectivity: the higher the connectivity level, the more wire. Further, connectivity is governed by the connectivity function defined in Eq. 5.12 which specifies, based on euclidean distance and a set of λ parameters, how different neuron types (sensory (S), interneuron (I) and motor (E)) should become connected together. **Of importance:** recall from Fig. 5.4 that the larger the λ value, the closer a pair of neurons have to be to become connected.

Fig. 8.11 displays the emergence of each of the four evolved λ parameters for each energy constrained setup. These are the salient points:

- When an energy constraint is incorporated into the evolutionary process, over evolutionary time, the λ values are increased which has the effect of reducing the connectivity level (unless of course the neurons end up closer together).

- We can further observe from Fig. 8.12, that statistically, except for connections forming between interneurons in adjacent segments ('segment-segment' plot in the figure), differences in property emerge early (at around the 300 generation mark with a 0.05 confidence level).

- There are no statistical differences in the λ values controlling connectivity between interneurons in adjacent segments ('segment-segment' plot) for any *a:b* ratio.

- There are no statistical differences in the λ values controlling connectivity between interneurons and effector neurons when zero (1.0:0.0) and marginal (0.9:0.1 and 0.8:0.2) ratios are compared.

Therefore, in terms of connectivity, the evolutionary process evolves energy-conserving agents first and foremost by pruning out those connections between interneurons and secondly, by pruning out those connections made from sensory neurons. We have already noted in Chapters 6 and 7 that in terms of Evo-Critter, optimal behaviour is not necessarily dependent on connections from sensory neurons, therefore, pruning them out in order to conserve energy will have a negligible (if indeed any) impact on behavioural fitness.

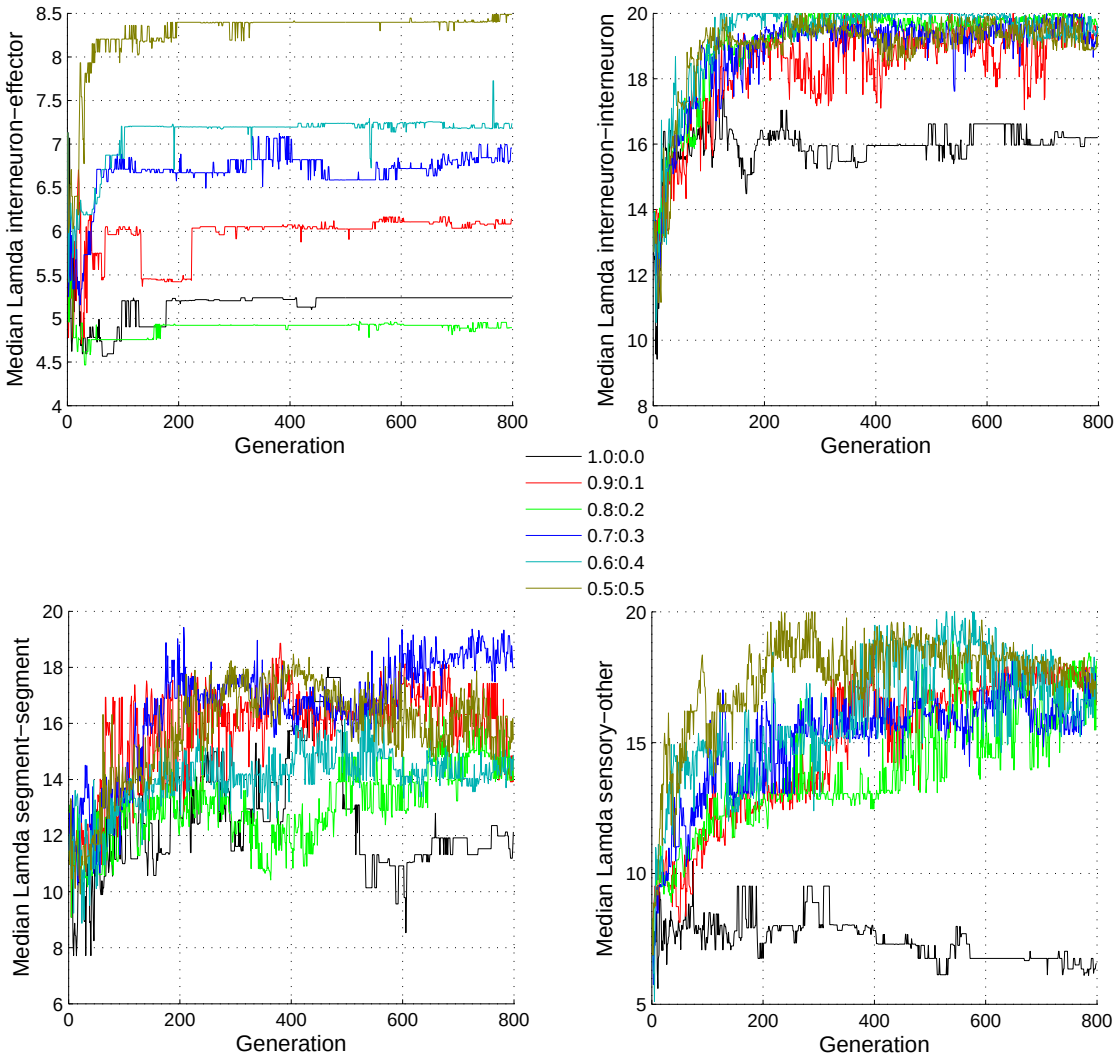

Figure 8.11: Evolutionary emergence of λ parameters for each of the different types of connectivity. As shown, for high energy constrained setups, there was a general tendency for the parameters to increase i.e. neurons had to be closer together if they were to become connected together.

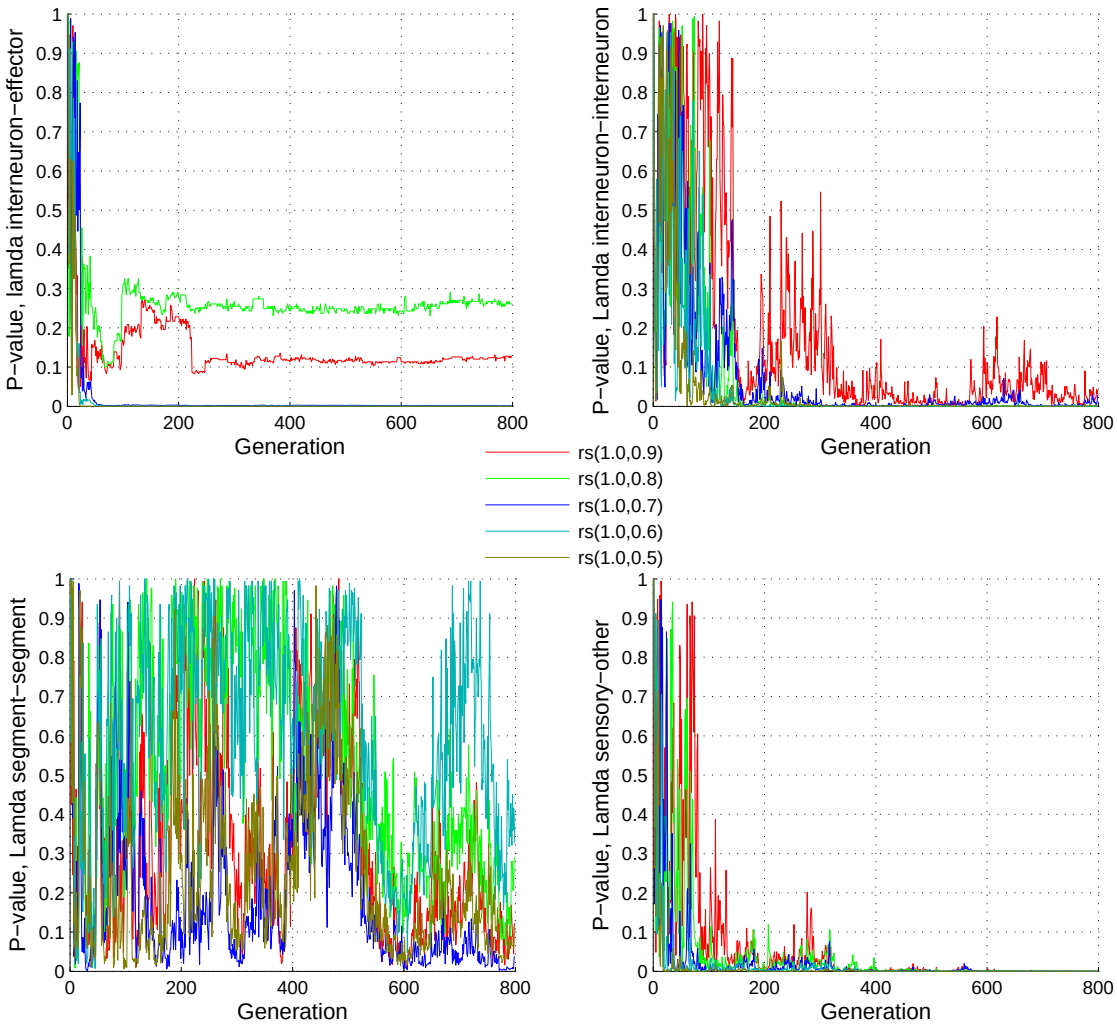

Figure 8.12: Statistical p-values generated when comparing the λ values of the 1.0:0.0 case (i.e. no energy constraint), with the λ values of cases having energy loss, as they emerged through evolution. In the legend, rs stands for ranksum, the statistical test used to compare the non-energy constrained agents (1.0:0.0) with 0.9:0.1, 0.8:0.2, etc. ratio agent setups. As shown, except for segment-segment connections, differences typically emerged early.

The fact that connections are only pruned out from between interneurons and effectors when the energy constraint is high (ratios 0.7:0.3, 0.6:0.4, 0.5:0.5), signifies the importance of this connection type. This makes sense because effector neurons are ultimately driven by the interneurons; thus, when the energy constraint is low, removing these connections will destroy those neural motifs necessary for correct behaviour. However, when the energy

constraint is turned up a few notches, energy loss as a penalty in the fitness function becomes more significant, thus, removal becomes more beneficial in order to keep the energy loss low and relative overall fitness high.

How does neuron pair distance depend on the connectivity level? In light of the above results, it is evident that evolution conserves energy by pruning out non-essential connections via an alteration of the λ connectivity parameters; we further observed how, given tests for significant difference, some types of connectivity (in particular those between interneurons and effector) are more fundamental in maintaining reasonable behavioural fitness levels. Thus we can infer that at certain levels of energy constraint, at a certain point in the evolutionary process, a trade-off is established in how energy should be conserved: on the one hand, by shortening the connection length and on the other, by pruning connections out entirely. To shed light on this trade-off, we can first compare the emergence of the average neuron pair distances with the emergence of theλ connectivity parameters (since these reflect connectivity levels). The results of having done this are plotted in Fig. 8.13. The main observations are as follows:

- The λ parameters depend on the level of energy constraint.
- In all but one case ('sensory-other'), there are no differences in neuron pair distances.
- In the case 'sensory-other', the larger the energy constraint, the further apart neurons become.

Therefore, it would appear that in terms of how evolution comes to minimise energy consumption, alteration in the level of connectivity takes precedence over an alteration in neuron pair distance. Only for connections between sensory- and interneurons, is energy minimised via an alteration of both properties: by increasing the λ connectivity parameter and by altering neuronal pair distance; however it should be noted that actually, in terms of this connection type, evolution appears to minimise energy loss not by bringing neurons closer together to thus shorten their connections, but by moving them further apart. Together with the larger λ connectivity parameter, which means that neurons need to be closer if connections are to form between them, this then has the effect of making neurons too far apart for connections to form between them. Connectivity is therefore ultimately reduced.

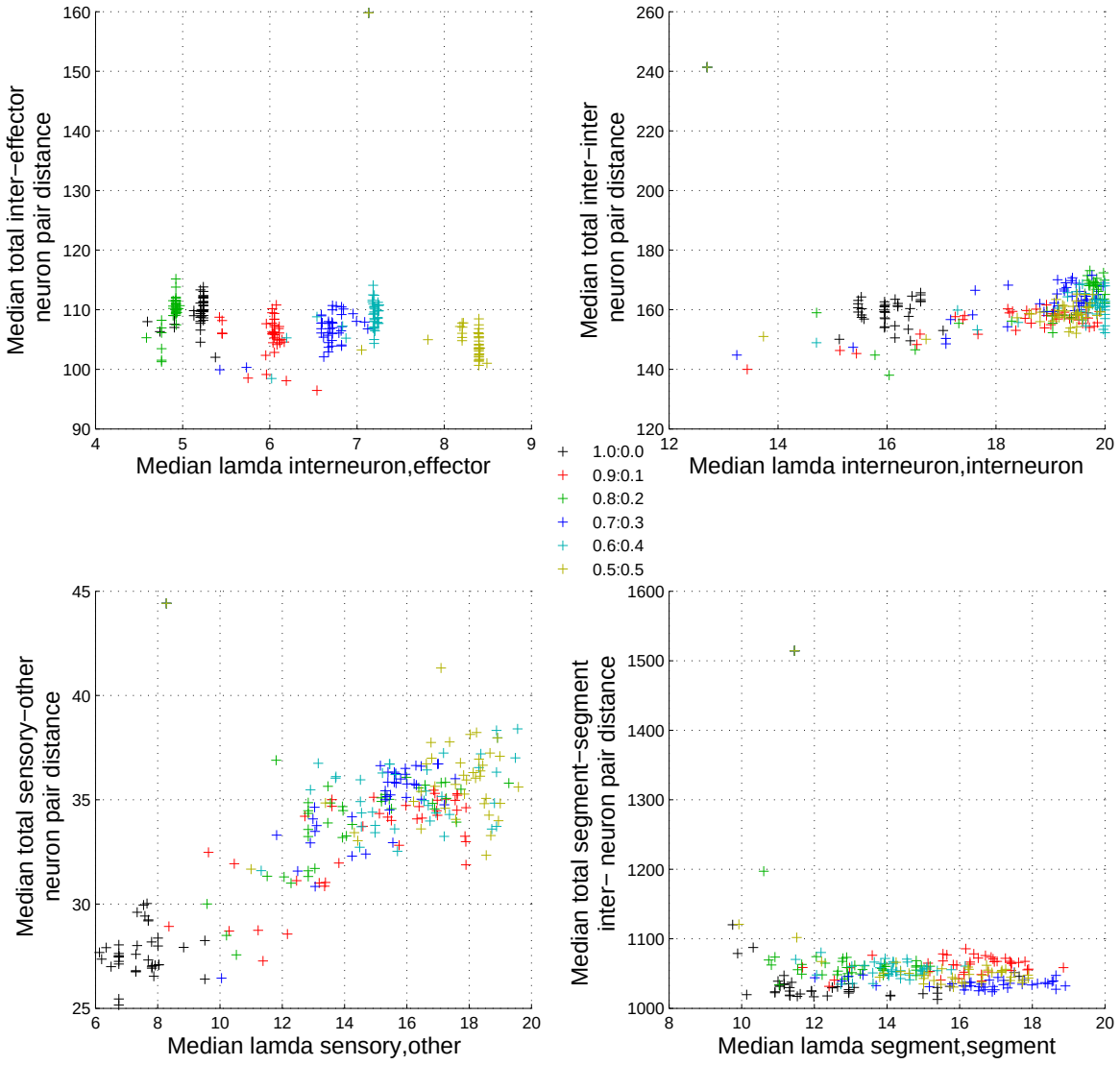

Figure 8.13: Neuron pair distances plotted against λ connectivity parameters. In a given subplot, a single point represents the median of 30 comparisons at the end of evolution.

Neural architectures The neural architectures of each set of 30 simulations have been plotted in Fig. 8.14.

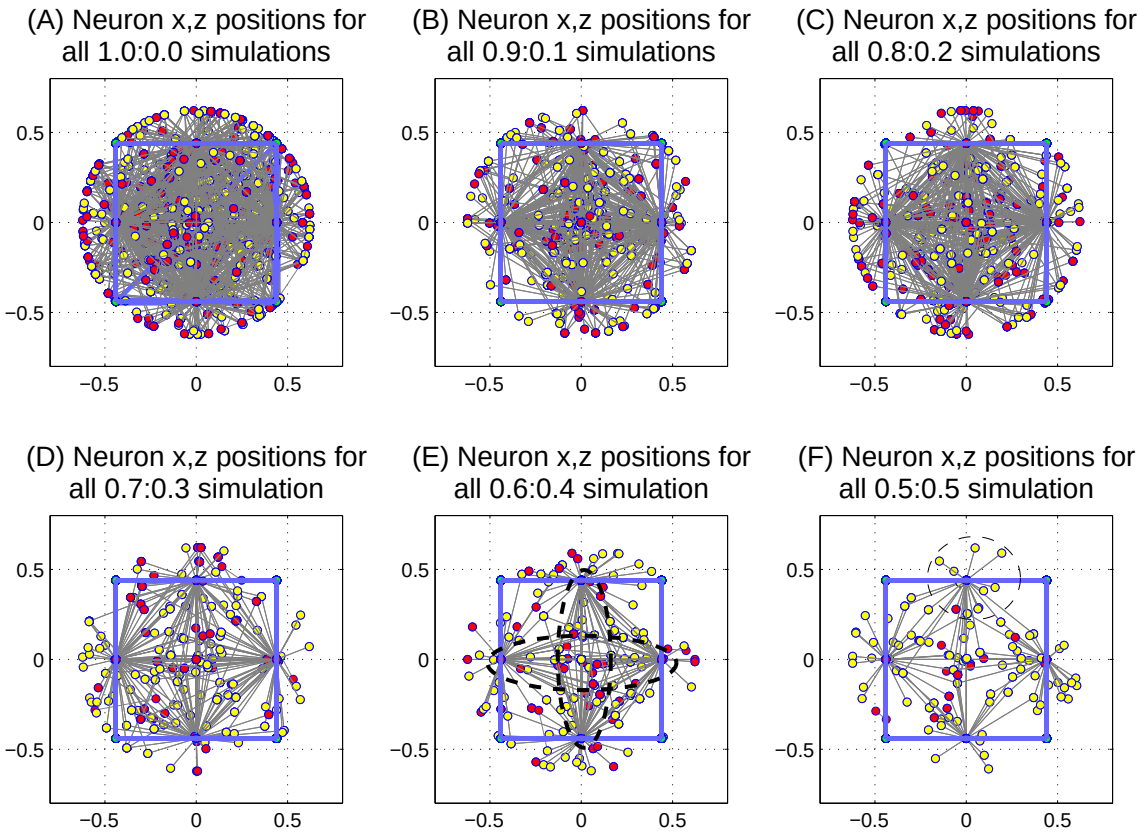

Figure 8.14: Neural architectures to have emerged for all simulations at the end of evolution (in each subplot, all 30 architectures are overlaid) when observing from the head end of the agent. Only neurons to have become connected, along with their connections, are visualised. Spheres are neurons (yellow=inhibitory; red=excitatory), grey lines are symmetric connections. The dashed ellipses in subplot (E) highlight some of the common architectural features that were found to emerge, and more prominently so, with higher energy constraints. The dashed ellipse in subplot (F) highlights 'leaf neurons', also found to emerge more prominently with higher energy constraints.

In subplot (A), the most dense connectivity can be observed for zero energy constraint. At the other extreme, in subplot (F), the most sparse connectivity can be observed for the 0.5:0.5 energy constraint. Also shown is how, with higher energy constraints, more 'leaf neurons' emerged. These are defined as those neurons that (due to evolutionary pressure) move towards and connect to the motors; an example is highlighted with a dashed ellipse in subplot (F). Notably, as the energy constraint increases, the connectivity gets sparser; those connections that remain are likely to be part of the functional motifs important for the

swimming behaviour. In particular, some very specific motifs were found to emerge during the course of evolution, the patterns of which have been highlighted with dashed ellipses in subplot (E). Generally, there is a tendency for 'cross-hair' motifs to emerge, whereby the centre neuron is a single inhibitory neuron. Examples of the neural motifs of body segment 2, for the best individuals to have emerged for each energy constraint experiment, are shown in Fig. 8.15.

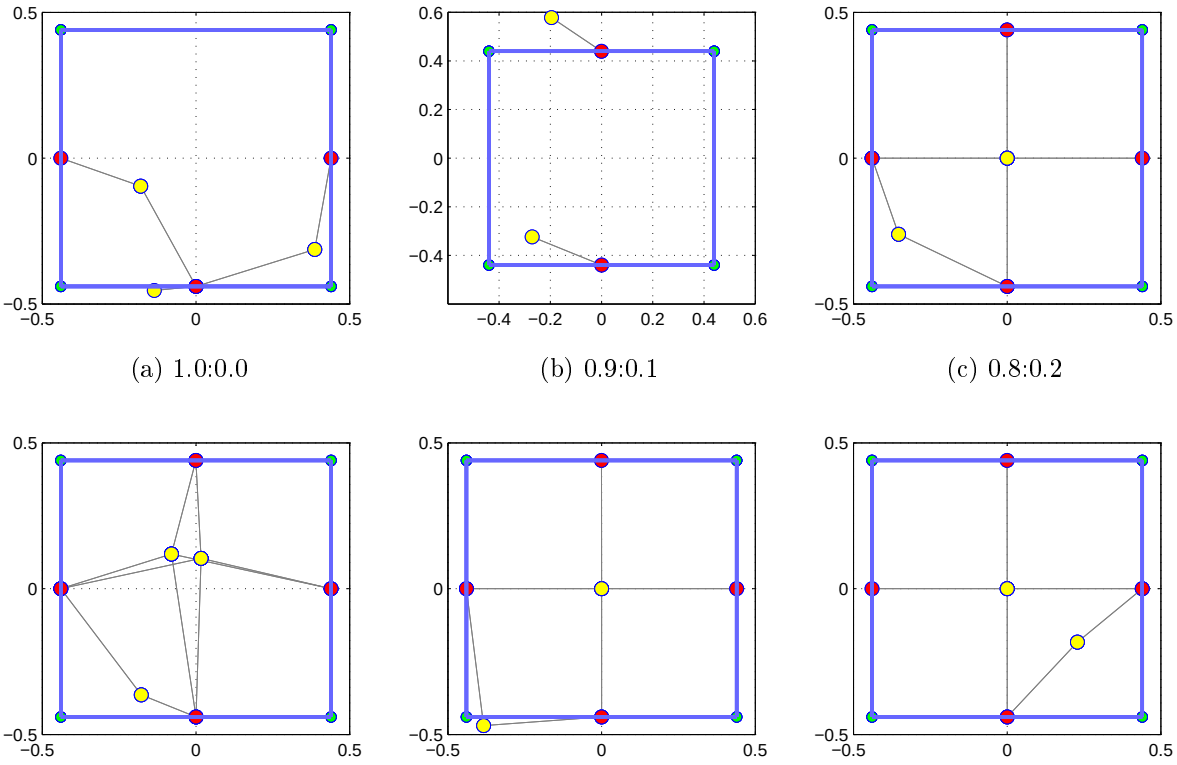

(a) 1.0:0.0 (b) 0.9:0.1 (c) 0.8:0.2

(d) 0.7:0.3 (e) 0.6:0.4 (f) 0.5:0.5

Figure 8.15: Common neural motifs to have emerged in the second body segment of the fittest individuals as generated by the best simulations. In (c), (e), and (f), a 'cross-hair' motif is seen to have emerged. This type of motif was found to be prevalent amongst all experiments. Note that a connection represented by a grey line is symmetric.

Influence of body segmentation characteristics We might hypothesise that in order to conserve energy, agents will evolve fewer body segments to reduce the number of neurons and therefore, the level of connectivity. This will have the effect of reducing the level of energy expenditure. However, statistically, there were found to be no differences. Therefore, in terms of conserving energy, evolution appears to either **(i)** prune out the extra connectivity that is

generated because of the extra body segments, or **(ii)** leave connections of computationally inactive neurons in place, since given the model, it is impossible for these to 'leak' any energy. Likewise, there are no statistical differences in body segment lengths between the different *a:b* experiments, even though the length of a segment constrains the distribution of neurons inside of it (for definitions, refer to Section 5.2.3). Thus in terms of conserving energy, connectivity between neurons is not altered by altering the lengths of body segments.

Motor Symmetry In Evo-Critter, motor symmetry determines which of the motor neurons actively drive the behavioural process. Thus by investigating the emergence of this property, we can investigate how symmetry is adapted not only to endow the agent with a reasonable behavioural fitness, but also to minimise its loss of energy. Fig. 8.16 shows the percentage of each type of motor symmetry to have emerged across all sets of 30 simulations. We can see that whilst the largest proportion of symmetry type to have emerged in agents with low energy constraint (1.0:0.0, 0.9:0.1 and 0.8:0.2) was fully bilateral, there was less preference for this symmetry type when the energy constraint was high. In order to shed light on this, Fig. 8.17 visualises the evolutionary emergence of motor symmetry of the individuals for which fitness and energy emergence have been plotted in Fig. 8.10.

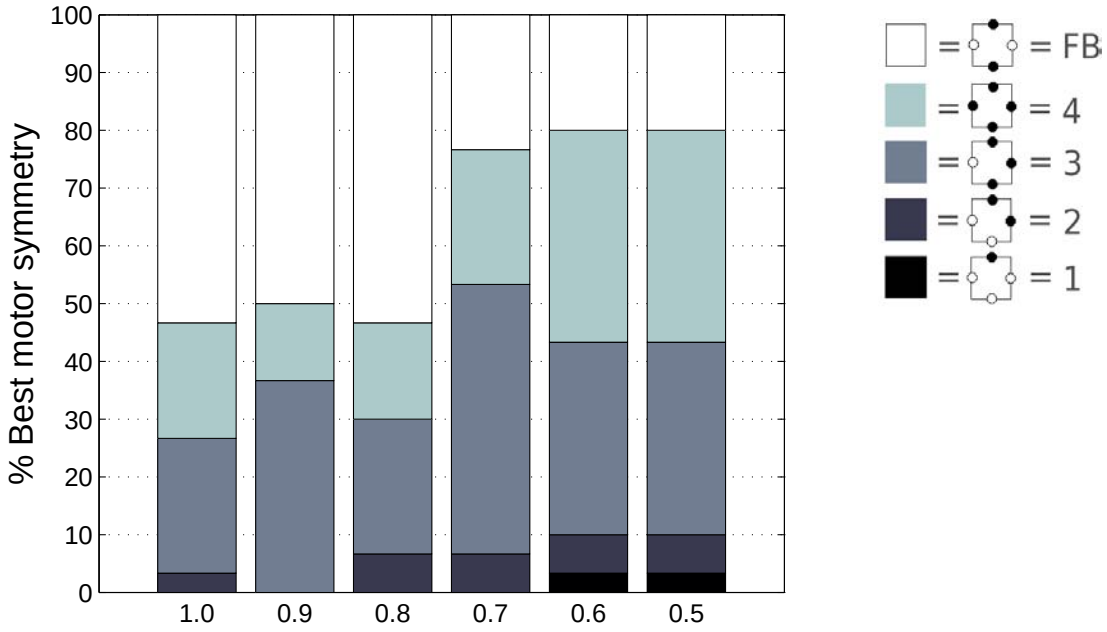

Figure 8.16: Motor symmetries to have emerged for the best individuals at the end of evolution, for each a:b setup. As shown, there was less of a tendency for bilaterally symmetric motor configurations to emerge when the energy constraint was high.

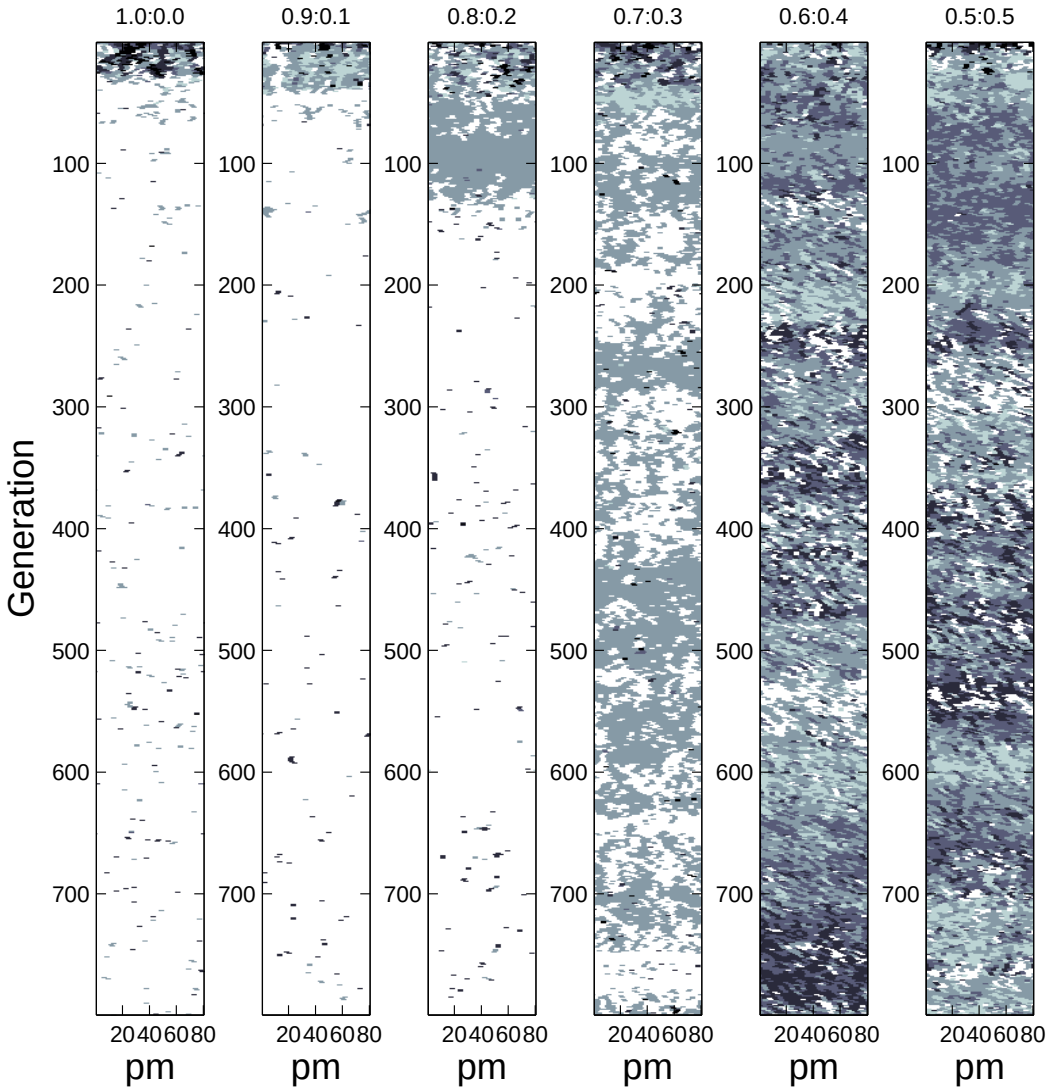

Figure 8.17: The evolutionary emergence of motor symmetry for the best population member of those members having the motor symmetry that was found to have emerged in largest proportion, for each a:b setup. In each subplot, y-axis is generation, x-axis is population member (0-80). Color represents type of symmetry (refer to legend in Fig. 8.16).

Our observations are thus:

- When the energy constraint is low (first three subplots), full bilateral symmetry, for these particular individuals, emerges early.
- For the first three individuals (relatively low energy constraint), full bilateral symmetry

takes progressively longer to emerge.

- When the energy constraint is high (second three subplots), motor symmetries 3 and 4 become more prominent during the evolutionary process.

Thus, when the energy constraint is high, the agent evolves to utilise more degrees of movement. By having motor symmetries that are not strictly fully bilateral, the agent can 'undulate' in more than just one dimension. It would therefore seem that when the energy constraint is overly large, the agent is forced to evolve in a way that allows it to 'do all it can' in locomoting, since the normal structural neural motifs that preclude optimal central pattern generating dynamics for full bilateral symmetry, are no longer necessarily in place. In terms of neural architecture, the agents evolve to harness 'what is available', forcing the agent to adapt and fit its motor symmetry around the energy constrained neural system.

8.3 Discussion and Conclusions

In Section 8.1, a novel ('Hydramat') framework that incorporates energy efficiency in organising nervous systems was suggested. This framework allowed us to take the first steps in understanding organisation of the most primitive of nervous systems, demonstrating how efficiency of information processing and minimisation of energy consumption emerges in evolution via interactions with the environment. The results further showed us how random perturbations facilitate the emergence of novel nervous architectures. We can speculate that the same holds for the biological radially symmetric organisms of the genus hydra, i.e., that the formation of ring structures around the hypostomal region, [63], is a result of selection pressure towards minimalistic structures which when coupled to body morphology results in similar neural architectures emerging. A further view is that the noisy effect of lifetime neural perturbations might increase robustness of the information processing system.

In Section 8.2, it was further explained how an energy loss term was added to the Evo-Critter fitness function. This enabled us to consolidate the view that a minimisation of energy consumption leads to an emergence of archetypal neural architectures which, due to a minimisation of connectivity, are invariably sparser and further, are often characterised by particular 'cross-hair' connectivity motifs and other minimal structures. Also, it was considered how a notion of energy loss should also reflect the level of agent movement given that effector neuron actuations are reflective of behavioural processes. Thus the main contribu-

tion of this secondary piece of work is a novel simulation environment in which the nervous system of an agent and the coupling to its body plan morphology, emerges in order that energy loss can be minimised (yet in a way that facilitates swimming behaviour). It was further demonstrated that under the constraints of energy, functional symmetry will emerge to encompass more degrees of freedom of movement, so that basically, the agent can do all it can in locomoting towards the environmental target.

Thus in summary, the contributions of this chapter are as follows:

- a presentation of the Hydramat framework, a tool that can be used to study the evolutionary emergence of neural organisation when under the constraint of energy loss minimisation / energy gain maximisation.

- a presentation of how an energy loss term can be incorporated into the Evo-Critter framework and thus demonstrate how energy is lost via both neural and motor activities. Also, the commensurate effect of this on neural architecture and body plan morphology.

- how neural organisation emerges to be minimal (especially in view of connectivity) when there exists a need to minimise the loss of energy.

- a demonstration of how energy loss minimisation due to both neural and motor activity can lead to minimal changes in body plan morphology: in comparison to the results presented in Chapter 6, no significant changes in segmentation characteristics were seen to occur.

- with very high energy constraint, bilateral motor symmetry emerges less often. This demonstrates a coupling between the need to conserve energy and the emergence of body symmetry properties.

Chapter 9

Conclusions

In the introduction of this thesis, the importance of shedding light on nervous system organisation was identified as a crucial endeavour in helping us to understand how nature has come to organise and process information efficiently and robustly. Doing so formed the aim of the thesis. It was then elucidated how we can turn to nature's least complex nervous systems, modeling them in simulated computer environments so that we can contribute towards the understanding of how different organisational aspects evolve and develop over time. This formed the basic methodology used throughout.

The above aim was met via several computational models designed to assess different levels of neural organisation. These models primarily placed an emphasis on neural architecture such that spatial characteristics would have a bearing on computational property. This meant that for a given agent, the neural architecture was largely responsible for eliciting behaviour, which thereby allowed us to directly observe and evaluate the impact of specific neural structures – e.g. nerve rings or central pattern generators – in very specific environments. Although the levels of abstraction were high, the implemented frameworks endowed us with a set of tools that could be used to investigate some of the core principles. Development of these models imparted a significant undertaking.

To begin with, based on an initial literature review of primitive nervous systems, the Hydramat Simulation Environment was developed to study the effect of energy consumption on the emergence of neural organisation within agents akin to the freshwater Hydra; this organism was identified in the literature review as having the most primitive of nervous systems. Thus, the Hydramat work was actually conducted before the Evo-Critter work, however, it was not until Chapter 8 that it was fully introduced since only at this point was

the impact of energy fully addressed.

The Evo-Critter framework was then later developed (but presented in the thesis earliest) due to the limitations posed by the Hydramat Simulation Environment. The fixed nature of the Hydramat agent's body plan meant that coevolution of body morphology could not be investigated. The Evo-Critter framework was designed to alleviate such problems by being as extensible as practically possible; one could, for example, easily modify it to investigate a variety of other neural models, agent types and evolutionary processes. The Evo-Critter framework further incorporated a notion of body-symmetry which was identified in the literature as being significant in evolutionary terms. Thus, it encompassed more of the investigatory targets.

In terms of implementational specifics, development of the Hydramat framework involved the creation of a three dimensional wire frame environment, incorporation of a spiking neural network simulator and artificial evolutionary processes. The Evo-Critter framework was more complex and accordingly took longer to be developed and tested. In addition to the 3D wire frame model which was essentially ported across from the Hydramat framework, development involved the implementation of a physics engine, a recurrent neural network model and different artificial evolutionary processes. The code bases for both the Hydramat Simulation Environment and the Evo-Critter framework were further parallelised using the Message Passing Interface (MPI)[1] allowing one to distribute a single evolutionary simulation amongst several computer nodes. This made things substantially faster; experiments that would normally have taken a week to complete could be carried out in a single day.

For both frameworks, in terms of the methodology, an agent would incorporate a neural control system that was *spatially embedded*. This point of methodology was determined to be crucial, since it enabled one to focus on the effect of the nervous system architecture in terms of its relation to important physical and dynamical properties. Interneuronal distance would determine synaptic efficacy (i.e. connection weight value), therefore, the neural dynamics would be largely determined by the neural system's spatial organisation which in itself would be constrained by the body plan morphology and energy constraint. Therefore, in a sense, architectural organisation of both the body plan and the nervous system were placed on an even keel.

Throughout the thesis, the research interest has primarily focused on biological literature and biophysical models. Accordingly, the Evo-Critter framework was developed with only a

[1] see http://en.wikipedia.org/wiki/Message_Passing_Interface

sparse consideration of prior 'Artificial Life'-based three dimensional models (for example, Karl Sims' models and derived works). It was only retrospectively that these other models were approached in the manner of enabling one to appraise one's own methodology. Moreover, the work has been grounded in scientific understanding as opposed to engineering. The models were devised to reflect principles of biological nervous systems as plausibly (and therefore, as scientifically accurately) as was practically possible. Thus the ultimate worth of the models we've explored lies in their capacity to shed light on real neurobiology. The findings endow us with many credible implications, some of which are discussed in Section 9.6.

The remainder of this chapter is set out as follows. The main contributions of this thesis are summarised in Sections 9.1 to 9.4. Some possibilities for future research avenues are summarised in Section 9.5. Finally, some of the wider implications are addressed in Section 9.6.

9.1 The Beginning: Towards Physical Couplings

To begin with, a model of an undulatory organism ('Evo-Critter') was developed with the primary aim of understanding how the nervous system should become architecturally coupled to the body plan morphology and how this morphology should further constrain neural organisation. Also, in order to observe how body symmetry should have an impact on behaviour, which, as we discussed throughout, is a major factor during the evolution of nervous systems, the Evo-Critter framework further incorporated a notion of functional symmetry. Thus the initial contributions are as follows:

- Evo-Critter, the model itself, as a tool capable of elucidating body plan - nervous system couplings via interactions with the environment.
- A demonstration of how certain symmetry is advantageous to the behaviour of an artificial agent. It is conceivable that symmetrical properties of biological organisms will also emerge to reflect functional necessity.
- An understanding that given the non-linear dependencies (couplings) between the different components, different combinations of phenotype traits will emerge to facilitate optimal behaviour. This was further demonstrated in light of constraining parts of the body plan morphology.

- The finding that neural architecture in many instances emerges to be minimal with much of the behavioural process governed by the dynamics of the moving body components (springs etc.). We observed this in terms of the wire length and connectivity levels. The most minimal neural structures were observed in agents for which all body plan components ('segmentation characteristics') were coevolved. Further, agents endowed with segment length coevolution were also shown to yield a minimal level of neural activity despite higher fitness levels, which again indicated how much of the behavioural process was being offloaded to the body dynamics.

9.2 The Middle: Towards a Dynamic Coupling

Secondly, it was demonstrated how body plan morphology and nervous system are not only physically coupled in the sense of structure, but also dynamically, given the behavioural interaction between the body kinematics and the nervous system dynamics. This was brought to the fore in Chapter 7, with the demonstration that a feedback mechanism strengthens the coupling. It was further suggested that this strengthening heightens a robustness to environmental perturbation. Thus, the next set of contributions are as follows:

- The finding that agents endowed with feedback evolve to have more minimalist neural architectures.

- The principle that agents endowed with sensory feedback have more of the computational (central pattern generating) process offloaded to the kinematics of the moving body parts.

- The finding that agents endowed with a feedback mechanism are more robust to environmental perturbation given the strengthened dynamic coupling between body kinematics and neural dynamics.

- The finding that structural regularity within the nervous system will ensure optimal connectivity levels: when the neural architecture is perturbed, the neural connectivity levels and therefore the behavioural process are disrupted.

9.3 The End: The Effect of Energy Loss Minimisation

In the third part of this thesis, we came to understand how the need to minimise energy loss and thus conserve energy (so that the agent may survive) also places constraint on the emergence of neural organisation. The main contributions of this part are several-fold:

- It was demonstrated how neural organisation in a radially symmetric agent should emerge to become minimalistic in structure, which corresponds closely to the neural organisation in biological organisms of the genus Hydra. Thus via interactions with the environment, evolution will strive towards minimalistic neural architectures.

- In extending an energy loss minimisation term to the fitness function of the Evo-Critter framework, it was demonstrated how a drive towards minimising energy loss can influence the organisation of the nervous system and, like the findings of the Hydramat work, drive neural architectures towards minimalistic structure.

- It was further demonstrated in the Evo-Critter framework that body symmetry – as it was defined in the Evo-Critter system (i.e. motor symmetry configuration) – will emerge in a way that minimises energy loss. It was found that such symmetries would enable the agent to swim in 'non-standard' ways (non-undulatory) and thus compensate for an imparted reduction in functional input from the neural system to the motors.

9.4 Tying it all together

We can see that with regards to all of the above described work, there is a common theme: the emergence of minimal neural structure as summarised:

- A significant reduction in wire when all body plan morphology characteristics were evolved (Chapter 6).

- A significant reduction in connectivity levels when sensory feedback is incorporated (Chapter 7).

- The emergence of minimal neural structure and connection motifs when a need to minimise energy loss is incorporated as an extra term in the fitness function (demonstrated in both the Hydramat and Evo-Critter work, Chapter 8).

Thus the primary contributions of the work presented in this thesis are as follows:

1. When the body plan morphology of an agent is unconstrained in the sense that it can be tuned by the evolutionary process, there is a tendency for the neural structure to emerge in a minimal fashion. Moreover, it would appear that when the behavioural process can be offloaded to the body morphology characteristics (due to an optimisation of spring lengths etc.) or that the body can directly influence the behavioural process (via a sensory feedback link), there is less of a need for neural structure, and in some cases, the neural activity is also commensurately lower, indicating less of a need for neural computation processes. Whilst the Evo-Critter model is highly abstract, we can conjecture that similar evolutionary forces are at play during the evolution of biological nervous systems, in which a minimisation of wire length together with the coupled evolution of optimal body plan morphology are both critical for ensured survival.

2. When a need to minimise energy is also incorporated into the evolutionary process, the neural architecture emerges minimally both in terms of wire length and geometrical structure. Thus demonstrably, functional energetics is also an important consideration in the evolution of neural organisation. Again, although the models are abstract, it is conceivable that given the need to minimise the wire length and thus conserve energy, such processes are at play during the evolution of biological organisms.

9.5 Future Work

A possible and very interesting avenue of future work concerns the amalgamation of the Hydramat framework and the Evo-Critter framework. This is in view of the following: firstly, on the one hand, the Hydramat framework attempts to model the most primitive of neural organisation evolution whilst on the other, the Evo-Critter framework is concerned with a more advanced evolutionary level. Secondly, the Hydramat is radially symmetric whilst the Evo-Critter is basically bilaterally symmetric (if we discount the functional symmetry component). Thus, by incorporating both frameworks, we can aim to model a smooth transition from radial symmetry to bilateral symmetry and observe the according changes in the coupled nervous system architecture. In order to allow for this, a range of different environments, extending from the 'food-drop' task of the Hydramat to the directional swimming behaviour of the Evo-Critter agent, will need to be created in order that the correct selection

mechanisms are in place. By doing this, specific environments will be better served by agents having specific body plan nervous system couplings.

An entropy transfer framework could also be used to further the Evo-Critter analysis by empirically measuring and therefore quantifying how certain events (environmental or internal) affect information flow. The idea is this: if the entropy change from component A to component B is observed to have been high, then a high level of information can be said to have propagated from A to B. With variable setups, we can take this idea and empirically measure how energy consumption or body plan morphology characteristics affect this process. The investigations of Lungarella and Sporns [71] can be used as a basis.

Other possible extensions are as follows:

- 'Complexifying' the environments so that any changes to nervous system architecture and body plan morphology characteristics, both with and without the constraint of energy consumption, can be observed. For example, what happens if the agent is tasked with 'tracking' a moving object? Intuitively, the neural system would have to be wired such that coordination between the neural circuits is made possible; this is especially interesting in lieu of the experimental findings presented in this thesis, that neural circuits would typically emerge to be decoupled.

- In the Evo-Critter framework, connections are currently symmetric; how do neural connection motifs emerge if connections are asymmetric?

- Subsets of neurons are restricted to geometrically reside in certain body segments; what happens if we remove this restriction? Will neural architecture emerge differently?

- With the addition of an evolvable feedback mechanism, we could observe how agents evolve in noisy environments. This will strengthen our understanding of robustness.

- A spiking neuron model could be incorporated to Evo-Critter to more realistically reflect the nervous systems of biological organisms.

- A cost of development could be incorporated into the fitness function; thus the actual construction of neural circuits – neurons, their respective connections, and body segments – could be taken into account. How will this constrain the emergence of functional neural connection motifs? (Note: a cost of movement could also be added

to the Hydramat framework. This is implicitly accounted for in the Evo-Critter framework already given the incorporation of motor neuron actuations into the energy loss formulation).

- A genetic regulatory network could be incorporated so that the growth processes of biological organisms can be more realistically reflected.

9.6 Wider Implications

The core of this thesis has presented the view that the evolutionary emergence of neural organisation is constrained by both an agent's body plan morphology and a need to conserve energy. It has been demonstrated that neural organisation will emerge to fit around these 'constraints' yet nonetheless in a way that maximises functional advantage – for example, the ability to undertake directional movement, or the acquisition of food particles. In other words, it has been demonstrated how, during the evolutionary process, physical and dynamical interdependencies become fitness-enhancing features – *units of selection* – all of which lend themselves to the survivability of the agent. It seems credible that animals have evolved to reflect this interdependency, that evolutionary transitions of nervous systems have been driven as much by such couplings as by the individual components themselves. Thus, in a fully encompassing framework, such 'body' and 'nervous system' couplings, and energy consumption, which is core in evolutionary process, cannot be ignored or assumed to have negligible importance.

Crucially, the results presented in this thesis suggest that neuroscientific investigations could benefit from moving beyond a conceptual treatment of the nervous system alone, since, as shown, physical and dynamic properties are as much governed by body plan characteristics and energetic constraints as by properties of the nervous system (and sometimes more so). In the very least, models and frameworks that have already been devised might be assessed to determine their palpability in incorporating such factors.

It is conceivable that primitive animals of both the invertebrate type (e.g., the hydra and platyhelminthe) and the vertebrate type (e.g., the lamprey) evolved in a fashion not entirely dissimilar to the artificial agents presented in this thesis, that during evolution, different components cooperatively 'aligned themselves' to maximise the efficiency of the whole animal. Precisely how this occurred is basically the subject of much evolutionary-developmental literature, yet, beyond evidence for genetic homology, the practical specifics

are open to debate. However, as with the artificial treatments made in this thesis, if the 'how' and 'why' of a naturally extant agent is similarly investigated, it might be possible to shed light on such specifics, for example, when certain features of the body-plan are simply 'switched off'. With such an (ideal) approach, scientific study can aim to disseminate precisely how different body-plan characteristics of a natural agent impact upon the dynamic and structural characteristics of the agent's (natural) nervous system. One might ask: if a 'fish' is prevented from moving, does its nervous system still exhibit the same central pattern generating dynamics as when the fish is allowed to move freely? If the answer is found to be 'no', then we might deduce that the dynamics of the moving fish body does indeed have a significant impact on the generation of the fish's neural dynamics.

We can also ask how in a natural agent framework, the wire length is affected; in most biological treatments, this has traditionally only been analysed in terms of energetic factors and, moreover, in an offline sense, whereby no interaction exists between the neural system and the surrounding environment. Yet, in view of the finding that neural circuitry has a tendency to emerge minimalistically – even without the constraint of energy conservation –, it is arguably paramount to incorporate at least some notion of a coupled body morphology when investigating the minimisation of wire length.

As an aside, the above suggestions may only come into fruition once greater dialogue has been established between neuroscientists and members of the artificial life community. By engaging together on a more frequent basis, it is expected that both parties will be able to benefit from the studies of each. Neuroscientists will have greater access to biologically plausible artificial life findings, and members of the artificial life community will be able to extend their models in a way that can basically overcome regimented engineering approaches.

Bibliography

[1] J. Albert. Computational modeling of an early evolutionary stage of the nervous system. *BioSystems*, 54(1–2):77–90, 1999.

[2] J. Albert. Modeling of an early evolutionary stage of the cnidarian nervous system and behaviour. In *Lecture notes in Computer Science*, volume 1674, pages 236–245. 1999.

[3] J. Albert. Towards a comprehensive alife-model of the evolution of the nervous system and adaptive behaviour. Technical report, Dept. of Comparative Physiology and Dept. of history and Philosophy of Science, Lorand Eotvos University, Budapest, 2000.

[4] P.A.V. Anderson. Cnidarian neurobiology: what does the future hold? *Hydrobiologia*, (530-531):107–116, 2004.

[5] D. Arendt, A.S. Denes, G. Jékely, and K. Tessmar-Raible. The evolution of nervous system centralization. *Philosophical Transactions of The Royal Society B*, 363(1496):1523–1528, 2008.

[6] J. Astor and C. Adami. Development and evolution of neural networks in an artificial chemistry. In *Third German Workshop on Artificial Life*, pages 15–30, Frankfurt, 1998. Harri Deutsch.

[7] T. Bäck and H.-P. Schwefel. An overview of evolutionary algorithms for parameter optimization. *Evolutionary Computation*, 1(1):1–23, 1993.

[8] D. S. Bassett and E. Bullmore. Small-world brain networks. *Neuroscientist*, 12(6):512–523, 2006.

[9] M. Beauregard and P.J. Kennedy. Robust simulation of lamprey tracking. In *Parallel Problem Solving from Nature IX*, pages 641–650, Berlin, 2006. Springer.

[10] R.D. Beer. On the dynamics of small continuous-time recurrent neural networks. *Adaptive Behavior*, 3(4):469–509, 1995.

[11] R.D. Beer. Toward the evolution of dynamical neural networks for minimally cognitive behavior. In *From Animals to Animats 4*, pages 421–429. MIT press, 1996.

[12] P. beim Graben, T. Liebscher, and J. Kurths. Neural and cognitive modeling with networks of leaky integrator units. In *Lectures in Supercomputational Neurosciences*, pages 195 – 223. Springer, Berlin, 2008.

[13] J. Blynel and D. Floreano. Levels of dynamics and adaptive behavior in evolutionary neural controllers. In *From animals to animats: The seventh international conference on simulation of adaptive behavior*, pages 272–281, Cambridge, MA, 2002. MIT Press.

[14] H.R. Bode. Continuous conversion of neuron phenotype in hydra. *Trends in Genetics*, 8(8):279–284, 1992.

[15] H.R. Bode. The interstitial cell lineage of hydra: a stem cell system that arose early in evolution. *Journal of Cell Science*, 109(66):1155–1164, 1996.

[16] H.R. Bode, S. Heimfeld, O. Koizumi, C.L. Littlefield, and M.S. Yaross. Maintenance and regeneration of the nerve net in hydra. *American Zoology*, 28:1053–1063, 1988.

[17] P.M. Bode, T.A. Awad, O. Koizumi, Y. Nakashima, C.J. Grimmelikhuijzen, and H.R. Bode. Development of the two-part pattern during regeneration of the head in hydra. *Development*, 102(1):223–235, 1988.

[18] J. Bongard and R. Pfeifer. Evolving complete agents using artificial ontogeny. In *Morpho-functional Machines: The New Species (Designing Embodied Intelligence)*, pages 237–258. Springer, Berlin, 2003.

[19] J.C. Bongard. *Incremental Approaches to the Combined Evolution of a Robot's Body and Brain*. PhD thesis, Mathematisch-naturwissenschaftlichen Fakultät der Universität Zürich, Zürich, 2003.

[20] J.C. Bongard and C. Paul. Investigating morphological symmetry and locomotive efficiency using virtual embodied evolution. In *From Animals to Animats: The Sixth International Conference on Simulation of Adaptive Behavior*, Cambridge, MA, 2000. MIT Press.

[21] T.C.G. Bosch and K. Khalturin. Patterning and cell differentiation in hydra: novel genes and the limits to conservation. *Canadian Journal of Zoology*, 80(10):1670–1677, 2002.

[22] V. Braitenberg. *Vehicles: Experiments in synthetic psychology*. MIT Press, Cambridge, Mass, 1984.

[23] M. Broun, S. Sokol, and H.R. Bode. Cngsc, a homologue of goosecoid, participates in the patterning of the head, and is expressed in the organizer region of Hydra. *Development*, 126:5245–5254, 1999.

[24] J. Chavas, C. Corne, P. Horvai, J. Kodjabachian, and J.-A. Meyer. Incremental evolution of neural controllers for robust obstacle-avoidance in khepera. In *Evolutionary Robotics*, pages 227–247, Berlin, 1998. Springer.

[25] B.L. Chen, D.H. Hall, and D.B. Chklovskii. Wiring optimization can relate neuronal structure and function. *Proceedings of the National Academy of Sciences of the United States of America*, 103(12):4723–4728, 2006.

[26] D.B. Chklovski and T. Schikorski. Wiring optimization in cortical circuits. *Neuron*, 34(3):341–347, 2002.

[27] D. B. Chklovskii. Exact solution for the optimal neuronal layout problem. *Neural Computation*, 16:2067–2078, 2004.

[28] J. Chvál. L-systems based generative mapping in the evolutionary design. *Slovensko-České rozpravy o umelej inteligencii (Kognícia a umelý život III)*, 3:309–314, 2003.

[29] R.B. Clark. *Dynamics in Metazoan Evolution: The Origin of the Coelom and Segments*. Clarendon Press, Oxford, 1964.

[30] D. Cliff. Computational neuroethology: a provisional manifesto. In *Proceedings of the first international conference on simulation of adaptive behavior on From animals to animats*, pages 29–39, Cambridge, MA, 1990. MIT Press.

[31] C.A. Coello Coello. A comprehensive survey of evolutionary-based multiobjective optimization techniques. *Knowledge and Information Systems*, 1:269–308, 1998.

[32] A.G. Collins and J.W. Valentine. Defining phyla: evolutionary pathways to metazoan body plans. *Evolution and Development*, 3(6):432–442, 2001.

[33] S. Conway-Morris. The Cambrian "explosion" of metazoans and molecular biology: would Darwin be satisfied? *International Journal of Developmental Biology*, 47(7-8):505–515, 2003.

[34] P. Eggenberger. Creation of neural networks based on developmental and evolutionary principles. In *Proceedings of the 7th International Conference on Artificial Neural Networks*, volume 1327, pages 337–343, London, 1997. Springer.

[35] P. Eggenberger. Evolving neural network structures using axonal growth mechanisms. In *International Joint Conference on Neural Networks*, volume 6, pages 591–595, Washington, DC, 2000. IEEE Computer Society.

[36] Ö. Ekeberg. A combined neuronal and mechanical model of fish swimming. *Biological Cybernetics*, 69(5-6):363–374, 1993.

[37] Ö. Ekeberg. An integrated neuronal and mechanical model of fish swimming. In *Computation in Neurons and Neural Systems*, pages 217–222, Washington, DC, 1994. Kluwer.

[38] O. Ekeberg and S. Grillner. Simulations of neuromuscular control in lamprey swimming. In *Philosophical transactions of the Royal Society of London. Series B, Biological sciences*, volume 354, pages 895–902. 1999.

[39] J.G. Ferry and C.H. House. The stepwise evolution of early life driven by energy conservation. *Molecular Biology and Evolution*, 23(6):1286–1292, 2006.

[40] J.R. Finnerty. The origins of axial patterning in the metazoa: how old is bilateral symmetry? *International Journal of Developmental Biology*, 47(7–8):523–529, 2003.

[41] D. Floreano, P. Dürr, and C. Mattiussi. Neuroevolution: from architectures to learning. *Evolutionary Intelligence*, 1(1):47–62, 2008.

[42] R.V. Florian. Biologically inspired neural networks for the control of embodied agents. Technical report, The Center for Cognitive and Neural Studies, Cluj-Napoca, Romania, 2003.

[43] W.O. Friesen and W.B. Kristan. Leech locomotion: swimming, crawling, and decisions. *Neurobiology of Behaviour*, 17(6):704–711, 2008.

[44] M.-O. Gewaltig and M. Diesmann. NEST. Scholarpedia, 2007.

[45] A. Ghysen. The origin and evolution of the nervous system. *International Journal of Developmental Biology*, 47(8):555–562, 2003.

[46] G.B. Gillis. Undulatory locomotion in elongate aquatic vertebrates: Angulliform swimming since Sir James Gray. *American Zoology*, 36:656–665, 1996.

[47] S. Grillner, A. Kozlov, P. Dario, C. Stefanini, A Menciassi, A Lansner, and J. Hellgren Kotaleski. Modeling a vertebrate motor system: pattern generation, steering and control of body orientation. *Progress in Brain Research*, 165, 2007.

[48] F. Gruau. *Neural Network Synthesis Using Cellular Encoding And the Genetic Algorithm*. PhD thesis, L'Universite Claude Bernard-Lyon I, Lyon, 1994.

[49] S. Haykin. *Neural Networks: A Comprehensive Foundation*. Prentice Hall, NJ, USA, 2nd edition, 1998.

[50] L.Z. Holland. Body-plan evolution in the bilateria: early antero-posterior patterning and the deuterostome-protostome dichotomy. *Current opinion in genetics and development*, 10(4):434–442, 2000.

[51] N.D. Holland. Early central nervous systems evolution: an era of skin brains? *Nature reviews*, 4(8):617–627, 2003.

[52] A. Ijspeert and J. Kodjabachian. Evolution and development of a central pattern generator for the swimming of a lamprey. *Artificial Life*, 5(3):247–269, 1999.

[53] A.J. Ijspeert and M. Arbib. Visual tracking in simulated salamander locomotion. In *Sixth International Conference of the Society for Adaptive Behavior*, pages 88–97, Cambridge, MA, 2000. MIT Press.

[54] A.J. Ijspeert, J. Hollam, and D. Willshaw. Evolving swimming controllers for a simulated lamprey with inspiration from neurobiology. *Adaptive Behavior*, 7(2):151–172, 1999.

[55] Y. Jin, L. Schramm, and B. Sendhoff. A gene regulatory model for the development of primitive nervous systems. In *Proceedings of the 15th International Conference on Neural Information Processing*, pages 48–55. Springer, 2008.

[56] B. Jones, Y. Jin, B. Sendhoff, and X. Yao. Evolving functional symmetry in a three dimensional model of an elongated organism. In *Artificial Life XI: Proceedings of the Eleventh International Conference on the Simulation and Synthesis of Living Systems*, pages 305–312, Cambridge, MA, 2008. MIT Press.

[57] B. Jones, Y. Jin, B. Sendhoff, and X. Yao. The effect of proprioceptive feedback on the distribution of sensory information in a model of an undulatory organism. In *Proceedings of the 10th European Conference on Artificial Life*, Berlin, 2009. Springer.

[58] B. Jones, Y. Jin, B. Sendhoff, and X. Yao. The evolutionary emergence of neural organization in a hydra-like animat. In *The Bernstein Conference of Computational Neuroscience*. Frontiers Research Foundation, 2009.

[59] B. Jones, Y. Jin, X. Yao, and B. Sendhoff. Evolution of neural organization in a hydra-like animat. In *Proceedings of the 15th International Conference on Neural Information Processing of the Asia-Pacific Neural Network Assembly*, volume 1, pages 216–223, Berlin, 2008. Springer.

[60] P.S. Katz. Evolution and development of neural circuits in invertebrates. *Current Opinion in Neurobiology*, 17(1):59–64, 2007.

[61] H. Kitano. Designing neural networks using genetic algorithms with graph generation system. *Complex Systems*, 4(4):461–476, 1990.

[62] J. Kodjabachian and J.-A. Meyer. Evolution and development of modular control architectures for 1D locomotion in six-legged animats. *Connection Science*, 10(3-4):211–237, 1998.

[63] O. Koizumi. Developmental neurobiology of hydra, a model animal of cnidarians. *Canadian Journal of Zoology*, 80(10):1678–1689, 2002.

[64] O. Koizumi. Nerve ring of the hypostome in hydra: is it an origin of the central nervous system of bilaterian animals? *Brain, Behavior and Evolution*, 69(2):151–159, 2007.

[65] O. Koizumi and H.R. Bode. Plasticity in the nervous system of adult hydra. III. Conversion of neurons to expression of a vasopressin-like immunoreactivity depends on axial location. *Journal of Neuroscience*, 11:2011–2020, 1991.

[66] O. Koizumi, N. Sato, and C. Goto. Chemical anatomy of hydra nervous system using antibodies against hydra neuropeptides: a review. In *Hydrobiologia*, volume 530-531, pages 41–47. Springer, Netherlands, 2004.

[67] T. Lacalli. Dorsoventral axis inversion: a phylogenetic perspective. *BioEssays*, 18(3):251–254, 1996.

[68] S.B. Laughlin, R.R. de Ruyter van Steveninck, and J.C. Anderson. The metabolic cost of neural information. *Nature Neuroscience*, 1:36–41, 1998.

[69] C. H. Leung and M. Berzins. A computational model for organism growth based on surface mesh generation. *Journal of Computational Physics*, 188(1):75–99, 2003.

[70] S.P. Leys, G.O. Mackie, and R.W. Meech. Impulse conduction in a sponge. *The Journal of Experimental Biology*, 202(9), 1999.

[71] M. Lungerella and O. Sporns. Mapping Information Flow in Sensorimotor Networks. *PLoS Computational Biology*, 2(10):1301–1312, 2006.

[72] J. Lynch and C. Desplan. 'De-evolution' of Drosophila toward a more generic mode of axis patterning. *International Journal of Developmental Biology*, 47(7-8):497–503, 2003.

[73] G.O. Mackie. The elementary nervous system revisited. *American Zoologist*, 30(4):907–920, 1990.

[74] G.O. Mackie. Central neural circuitry in the jellyfish Aglantha: a model 'simple nervous system'. *Neurosignals*, 13(1-2):5–19, 2004.

[75] G.O. Mackie. Epithelial conduction: recent findings, old questions, and where do we go from here? *Hydrobiologia*, 530-531(1-3):73–80, 2004.

[76] E. Marder and D. Bucher. Central pattern generators and the control of rhythmic movements. *Current Biology*, 11(23):986–996, 2001.

[77] M.Q. Martindale, J.R. Finnerty, and J.Q. Henry. The Radiata and the evolutionary origins of the bilaterian body plan. *Molecular Phylogenetics and Evolution*, 24(3):358–365, 2002.

[78] W.S. McCulloch and W. Pitts. A logical calculus of the ideas immanent in nervous activity. *Bulletin of Mathematical Biology*, 5(4):115–133, 1943.

[79] S. McMillan. *Computational dynamics for robotic systems on land and under water*. PhD thesis, The Ohio State University, Ohio, Columbus, 1995.

[80] H. Meinhardt. Organizer and axes formation as a self-organizing process. *International Journal of Developmental Biology*, 45:177–188, 2001.

[81] H. Meinhardt. The radial-symmetric hydra and the evolution of the bilateral body plan: an old body become a young brain. *BioEssays*, 24(2):185–191, 2002.

[82] H. Meinhardt. Different strategies for midline formation in bilaterians. *Nature*, 5:502–510, 2004.

[83] S. Minobe, O. Koizumi, and T. Sugiyama. Nerve cell differentiation in nerve-free tissue of epithelial hydra from precursor cells introduced by grafting: I. Tentacles and hypostome. *Developmental Biology*, 172(12):170–181, 1995.

[84] O. Mokady, M.H. Dick, D. Lackschewitz, B. Schierwater, and L.W. Buss. Over one-half billion years of head-conservation? Expression of an *ems* class gene in *Hydractinia symbiolongicarpu* (Cnidaria: Hydrozoa). *Proceedings of the National Academy of Sciences of the United States of America*, 95(7):3673–3678, 1998.

[85] U.K. Müller, J. Smit, E.J. Stamhuis, and J.J. Videler. How the body contributes to the wake in undulatory fish swimming: flow fields of a swimming eel (*Anguilla Anguilla*). *The Journal of Experimental Biology*, 204(16):2751–2762, 2001.

[86] Y. Murakami, K. Uchida, F.M. Rijli, and S. Kuratani. Evolution of the brain developmental plan: insights from agnathans. *Developmental Biology*, 280(2):249–259, 2005.

[87] H. Nakano, N. Murabe, S. Amemiya, and Y. Nakajima. Nervous system development of the sea cucumber *Stichopus japonicus*. *Developmental Biology*, 292(1):205–212, 2006.

[88] S.A. Newman. Is segmentation generic? *BioEssays*, 15(4):277–283, 1993.

[89] J. Nishii. A learning model of a periodic locomotor pattern by the central pattern generator. *Adaptive Behavior*, 7(2):137–149, 1999.

[90] K.C. Nishikawa. Evolutionary convergence in nervous systems: Insights from comparative phylogenetic studies. *Brain, Behavior and Evolution*, 59(5-6):240–249, 2002.

[91] Y. Niv, D. Joel, I. Meilijson, and E. Ruppin. Evolution of reinforcement learning in uncertain environments: a simple explanation for complex foraging behaviors. *Adaptive behavior*, 10(1):5–24, 2002.

[92] J.E. Niven. Brain evolution: Getting better all the time? *Current Biology*, 15(16):624–626, 2005.

[93] J.E. Niven, J.C. Anderson, and S.B. Laughlin. Fly photoreceptors demonstrate energy-information trade-offs in neural coding. *PLoS Biology*, 5(4):e166, 2007.

[94] J.E. Niven and S.B. Laughlin. Energy limitation as a selective pressure on the evolution of sensory systems. *Journal of Experimental Biology*, 211(11):1792–1804, 2008.

[95] S. Nolfi and D. Parisi. Growing neural networks. Technical Report PCIA-91-15, Institute of Psychology C.N.R., Rome.

[96] B.A. Olshausen and D.J. Field. Sparse coding of sensory inputs. *Current Opinion in Neurobiology*, 14(4):481–487, 2004.

[97] K.J. Peterson, R.A. Cameron, and E.H. Davidson. Bilaterian origins: significance of new experimental observations. *Developmental Biology*, 219(1):1–17, 2000.

[98] R. Pfeifer and F. Iida. Morphological computation: Connecting brain, body, and environment. In *Biologically Inspired Approaches to Advanced Information Technology*, volume 3853, pages 2–3. Springer, Berlin, 2006.

[99] J. Piatigorsky and Z. Kozmik. Cubozoan jellyfish: an evo/devo model for eyes and other sensory systems. *International Journal of Developmental Biology*, 48(8–9):719–729, 2004.

[100] M. Reuter and M.K.S. Gudtaffson. The flatworm nervous system: Pattern and phylogeny. *EXS*, 72:25–59, 1995.

[101] M. Reuter, K. Mäntylä, and M.K.S Gustafsson. Organization of the orthogon – main and minor nerve cords. *Hydrobiologia*, 383(1-3):175–182, 1998.

[102] F. Rosenblatt. The perceptron: a probabilistic model for information storage and organization in the brain. *Psychological Review*, 65(6):386–408, 1958.

[103] A.G. Rust, R. Adams, and H. Bolouri. Towards computational neural systems through developmental evolution. In *Emergent Neural Computational Architectures based on Neuroscience*, volume 2036, pages 188–202, Hiedelberg, 2001. Springer.

[104] J. Sarma and K. De Jong. An analysis of the effects of neighborhood size and shape on local selection algorithms. In *Parallel Problem Solving from Nature – PPSN IV*, volume 1141, pages 236–244, Berlin, 1996. Springer.

[105] L. Schramm. A model for nervous systems development controlled by a gene regulatory network. Diploma thesis. Master's thesis, Technische Universität Darmstadt, Darmstadt, 2007.

[106] L. Schramm, Y. Jin, and B. Sendhoff. Emerged coupling of motor control and morphological development in evolution of multi-cellular animats. In *Proceedings of the 10th European Conference on Artificial Life*. Springer, 2009.

[107] M. Sfakiotakis and D.P. Tsakiris. Simuun: A simulation environment for undulatory locomotion. *International Journal of Modelling and Simulation*, 26(4):350–358, 2006.

[108] M.A. Shenk, H.R. Bode, and R.E. Steele. Expression of Cnox-2, a HOM/HOX homeobox gene in hydra, is correlated with axial pattern formation. *Development*, 117:657–667, 1993.

[109] K. Sims. Evolving 3D morphology and behavior by competition. *Artificial Life*, 1(4):353–372, 1994.

[110] K. Sims. Evolving virtual creatures. In *Proceedings of the 21st annual conference on Computer graphics and interactive techniques*, pages 15–22, New York, NY, 1994. ACM.

[111] A. Soltoggio, J.A. Bullinaria, C. Mattiussi, P. Dürr, and D. Floreano. Evolutionary Advantages of Neuromodulated Plasticity in Dynamic, Reward-based Scenario. In *Artificial Life XI: Proceedings of the Eleventh International Conference on the Simulation and Synthesis of Living Systems*, Cambridge, MA, 2008. MIT Press.

[112] A. Soltoggio, P. Dürr, C. Mattiussi, and D. Floreano. Evolving neuromodulatory topologies for reinforcement learning-like problems. In *Proceedings of the 2007 IEEE Congress on Evolutionary Computation*, pages 2471–2478, New York, 2007. IEEE Press.

[113] W. Song, M. Onishi, L. Y. Jan, and Y. N. Jan. Peripheral multidendritic sensory neurons are necessary for rythmic locomotion behaviour in drosophila larvae. *Proceedings of the National Academy of Sciences of the United States of America*, 104(12):5199–5204, 2007.

[114] J. Spring, N. Yanze, C. Josch, A.M. Middel, B. Winninger, and V. Schmid. Conservation of *Brachyury*, *Mef2*, and *Snail* in the myogenic lineage of jellyfish: A connection to the mesoderm of bilateria. *Developmental Biology*, 244(2):372–384, 2002.

[115] K.O. Stanley and R. Miikkulainen. Efficient evolution of neural network topologies. In *Proceedings of the 2002 Congress on Evolutionary Computation*, pages 1757–1762, Washington, DC, 2002. IEEE Computer Society.

[116] Larry W. Swanson. *Brain Architecture: Understanding the Basic Plan*, chapter 2: The Simplest Nervous Systems. Oxford University Press, Oxford, 2003.

[117] T. Taylor and C. Massey. Recent developments in the evolution of morphologies and controllers for physically simulated creatures. *Artificial Life*, 7(1):77–87, 2000.

[118] D. Terzopoulos, T. Rabie, and R. Grzeszczuk. Perception and learning in artificial animals. In *Artificial Life V: Proceedings of the Fifth International Conference on the Synthesis and Simulation of Living Systems*, pages 313–320, Cambridge, MA, 1996. MIT Press.

[119] D. Terzopoulos, X. Tu, and R. Grzeszczuk. Artificial fishes: autonomous locomotion, perception, behavior, and learning in a simulated physical world. *Artificial Life*, 1(4):327–351, 1994.

[120] D.P. Tsakiris, A. Menciassi, M. Sfakiotakis, G. La Spina, and P. Dario. Undulatory locomotion of polychaete annelids: mechanics, neural control and robotic prototypes. In *The Annual Computational Neuroscience Meeting*, Greece, 2004. Institute of Computer Science - FORTH, Vassilika Vouton, Greece.

[121] B.T. Vincent and R.J. Baddeley. Synaptic energy efficiency in retinal processing. *Vision Research*, 43(11):1285–1292, 2003.

[122] B.T. Vincent, R.J. Baddeley, T. Troscianko, and I.D. Gilchrist. Is the early visual system optimised to be energy efficient? *Network: Computation in Neural Systems*, 16(2-3):175–190, 2005.

[123] J. Vreeken. Spiking neural networks, an introduction. Technical report, Adaptive Intelligence Laboratory, Intelligent Systems Group, Institute for Information and Computing Sciences, Utrecht University, Utrecht, 2003.

[124] D.J. Watts and S.H. Strogatz. Collective dynamics of 'small-world' networks. *Nature*, 393(6684):440–442, 1998.

[125] E. W. Weisstein. Savitzky-golay filter. From MathWorld–A Wolfram Web Resource. http://mathworld.wolfram.com/Savitzky-GolayFilter.html.

[126] P. Willmer. *Invertebrate Relationships: Patterns in Animal Evolution*. Cambridge University Press, Cambridge, 1990.

[127] X. Yao. Evolving artificial neural networks. In *Proceedings of the IEEE*, number 87 in 9, pages 1423–1447, September 1999.